



Comparison of inclusive and photon-tagged jet suppression in 5.02 TeV Pb+Pb collisions with ATLAS



The ATLAS Collaboration*

ARTICLE INFO

Article history:

Received 29 March 2023

Received in revised form 21 July 2023

Accepted 23 August 2023

Available online 29 August 2023

Editor: M. Doser

Dataset link: <https://hepdata.cedar.ac.uk>

ABSTRACT

Parton energy loss in the quark-gluon plasma (QGP) is studied with a measurement of photon-tagged jet production in 1.7 nb^{-1} of Pb+Pb data and 260 pb^{-1} of pp data, both at $\sqrt{s_{\text{NN}}} = 5.02 \text{ TeV}$, with the ATLAS detector. The process $pp \rightarrow \gamma + \text{jet} + X$ and its analogue in Pb+Pb collisions is measured in events containing an isolated photon with transverse momentum (p_T) above 50 GeV and reported as a function of jet p_T . This selection results in a sample of jets with a steeply falling p_T distribution that are mostly initiated by the showering of quarks. The pp and Pb+Pb measurements are used to report the nuclear modification factor, R_{AA} , and the fractional energy loss, S_{loss} , for photon-tagged jets. In addition, the results are compared with the analogous ones for inclusive jets, which have a significantly smaller quark-initiated fraction. The R_{AA} and S_{loss} values are found to be significantly different between those for photon-tagged jets and inclusive jets, demonstrating that energy loss in the QGP is sensitive to the colour-charge of the initiating parton. The results are also compared with a variety of theoretical models of colour-charge-dependent energy loss.

© 2023 The Author(s). Published by Elsevier B.V. This is an open access article under the CC BY license (<http://creativecommons.org/licenses/by/4.0/>). Funded by SCOAP³.

Contents

1. Introduction	1
2. ATLAS detector	3
3. Event reconstruction	3
4. Simulation	3
5. Analysis	4
6. Systematic uncertainties	5
7. Results	6
8. Discussion	7
8.1. Fractional energy loss analysis	7
8.2. Theoretical comparisons	8
9. Conclusion	9
Declaration of competing interest	9
Data availability	9
Acknowledgements	9
References	10
The ATLAS Collaboration	11

1. Introduction

Ultra-relativistic collisions of heavy nuclei at the Large Hadron Collider (LHC) and the Relativistic Heavy Ion Collider (RHIC) produce a hot, deconfined nuclear medium known as the quark-gluon

plasma (QGP). The QGP exhibits interesting emergent phenomena, such as a collective evolution that suggests it is a strongly coupled fluid well described by hydrodynamics [1–3]. The dense colour field arising from the deconfined colour charges that makes up the QGP is opaque to high-energy quarks and gluons attempting to pass through it. This results in hard-scattered partons suffering energy loss and a modification of their showering processes as they traverse the QGP. This phenomenon is known as *jet quench-*

* E-mail address: atlas.publications@cern.ch.

ing, and results in a wide variety of experimental signatures – see Ref. [4] for a recent review.

A straightforward and broadly used signature of jet quenching is the suppression of jet production at fixed transverse momentum¹ (p_T) in Pb+Pb collisions compared to pp collisions. This is quantified by the nuclear modification factor, R_{AA} , which is defined as the ratio of the observed yield in Pb+Pb collisions to the expectation from an equivalent number of nucleon–nucleon (NN) collisions, i.e., without jet quenching effects from the formation of a QGP. This expectation is calculated as the cross-section in pp collisions, scaled by the mean value of the nuclear thickness function in the corresponding Pb+Pb collisions, $\langle T_{AA} \rangle$ [5]. The R_{AA} is therefore defined as

$$R_{AA} = \frac{1}{N_{\text{evt}}} \frac{d^2 N^{\text{Pb+Pb}}}{dp_T d\eta} / \langle T_{AA} \rangle \frac{d^2 \sigma^{pp}}{dp_T d\eta}, \quad (1)$$

where $d^2 N^{\text{Pb+Pb}}/dp_T d\eta$ is the differential jet yield in N_{evt} Pb+Pb events in a given centrality range, $d^2 \sigma^{pp}/dp_T d\eta$ is the jet cross-section in pp collisions, and $\langle T_{AA} \rangle$ can be considered as a luminosity of nucleons per Pb+Pb collision. Therefore, the term in the denominator is the expected yield in Pb+Pb collisions in the absence of any nuclear effects.

In central Pb+Pb collisions, the nuclei collide head on and create a large and long-lived volume of QGP. The developing showers of high- p_T partons undergo substantial interactions with the QGP, such that part of their momentum is transferred to large angles relative to the initial parton direction [6,7]. Therefore, the total momentum in a fixed-size jet cone is decreased compared to the process with analogous initial kinematics occurring in pp collisions, and the jets can be thought of as migrating to lower p_T values in Pb+Pb events. Since the jet spectrum is steeply falling with p_T , this results in an R_{AA} below unity with a magnitude that depends on the amount of transported energy and the local shape of the spectrum. In central Pb+Pb events at the LHC, the R_{AA} for inclusive jets is suppressed by approximately a factor of two at $p_T \approx 100$ GeV [8–10]. While the R_{AA} is expected to be impacted by other effects, such as the modification of parton densities in the nucleus (nPDFs), these are understood to be modest for inclusive jets and thus most of the signal is due to jet energy loss [11–13].

A key aspect to the theoretical description of jet quenching is its sensitivity to the colour charge of the initiating parton, i.e., whether that parton is a quark or a gluon [14–25]. If the jet-medium interaction is predominantly described as proceeding by radiative emission (medium-induced gluon radiation by strong colour charges), quarks and gluons are generally expected to lose energy in proportion to their QCD colour factors for gluon emission of 4/3 and 3, respectively. Thus, gluon-initiated jets are expected to lose significantly more energy than quark-initiated ones. While the developing parton shower eventually contains both quarks and gluons, theoretical models indicate that the charge of the initiating parton should have a significant impact. At LHC energies, inclusive jet production in the region $p_T < 200$ GeV is dominated by gluon-initiated jets.

Several previous measurements have attempted to explore the colour charge dependence of jet suppression, but with additional effects that may complicate its extraction. For example, Ref. [8] measured jet suppression as a function of jet rapidity, which

changes the quark/gluon-initiated jet fraction, but may also sample different regions of the QGP medium [23]. Refs. [26,27] report the suppression of b -jets, which have a significantly larger quark-initiated fraction than inclusive jets, but have additional effects from the large mass of b -quarks.

An alternative strategy, including the one employed in this Letter, is to measure jets produced in association with an isolated photon or other electroweak (EW) boson, for example through Compton scattering ($gq \rightarrow q\gamma$). These jets are substantially more likely to be initiated by a quark than inclusive jets at the same p_T . Importantly, the kinematics of the colourless photon or EW boson are not significantly modified by the QGP [28–31]. Therefore ATLAS has used an isolated photon or Z boson as a way to select partons with a known distribution of initial kinematics before jet quenching [32] and to study how the resulting jet [33] or hadron [34,35] distributions are modified in particular selections of boson p_T , compared to those in pp collisions.

This Letter presents a measurement of the process pp (or NN) $\rightarrow \gamma + \text{jet} + X$, as a function of jet p_T . Unlike previous measurements mentioned above (Ref. [33–35]), the results in this paper are not normalized per-photon, but measure the full photon-associated jet production cross-section. The measurement is performed using 260 pb⁻¹ and 1.7 nb⁻¹ of pp and Pb+Pb collisions, respectively, at an NN centre-of-mass energy $\sqrt{s_{\text{NN}}} = 5.02$ TeV recorded with the ATLAS detector at the LHC. Events are required to have an isolated photon with $p_T^\gamma > 50$ GeV and $|\eta^\gamma| < 2.37$ (excluding the region $1.37 < |\eta^\gamma| < 1.52$). At leading order (LO), the photon isolation requirement predominantly selects direct photons, which are those produced directly in the hard scattering, but also a contribution from fragmentation photons that are radiated in a parton shower after the scattering. All jets with $|\eta^{\text{jet}}| < 2.8$ and $p_T^{\text{jet}} > 50$ GeV in an opposing azimuthal direction to the photon ($\Delta\phi_{\gamma,\text{jet}} > 7\pi/8$) are included in the measurement. This requirement selects a set of jets with a steeply falling p_T distribution, with a large quark-initiated fraction.

The resulting jet production rates in Pb+Pb and pp collisions are used to report R_{AA} and the fractional energy loss quantity, S_{loss} , originally developed by the PHENIX Collaboration at RHIC [36–38] that is conceptually similar to the ‘pseudo-quantile’ described in Ref. [39]. For a given amount of energy loss, the particular magnitudes of the R_{AA} values are known to depend strongly on the steepness of the pp spectrum. The S_{loss} formulation is designed as an alternative way to characterize the energy loss while removing this dependence. Schematically, S_{loss} is the fractional decrease in p_T^{jet} at which the $\langle T_{AA} \rangle$ -scaled jet yield in Pb+Pb events reaches the same magnitude as the cross-section in pp events at the original p_T^{jet} . Quantitatively, for each value of the p_T^{jet} in pp collisions, p_T^{pp} , the shift function, $\Delta p_T(p_T^{pp})$, is defined as

$$\Delta p_T = p_T^{pp} - p_T^{\text{Pb+Pb}} \quad (2)$$

where $p_T^{\text{Pb+Pb}}$ is the value for which

$$\begin{aligned} \frac{1}{\langle T_{AA} \rangle} \frac{1}{N_{\text{evt}}} \frac{d^2 N^{\text{Pb+Pb}}(p_T^{\text{Pb+Pb}} = p_T^{pp} - \Delta p_T)}{dp_T^{\text{Pb+Pb}} d\eta} \\ = \frac{d^2 \sigma^{pp}(p_T^{pp})}{dp_T^{pp} d\eta} \times \left[1 + \frac{d\Delta p_T}{dp_T^{pp}} \right] \end{aligned} \quad (3)$$

where the expression in square brackets is the Jacobian term necessary to, e.g., preserve the total number of jets. The fractional energy loss is given by $S_{\text{loss}}(p_T^{pp}) = \Delta p_T/p_T^{pp}$. It is related to, but not identical to, the average energy lost by jets originating at a given p_T in pp collisions, and is a useful way to characterize the magnitude of energy loss in a way that does not depend on the local shape of the spectrum.

¹ ATLAS uses a right-handed coordinate system with its origin at the nominal interaction point (IP) in the centre of the detector and the z -axis along the beam pipe. The x -axis points from the IP to the centre of the LHC ring, and the y -axis points upward. Cylindrical coordinates (r, ϕ) are used in the transverse plane, ϕ being the azimuthal angle around the z -axis. The pseudorapidity is defined in terms of the polar angle θ as $\eta = -\ln \tan(\theta/2)$.

The R_{AA} and S_{loss} results for photon-tagged jets are then compared with the analogous ones for inclusive jets [8], whose production in this kinematic range has a significantly smaller quark-initiated fraction. Since the main difference between the jet populations is in their quark and gluon composition, this comparison allows a controlled examination of the impact of the initiating parton's QCD colour charge on jet energy loss.

2. ATLAS detector

The ATLAS detector [40] at the LHC is a multipurpose particle detector with a forward–backward symmetric cylindrical geometry and a near 4π coverage in solid angle. Its inner tracking detector is surrounded by a thin superconducting solenoid providing a 2 T axial magnetic field, and electromagnetic (EM) and hadron calorimeters. The inner tracking detector covers the pseudorapidity range $|\eta| < 2.5$. It consists of silicon pixel, silicon microstrip, and transition radiation tracking detectors. Lead/liquid-argon (LAr) sampling calorimeters provide EM energy measurements with high granularity. A steel/scintillator-tile hadron calorimeter covers the central pseudorapidity range ($|\eta| < 1.7$). The endcap and forward regions are instrumented with LAr calorimeters for both the EM and hadronic energy measurements up to $|\eta| = 4.9$. A zero-degree calorimeter (ZDC) was situated at $|\eta| > 8.3$ during Pb+Pb data-taking. It is composed of alternating layers of quartz rods and tungsten plates and is mostly sensitive to spectator neutrons from fragmenting nuclei in Pb+Pb collisions.

A two-level trigger system is used to select events [41]. The first-level trigger is implemented in hardware and uses a subset of the detector information to accept events at a rate below 100 kHz. This is followed by a software-based trigger that reduces the accepted event rate to 1 kHz on average depending on the data-taking conditions. An extensive software suite [42] is used in data simulation, in the reconstruction and analysis of real and simulated data, in detector operations, and in the trigger and data acquisition systems of the experiment.

3. Event reconstruction

Events were selected using triggers that required a reconstructed photon with p_T above 35 GeV (20 GeV) in pp (Pb+Pb) collisions [41,43]. The trigger sampled the full luminosity corresponding to 260 pb^{-1} of pp data in 2017 and 1.7 nb^{-1} of Pb+Pb data in 2018, and was fully efficient for the photon selection described below. Events are required to satisfy detector and data-quality requirements and, in Pb+Pb collisions, to have a reconstructed vertex.

The Pb+Pb event centrality is characterized by the sum of the transverse energy, ΣE_T^{FCal} in the forward calorimeters, $3.2 < |\eta| < 4.9$. Events in different ranges of ΣE_T^{FCal} are associated with an underlying Pb+Pb collision geometry according to a Monte Carlo (MC) Glauber simulation [5,44]. This analysis uses three centrality intervals corresponding to the following fractions of the ΣE_T^{FCal} distribution in minimum-bias events: 0–10% ('central' events, with a large nuclear overlap and large ΣE_T^{FCal} values), 10–30%, and 30–80% ('peripheral' events).

Photons are reconstructed following the method used previously in Pb+Pb collisions [28,33,35], which applies the procedure used in pp collisions [45] after an event-by-event estimation and subtraction of the underlying event (UE) contribution to the energy deposited in each calorimeter cell [46] (described further below). Photon candidates are required to satisfy 'tight' shower shape requirements designed to reject photons arising from neutral meson decays and from the start of hadronic showers in the EM calorimeter [47]. In pp collisions, photons are further required to be isolated by requiring that the sum of the transverse energy in calorimeter cells within $\Delta R = 0.3$ (not including the contribution from the

photon itself) is less than 3 GeV. In Pb+Pb collisions, the UE fluctuations within the isolation cone result in a substantial broadening of the isolation E_T distribution. Thus, in Pb+Pb collisions, the isolation energy requirement depends continuously on the centrality of the event and is chosen so that its efficiency for prompt photons is 90%, as determined from simulations of photon+jet events overlaid with Pb+Pb minimum-bias data (described in Section 4 below). This upper limit on the isolation energy is approximately 10 GeV in 0–10% Pb+Pb events, but quickly decreases in more peripheral events and converges to the pp value.

Jets are reconstructed following the procedure used in Pb+Pb collisions [8,46], which is summarized here. Calorimeter cells in all layers are evaluated at the EM energy scale and regrouped into $\Delta\eta \times \Delta\phi = 0.1 \times \pi/32$ logical towers, and the anti- k_t algorithm [48,49] with parameter $R = 0.4$ is applied to the towers. After the initial jet-finding, the contribution to the energy deposited in towers by the UE is estimated on an event-by-event basis, allowing for the variation of the UE as a function of η and ϕ (the latter arising from the global collective flow in Pb+Pb collisions). Information from towers within $\Delta R = 0.4$ of jet candidates is excluded to avoid biasing the UE estimate. The kinematics of the tower energies are updated to subtract the estimated UE contribution, and the UE procedure is iterated using a better-defined set of jets to define the exclusion regions. The resulting set of jet kinematics is corrected using p_T - and η -dependent factors, determined from simulation, to account for the response of the calorimeter to jets [50]. An additional correction for the absolute response in data is based on *in situ* studies of jets recoiling against photons, Z bosons, and jets in other regions of the calorimeter in pp collisions [51]. This calibration is followed by a 'cross-calibration' that relates the jet energy scale (JES) in high-luminosity 13 TeV pp collisions [52] to the jets reconstructed by the procedure outlined above in the 5.02 TeV data to account for additional differences between the data and simulations.

4. Simulation

Samples of MC-simulated events are used to evaluate the performance of the photon and jet reconstruction and to correct the measured distributions for detector effects. The main MC sample corresponding to photon+jet production in pp data consists of PYTHIA 8 [53] events, produced with the A14 [54] set of tuned parameters (tune) and the NNPDF 2.3 LO [55] parton distribution function (PDF) set, including direct and fragmentation contributions. As alternatives, photon+jet events were also produced using two additional generators. The SHERPA 2.2.4 [56,57] generator was run at next-to-leading order (NLO) with the NNPDF 3.0 NNLO [58] PDF set to produce a sample of events containing a photon plus up to three other partons. The HERWIG 7.2 [59] generator was run at leading order with the MMHT2014lo [60] PDF set, with separate samples produced for direct and fragmentation photons. The three sets of events were simulated [42] using a GEANT4 [61] description of the ATLAS detector and were digitized and reconstructed in a manner identical to that of the data. The generator-level final state photons in the MC samples are required to be isolated by requiring that the sum of the transverse energy of all the final state particles, excluding the photon itself, within a $\Delta R = 0.4$ cone is less than 5 GeV.

The fraction of quark-initiated jets, as defined in simulation in Ref. [62], is estimated by using three different MC generators (PYTHIA 8, HERWIG and SHERPA) for the photon-tagged jets, and is compared with that for inclusive jets [8] in Fig. 1. The generators predict that 75–80% of all photon-tagged jets at $p_T^{\text{jet}} = 50 \text{ GeV}$ are initiated by quarks, while this is true for only 30–40% of inclusive jets at the same p_T^{jet} . At higher p_T^{jet} , the quark-initiated fractions for photon-tagged and inclusive jets slowly fall and rise, respectively,

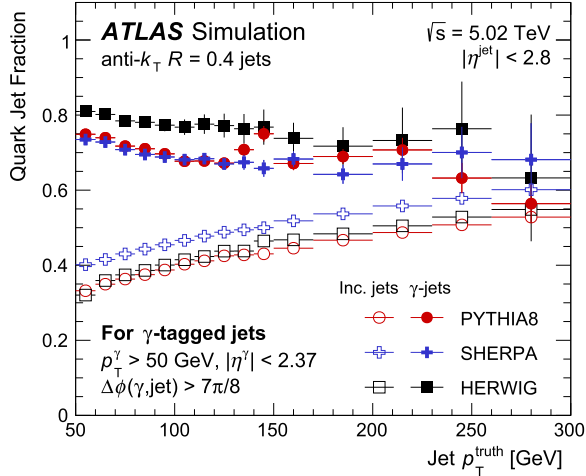


Fig. 1. Fraction of photon-tagged jets (filled markers) and inclusive jets (open markers) initiated by a quark, as a function of generator-level p_T^{jet} , in the PYTHIA 8 (circles), HERWIG (squares), and SHERPA (crosses) event generators. The vertical bars associated with symbols indicate the statistical uncertainties.

reaching 50–60% for both samples at 300 GeV. Thus, according to the MC generators, these two samples contain significantly different quark-initiated jet fractions with $p_T^{\text{jet}} \lesssim 200$ GeV.

To simulate photon+jet events in Pb+Pb data, the events described above were overlaid at the detector-hit level with a sample of Pb+Pb data events recorded with minimum-bias and central-event triggers. The combination of the simulated and data event was then reconstructed as a single event. These ‘Pb+Pb data overlay’ events are re-weighted to match the observed ΣE_T^{Fcal} distribution for photon+jet events in Pb+Pb data. In this way, the features of the Pb+Pb UE in the simulated samples which are uncorrelated with the photon+jet process, such as the flow and transverse energy distributions, are identical to those in real minimum-bias Pb+Pb events.

Finally, to evaluate the possible impact of nuclear effects, such as the modification of PDFs on the measurement, samples of generator-level PYTHIA 8 events were produced for photon+jet and inclusive jet events, again including both direct and fragmentation photons and the generator-level isolation requirement. For both of these processes, separate samples were generated for pp , proton-neutron (pn), and neutron-neutron (nn) events, and the cross-section in simulated Pb+Pb events was constructed via a weighted sum $(Z^2\sigma^{pp} + 2Z(A-Z)\sigma^{pn} + (A-Z)^2\sigma^{nn})/A^2$, where A and Z are the mass and atomic number of Pb, respectively. In a separate procedure, the cross-section in the pp samples was evaluated after being weighted on an event-by-event basis with the central values of the EPPS16 nPDF set [63], at NLO and configured for the lead nucleus with the grid file EPPS16NLOR_208.

5. Analysis

The signal definition for this measurement is $R = 0.4$ jets with $p_T^{\text{jet}} > 50$ GeV that are $\Delta\phi_{\gamma,\text{jet}} > 7\pi/8$, i.e. $|\Delta\phi_{\gamma,\text{jet}} - \pi| < \pi/8$, from a $p_T^{\gamma} > 50$ GeV isolated photon, with all candidate jets in a given event included in the measurement. The two-dimensional yield $(p_T^{\gamma}, p_T^{\text{jet}})$ is constructed for photons and their associated jets, but using thresholds of 40 GeV on the photon and jet p_T , to allow for the correction of bin migration effects (discussed below).

Fig. 2 shows the signal $p_T^{\text{jet}}/p_T^{\gamma}$ distributions in pp data at the reconstructed-level (i.e., without any of the corrections for photon purity, efficiency, and unfolding described below), compared with the same in simulated PYTHIA 8 events. The contributions from direct and fragmentation photons in PYTHIA 8 are shown separately

as shaded histograms, with the former contribution peaking near unity due to the back-to-back kinematics, and the latter distribution extending to large $p_T^{\text{jet}}/p_T^{\gamma}$ values. At the lowest p_T^{jet} bin of $50 < p_T^{\text{jet}} < 60$ GeV, the $p_T^{\text{jet}}/p_T^{\gamma}$ distribution in data has no entries above 1.2 because of the kinematic selection on the photons ($p_T^{\gamma} > 50$ GeV), and thus the comparison with simulation suggests that direct photons are dominant. However, at high p_T^{jet} values (e.g., in the right most panel), there is a growing contribution from fragmentation photons, which may contribute to the decreasing quark-initiated jet fraction in Fig. 1.

Notably, PYTHIA 8 does not precisely match the $p_T^{\text{jet}}/p_T^{\gamma}$ distribution in data, in particular over-estimating the relative magnitude of the fragmentation photon contribution. A similar conclusion was reached in the study of photon+jet events in pp collisions at 7 TeV [64], where PYTHIA 8 better describes the data after an increased (decreased) weighting of the direct (fragmentation) contributions in that generator. While this exercise is not repeated in this measurement, the dashed line in Fig. 2 indicates how de-weighting the fragmentation photon contribution in PYTHIA 8 by, e.g., a factor of two would modify the jet p_T distribution in that generator. Therefore this study highlights the need for the pp baseline in theoretical calculations of jet quenching to properly model the relative direct and fragmentation photon contributions in photon+jet processes.

The initial $(p_T^{\gamma}, p_T^{\text{jet}})$ yield in Pb+Pb collisions contains jets that do not arise from the same hard scattering as the photon, but rather from an unrelated NN scattering, or from jets that are reconstructed from the localized fluctuations of the UE. This combinatoric contribution is estimated through a ‘mixing’ technique in which high- p_T photons in data are correlated with jets in minimum-bias Pb+Pb events that match the overall properties of the original, photon-containing event. These matched properties include the ΣE_T^{Fcal} and flow plane angle. The resulting combinatoric jet contribution is observed to be flat in $\Delta\phi$, as expected for unrelated pairs. For the lowest p_T^{jet} values in the most central events, the background contribution is approximately half of the total yield, but this fraction falls very rapidly with increasing p_T^{jet} or in less central events. The contribution is statistically subtracted from the initial yields.

Even after the photon identification and isolation conditions above are applied to data, the selected photons still include a considerable contribution from backgrounds, dominantly from neutral hadron decays (e.g., $\pi^0, \eta \rightarrow \gamma\gamma$). These decay photons may be reconstructed as a single cluster that satisfies the ‘tight’ identification and the isolation conditions. Thus, the photon-associated jet yields contain a contribution from, e.g., π^0 -associated jet yields. To correct for this, the purity of prompt, isolated photons in the selected data sample is determined by using a data-driven, double-sideband method widely used in ATLAS photon measurements [65–68], separately for each selection in event centrality and p_T^{γ} . The purity has a minimum of $\approx 75\%$ in central Pb+Pb events at the lowest p_T^{γ} values, but then increases rapidly with p_T^{γ} and in more peripheral Pb+Pb or pp events to a plateau of $\approx 95\%$. The shape of the p_T^{jet} contribution from this background is determined by performing the same analysis but using an inverted signal selection on the photon. This selection requires the photon to still be isolated, but fail to satisfy several shower shape requirements in a way that is designed to greatly enhance the neutral hadron background. Finally, the background level is scaled according to the purity in each p_T^{γ} and centrality selection, and statistically subtracted from the yields.

To correct for the bin-to-bin migration in the p_T^{γ} and p_T^{jet} distributions arising from the finite detector resolution and residual defects in the JES, a two-dimensional unfolding procedure on the background-subtracted $(p_T^{\gamma}, p_T^{\text{jet}})$ yields is used. The PYTHIA 8 sim-

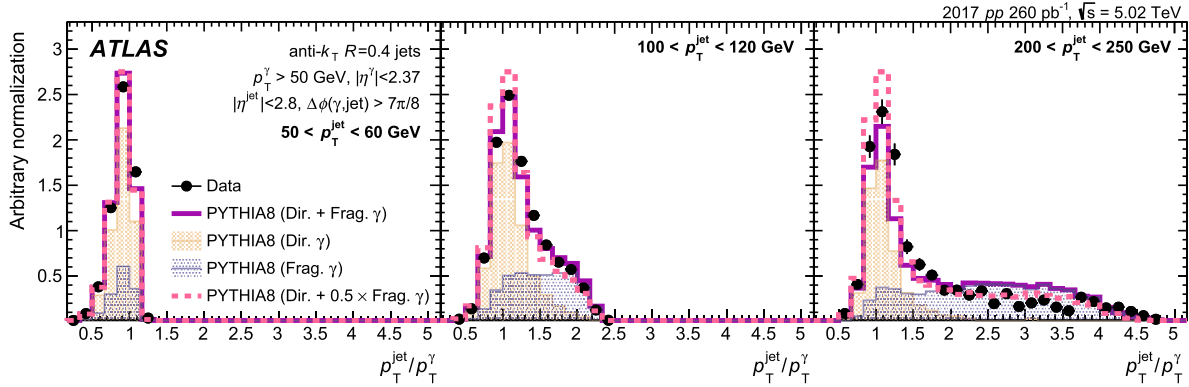


Fig. 2. Reconstructed-level $p_T^{\text{jet}}/p_T^{\gamma}$ distributions for different p_T^{jet} bins: (left panel) $50 < p_T^{\text{jet}} < 60 \text{ GeV}$ (middle panel) $100 < p_T^{\text{jet}} < 120 \text{ GeV}$ and (right panel) $200 < p_T^{\text{jet}} < 250 \text{ GeV}$. The data (filled circles) is compared with reconstructed-level PYTHIA 8 (solid line), which is normalized to the data. The shaded histograms show the breakdown of PYTHIA 8 contributions from photon-production processes: direct (checkered hatching) and fragmentation (dashed hatching) photons. The dashed-line histogram represents PYTHIA 8 events, including all direct photon events with the fragmentation photon events scaled down by a factor of two.

ulation samples are used to generate independent response matrices for pp events and for each centrality range in $\text{Pb}+\text{Pb}$ events, after reweighting the p_T^{jet} distributions in simulation to match those measured in data. The iterative Bayesian method [69] is used with the RooUnfold software package [70]. The number of iterations used in the unfolding is determined by minimizing the sum in quadrature of the total statistical uncertainty and the differences in the unfolded distribution between consecutive iterations. This number is two or three depending on the event centrality. The unfolding procedure also accounts for the finite reconstruction and selection efficiency for photons, which is $\approx 70\%$ at low- p_T^{γ} in central $\text{Pb}+\text{Pb}$ events, but rises rapidly with p_T^{γ} and in more peripheral events to a plateau of $\approx 85\%$, and for a small inefficiency for jets at low p_T^{jet} . When tested in simulation, this unfolding procedure leads to a recovery of the original generator-level distribution within the statistical uncertainties of the test sample.

6. Systematic uncertainties

The main sources of systematic uncertainty in this measurement are those associated with the photon, jet, and unfolding components. For most of the sources described below, the entire analysis is repeated with a given variation, and the change in the results is taken as the corresponding uncertainty. These individual uncertainties are treated as independent and added in quadrature to quantify the full uncertainties.

The photon measurement includes several uncertainty components. First, the reconstructed energy of photons in simulation is varied according to the uncertainties in the photon energy scale and resolution [71]. Second, the reconstructed shower shape variables used to identify photons are varied in simulation [47]. Third, the isolation and identification sideband boundaries used in purity determination are varied in a manner similar to that in Refs. [33,35]. Fourth, the difference between using the nominal purity values and the results of a smooth fit to those values is considered. Finally, the reconstruction-level isolation energy requirement is varied such that isolation efficiency for signal photons is 85% and 95%, instead of the nominal 90%. These variations result in different estimates of the photon purity, and thus test the stability of the extracted yield to any potentially imperfect description of photon isolation energy distributions in simulations. The uncertainty in the yields from all these sources is typically 3–6% in pp collisions (4–15% in central $\text{Pb}+\text{Pb}$ collisions), rising with jet p_T .

For the jet-related uncertainties, the reconstructed jet energy in simulation is varied according to the uncertainties in the JES and jet energy resolution (JER). As in other Run 2 heavy-ion jet

measurements [8,33,35,72], the JES uncertainties have four main components. First, a centrality-independent baseline component determined from *in situ* studies of the calorimeter response to jets reconstructed following the procedure used in 13 TeV pp collisions [51,73]. Second, a centrality-independent component accounting for the relative energy scale difference between the heavy-ion jet reconstruction in this analysis and that used for 13 TeV pp collisions [52]. Third, a component that accounts for potential inaccuracies in the relative abundances of jets initiated by quarks and gluons, and of their different calorimetric response, in simulation. This uncertainty was evaluated by using the flavour fractions and flavour-dependent response in the HERWIG, instead of PYTHIA 8, simulation samples. Finally, a centrality-dependent component accounting for a different structure and possibly a different detector response of jets in $\text{Pb}+\text{Pb}$ collisions that is not modelled in simulation. This uncertainty is determined by the method used for 2015 and 2011 data [52] that compares the calorimeter p_T^{jet} with the p_T sum of the charged particles in the jets in data and simulation. For the JER uncertainty, the reconstructed p_T^{jet} in simulation is smeared by a factor evaluated using an *in situ* technique in 13 TeV pp data [74,75], and by an additional contribution to account for the differences between the heavy-ion jet reconstruction and that in the 13 TeV pp data. The JES and JER uncertainties in the jet yields are typically 3–7% in pp collisions, rising slowly with jet p_T , and are modestly higher in $\text{Pb}+\text{Pb}$ collisions due to the final uncertainty source described above.

Two uncertainties associated with the unfolding procedure are evaluated. First, the impact of a different prior in the response matrices was determined by not applying the reweighting factors to account for the difference in the distributions between data and simulation. These were at most 5% at low p_T^{jet} , decreasing to 1% at high p_T^{jet} . Second, a resampling study is used to determine the impact on the results from the limited size of the simulated samples. These are included as part of the statistical uncertainties, but they are typically much smaller than the statistical uncertainties in data.

The mixed event technique was tested in the simulation samples, where the combinatoric contribution is exactly known. Any “non-closure” in the procedure (i.e. failure to fully subtract the combinatoric contribution) is considered as a source of uncertainty. Finally, there are uncertainties in the overall normalization of the measurements. For the pp cross-section, these arise from the luminosity of the pp data and are estimated to be 1.6% using the beam separation scan analysis methods similar to that in Ref. [76]. For the $1/\langle T_{AA} \rangle$ -scaled yields in $\text{Pb}+\text{Pb}$ collisions, the uncertainties are determined by adjusting the parameters in the Glauber

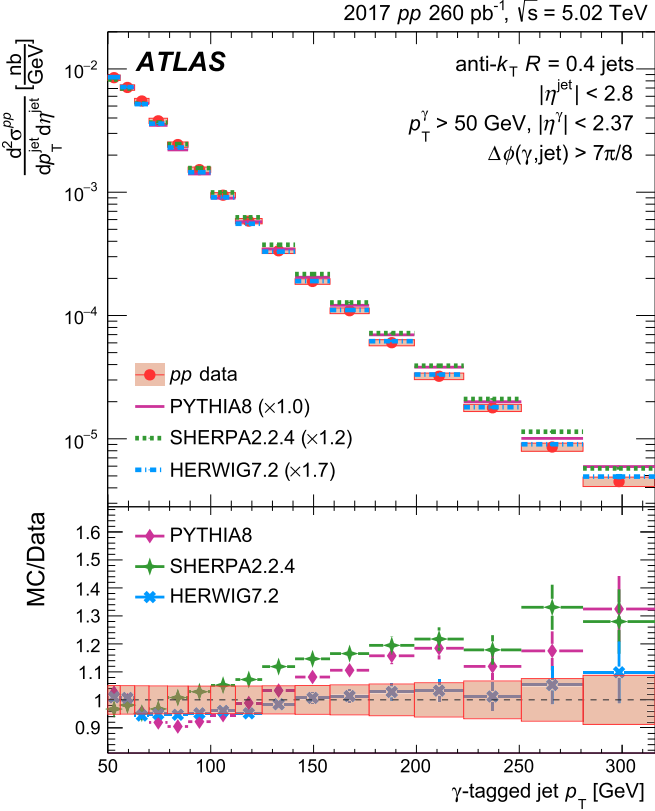


Fig. 3. Top panel: The differential cross-section of photon-tagged jets as a function of p_T^{jet} in pp data, compared with that in PYTHIA 8 (solid line), SHERPA 2.2.4 (dotted line) and HERWIG 7.2 (dash-dotted line) MC samples. The statistical uncertainties in the data are small and hidden by the symbols, and are drawn as vertical bars for the MC samples. The total systematic uncertainties in the data are shown as boxes in each p_T^{jet} bin. The MC distributions are normalized using the factors shown in parentheses to have the same total cross-sections as the data. Bottom panel: The ratio of cross-sections from different MC generators to the data.

analysis [5,44], and vary from 0.5% to 2.8% in central to peripheral collisions, respectively.

Uncertainty sources that are correlated between Pb+Pb and pp collisions, which include most of the jet- and photon-related uncertainties, typically cancel out to a large degree in R_{AA} . The most significant uncorrelated uncertainties are the centrality-dependent JES and unfolding ones.

For both the cross-section and R_{AA} measurements, the unfolding (photon purity) uncertainties are dominant at $p_T^{\text{jet}} < 80$ GeV for the 0–10% and 10–30% centrality intervals (30–80% centrality interval and in pp collisions). At $80 < p_T^{\text{jet}} < 200$ GeV, the JES, JER and photon purity uncertainties are dominant in all centrality bins and in pp collisions. The photon isolation uncertainties are dominant at $p_T^{\text{jet}} > 200$ GeV in all centrality bins and in pp collisions. In comparisons of the value of R_{AA} reported in this paper to that measured for inclusive jets [8], the uncertainties in the two measurements are treated as uncorrelated. For the S_{loss} analysis, these uncertainties are propagated as part of the S_{loss} determination procedure, described below in Section 8.1.

7. Results

Fig. 3 shows the measured cross-section for photon-tagged jet production in pp collisions, compared with the same quantity in the PYTHIA 8, HERWIG, and SHERPA event generators. The distributions of the generators are normalized to have the same total cross-sections as the data. The data is best described by HERWIG, which has a shape compatible with the data within its uncertain-

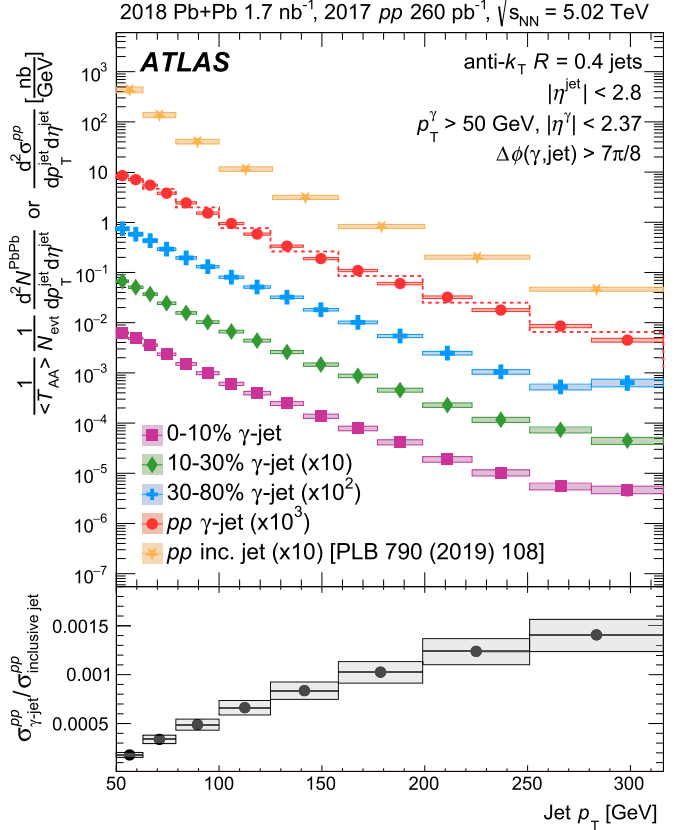


Fig. 4. Top panel: The yields of photon-tagged jets as a function of p_T^{jet} in Pb+Pb events for 0–10% (squares), 10–30% (diamonds) and 30–80% (crosses) centrality bins and the differential cross-section in pp events (circles). The spectra are scaled by the factors shown in the legend for clarity. The inclusive jet cross-section in pp collisions [8] (stars) is shown for comparison. The statistical uncertainties are small and hidden by the symbols. The total systematic uncertainties are shown as boxes in each p_T^{jet} bin. The photon-tagged jet pp data is also re-binned to match the binning of inclusive jet data (shown as dotted line). Bottom panel: The ratio of cross-sections between photon-tagged jets and inclusive jets in pp collisions. The boxes associated with the data points represent the sum in quadrature of the systematic uncertainties for photon-tagged jets and inclusive jets.

ties over the entire measured p_T^{jet} range. PYTHIA 8 and SHERPA are compatible with the data in the low p_T^{jet} region ($p_T^{\text{jet}} < 100$ GeV) but have a higher relative cross-section than the data at higher p_T^{jet} . The level of agreement between the MC generators and the data has a similar magnitude and p_T dependence as that observed in previous measurements in pp collisions at 7 TeV [64].

Fig. 4 shows the $\langle T_{AA} \rangle$ -scaled photon-tagged jet yields for different centrality bins in Pb+Pb collisions and the cross-section in pp collisions. The ratio of cross-sections for photon-tagged jets to that for inclusive jets in pp collisions is shown in the bottom panel. Both the pp inclusive jet and photon-tagged jet cross-sections are steeply falling as a function of p_T^{jet} , but the photon-tagged jet cross-section has a less steep spectrum, i.e., it decreases more slowly with p_T^{jet} . As described above, the R_{AA} depends on the convolution of the energy loss due to jet quenching with the slope of the p_T^{jet} spectrum and this must be taken into account when comparing results between inclusive and photon-tagged jets.

The R_{AA} values of photon-tagged jets are computed according to Eq. (1) above, and are shown in Fig. 5 as a function of p_T^{jet} in different centrality intervals. In 0–10% Pb+Pb collisions, the R_{AA} for photon-tagged jets is suppressed below unity, as expected from jet energy loss, and ranges between 0.60–0.75 depending on the jet p_T . Below 70 GeV, as the jet p_T decreases, the R_{AA} values systematically increase. As the R_{AA} depends not only on the energy loss

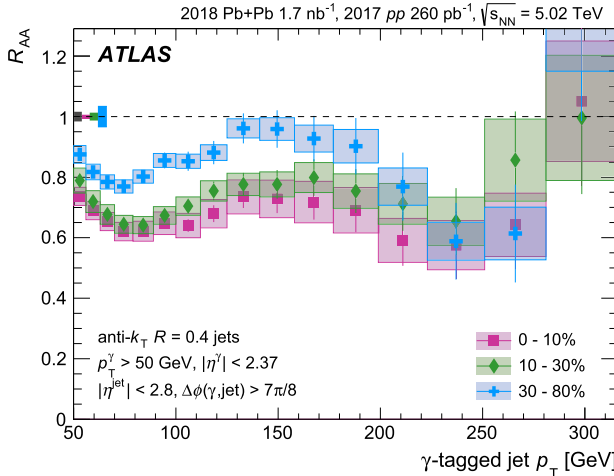


Fig. 5. The R_{AA} of photon-tagged jets as a function of p_T^{jet} for 0–10%, 10–30%, and 30–80% centrality intervals. The vertical bars associated with symbols indicate the statistical uncertainties. The total systematic uncertainties are shown as boxes in each p_T^{jet} bin. The shaded bars on the left of the axis at $R_{AA} = 1$ indicate the p_T -independent uncertainties associated with the luminosity in pp collisions and $\langle T_{AA} \rangle$ for 0–10%, 10–30%, and 30–80% Pb+Pb collisions, respectively. The highest p_T^{jet} data point in the 30–80% centrality interval is $1.42 \pm 0.43 \text{ (stat.)} \pm 0.25 \text{ (syst.)}$ and extends off the vertical scale.

but on the local shape of the initial spectrum, this increase may be related to the flattening of the spectrum near $p_T^{\text{jet}} = 50$ GeV, which is caused by the kinematic selection $p_T^{\gamma} > 50$ GeV. In the region $p_T^{\text{jet}} < 200$ GeV, the R_{AA} is found to be larger in the 30–80% Pb+Pb collisions than in the 0–10% Pb+Pb collisions, indicating more suppression in central Pb+Pb collisions as expected due to a larger jet quenching effect in collisions with a larger volume and higher temperature QGP.

8. Discussion

Fig. 6 compares the photon-tagged jet R_{AA} results to the previously published ATLAS inclusive jet results [8]. The R_{AA} of photon-tagged jets is significantly higher than the corresponding values for inclusive jets for $p_T^{\text{jet}} < 200$ GeV. For $p_T^{\text{jet}} > 200$ GeV, the statistical and systematic uncertainties in the photon-tagged jet results are larger and the two sets of R_{AA} values become compatible.

A primary goal of this measurement is to isolate the effect of colour charge on jet quenching. Indeed, in the range of p_T^{jet} where the quark-initiated fraction is significantly higher in photon-tagged jets (see Fig. 1), the R_{AA} is significantly higher than that for inclusive jets. However, the R_{AA} is known to depend on the shape of the initial production spectrum with, e.g., a steeper spectrum resulting in a lower R_{AA} for the same magnitude of energy loss. Indeed, Fig. 4 shows that although the jet p_T spectra for photon-tagged and inclusive jets are both steeply falling, the latter is systematically steeper than the former. Thus, it is important for theoretical calculations attempting to describe the R_{AA} results to first correctly describe the photon-tagged and inclusive jet cross-sections in pp collisions, i.e., before applying any jet quenching.

8.1. Fractional energy loss analysis

An alternative way to characterize the energy loss with a greatly reduced sensitivity to the spectral shape is through the fractional energy loss quantity, S_{loss} , introduced in Section 1.

To determine S_{loss} for the photon-tagged jet case, the distributions in pp and Pb+Pb collisions are fit using the ‘extended power law’ function introduced in Ref. [14], $f(p_T) =$

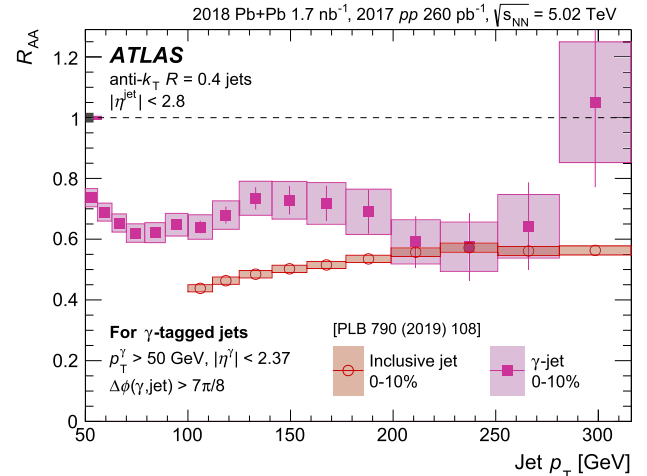


Fig. 6. The R_{AA} of photon-tagged jets (filled squares) as a function of p_T^{jet} for 0–10% Pb+Pb events are overlaid with that of inclusive jets [8] (open circles) in the same centrality range for comparison. The vertical bars associated with symbols indicate the statistical uncertainties. The total systematic uncertainties are shown as boxes in each p_T^{jet} bin. The shaded bars on the left of the axis at $R_{AA} = 1$ indicate the p_T -independent uncertainties associated with the luminosity in pp collisions and $\langle T_{AA} \rangle$ for 0–10% Pb+Pb collisions, respectively.

$A(p_{T,0}/p_T)^{n+\beta \log(p_T/p_{T,0})}$, in the region $p_T > 100$ GeV. An initial estimate of Δp_T in Eq. (2) is performed by first assuming that the Jacobian term in Eq. (3), $(1 + d\Delta p_T/dp_T^{pp})$, is unity, i.e. $d\Delta p_T/dp_T^{pp} = 0$, and determining $\Delta p_T(p_T^{pp})$ from the fitted functions. This estimate is then iteratively improved by applying the Jacobian factor to the pp spectrum and repeating the procedure to obtain an updated estimate of Δp_T . To determine the systematic uncertainty in Δp_T , and thus S_{loss} , the procedure is performed separately under each of the systematic variations detailed in Section 6, with the variations from sources that are correlated between pp and Pb+Pb applied to both distributions simultaneously. An additional uncertainty is assigned to account for the sensitivity of the extracted S_{loss} values to the choice of fit range, which is sub-dominant to the other sources described in Section 6.

To determine S_{loss} for the inclusive jet case, this procedure is repeated with two modifications. First, to provide a better description of the data, the fit function for the inclusive jet distributions includes an additional term in the exponent that is linear in p_T . Second, an alternative procedure is used to account for the correlated uncertainties between the pp and Pb+Pb distributions. The $\langle T_{AA} \rangle$ -scaled Pb+Pb yields are re-calculated by taking the R_{AA} values (including their uncertainties, which account for the correlation between pp and Pb+Pb) and multiplying them by the central values of the pp cross-section. Then, the uncertainties in Δp_T , and thus in S_{loss} , are calculated by propagating the uncertainty in the determined value of $p_T^{\text{Pb+Pb}}$ using Eq. (2).

The extracted Δp_T and S_{loss} values are shown in Fig. 7 for photon-tagged jets and inclusive jets for the 0–10% centrality interval. For photon-tagged jets, Δp_T ranges from 10–30 GeV, and S_{loss} from 0.07–0.10. For both samples, Δp_T increases with jet p_T . In the inclusive jet case, this increase is slower than the jet p_T , resulting in S_{loss} values that instead decrease systematically with increasing p_T . For the photon-tagged jet case, the S_{loss} values are approximately constant within uncertainties over this p_T^{jet} range. In the region $100 < p_T^{\text{jet}} \lesssim 200$ GeV, the S_{loss} values for photon-tagged jets are significantly smaller than those for inclusive jets, again suggesting a significant colour-charge dependence to jet energy loss. At higher p_T^{jet} , the two S_{loss} curves are compatible within uncertainties, potentially due to the quark fractions of the two samples becoming more similar in this p_T region (Fig. 1).

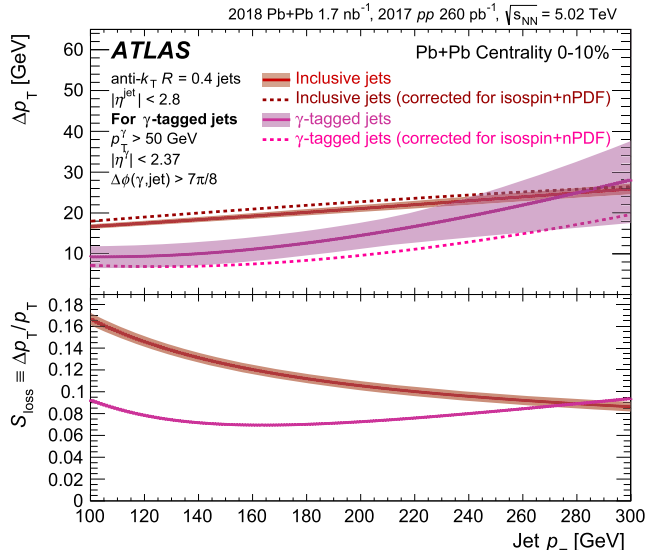


Fig. 7. Top panel: The energy loss Δp_T as a function of p_T^{jet} for photon-tagged jets (lower bands) and inclusive jets (upper bands) for the 0–10% centrality interval. The bands around the solid lines indicate the systematic uncertainties. The dashed lines show the updated estimate of Δp_T when the data are corrected for isospin and nPDF effects (see text). Bottom panel: The fractional energy loss S_{loss} .

Importantly, $S_{\text{loss}}(p_T)$ should not be interpreted as the fraction of the energy lost in the QGP for jets that emerge with the given p_T in Pb+Pb collisions. As detailed in Refs. [37,38], this extracted value is smaller than the true average energy loss. This is due to the steeply falling p_T spectrum and jet-to-jet fluctuations in the energy loss, which result in the fact that jets observed in Pb+Pb at a given p_T are more likely to be those with smaller than average energy loss. Nevertheless, the procedure above is clearly defined and is a useful way to quantify the difference in the magnitude of energy loss between different scenarios.

Even though the determination of S_{loss} is not strongly sensitive to the initial p_T^{jet} shape in pp collisions, there are other effects that modify the jet spectra in Pb+Pb collisions compared to those in pp collisions, which do not arise from energy loss but may impact the extracted S_{loss} values. These include effects originating from isospin (i.e., the different up- and down-quark composition of the nucleus compared to the proton, which decreases the rate of processes such as photon+jet production, as previously observed in p +Pb collisions [77]) and the modification of the PDFs in nuclei compared to those in free nucleons.

The possible quantitative impact of these effects can be explored using the generator-level simulation samples described at the end of Section 4. To determine the impact of the isospin and nPDF effects, the simulated cross-section in Pb+Pb events or in nPDF-weighted pp events, respectively, was compared with that in the original sample of pp events. The ratios of these modified cross-sections to the cross-section in pp collisions are shown in Fig. 8 separately for photon-tagged and inclusive jets. While the isospin effect for inclusive jets is negligible, it causes the photon-tagged jet spectrum (and thus R_{AA}) in Pb+Pb collisions to decrease by 10–20% in the p_T^{jet} range of 100–300 GeV. The isospin effect is stronger at larger p_T^{jet} as the parton in the nucleus involved in the parton-parton scattering is more likely to come from a valence (up/down) quark at large Bjorken- x range. The nPDF effects on the photon-tagged and inclusive jet R_{AA} are similar, leading to approximately a 5% enhancement at 100 GeV (an increase in the nuclear parton densities in the ‘anti-shadowing’ region) that then decreases with increasing p_T . Given the similar nPDF effects, it can be seen that the isospin effect for photon-tagged jets has the domi-

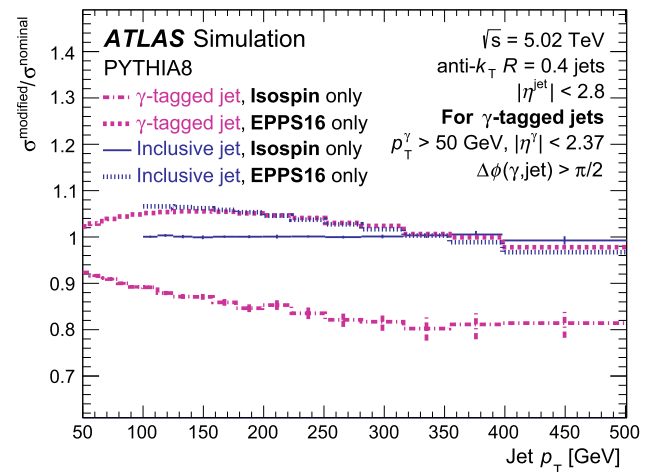


Fig. 8. PYTHIA 8-based evaluation of the impact of the isospin and nPDF effects for the two jet samples, shown as the ratio of the modified cross-section to the nominal one in pp collisions. The isospin (nPDF) effect for inclusive jets is shown as a solid (dotted) line, and for photon-tagged jets as dot-dashed (dashed) line.

nant impact in the comparisons. It decreases the photon-tagged jet yield in Pb+Pb events, thus causing an overestimate of the energy loss effects under the naive interpretation of S_{loss} and R_{AA} .

To test the potential impact of these effects on the S_{loss} results, the energy loss study is repeated after dividing the measured R_{AA} values by the simulation-derived values in Fig. 8 to approximately correct for these effects. The updated S_{loss} values are shown as dashed lines in Fig. 7. It can be seen that the differences in energy loss between photon-tagged jets and inclusive jets become even larger after accounting for the isospin and nPDF effects, further strengthening the evidence that quark-initiated jets lose less energy than gluon-initiated ones.

8.2. Theoretical comparisons

The R_{AA} results are compared with theoretical calculations of jet energy loss in the QGP that model the colour-charge dependence of the parton-QGP interaction in various ways. As discussed above, it is important for such calculations to properly model details such as the photon production processes (i.e., including fragmentation photons), the spectral shape, and the impact of the isospin and nPDF for a consistent comparison with the data. The five calculations described below typically meet most but not necessarily all these criteria.

The calculation from Takacs *et al.* [15,16] includes a resummation of energy loss effects from hard, vacuum-like emissions occurring in the medium and the modelling of soft energy flow and recovery at the jet cone. The Takacs *et al.* calculations are presented with a range of the jet-medium coupling parameter $g_{\text{med}} = 2.2\text{--}2.3$. The predictions in Refs. [17,18] are based on a linearised Boltzmann equation with diffusion model (LIDO). The LIDO calculations are presented with a range of values for the parameter $\mu = 1.3\pi T\text{--}1.8\pi T$, where T is the medium temperature and μ controls the strength of the parton coupling to the medium. The predictions labelled SCET_G are perturbative calculations performed within the framework of soft-collinear effective field theory with Glauber gluons in the soft-gluon-emission (energy-loss) limit [20–22], with the width of the band in the Figures corresponding to the range of jet-medium coupling $g = 2.0 \pm 0.2$. The linear Boltzmann transport (LBT) model predictions [23] include elastic and inelastic processes based on perturbative QCD for both jet shower and recoil medium partons as they propagate through a QGP. JEWEL [78] is a MC event generator that simulates QCD jet evolution in heavy-ion collisions, including radiative and elas-

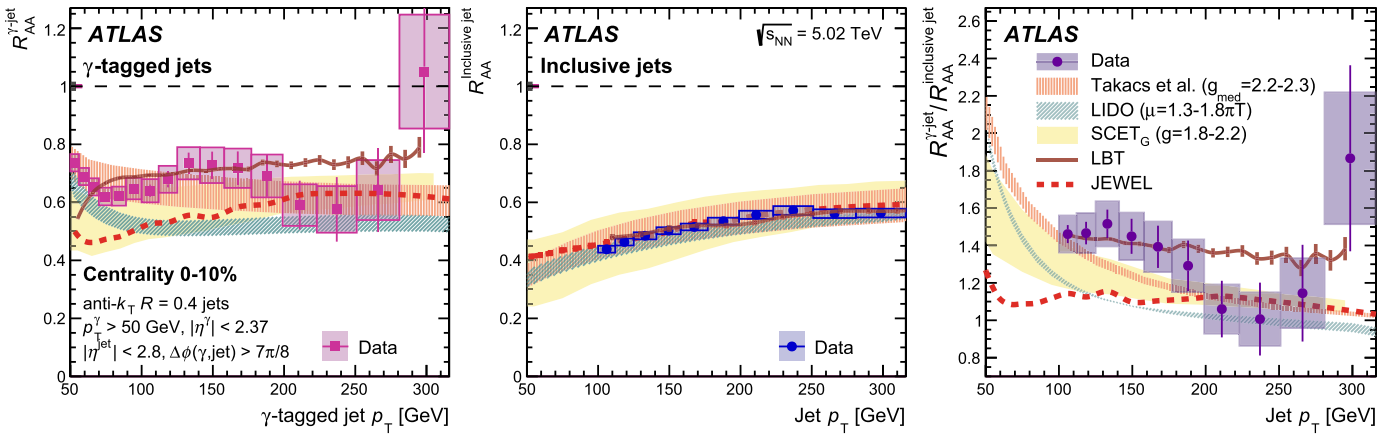


Fig. 9. Comparison of R_{AA} between data and various theoretical predictions for (left panel) photon-tagged jets and (middle panel) inclusive jets. The right panel shows $R_{AA}^{\gamma\text{-jet}} / R_{AA}^{\text{inclusive jet}}$ compared between data and theory predictions. The vertical bars associated with symbols of the photon-tagged jet data indicate the statistical uncertainties and the total systematic uncertainties are shown as boxes in each p_T^{jet} bin. For inclusive jets, the boxes around the points indicate combined statistical and systematic uncertainties, although they are dominated by the latter. The bands of the theoretical calculations represent ranges of model parameters (see text). The vertical bars associated with the LBT calculation indicate the statistical uncertainties. The shaded bars on the left of the axis at $R_{AA} = 1$ indicate the p_T -independent uncertainties associated with the luminosity in pp collisions and $\langle T_{AA} \rangle$ for 0–10% Pb+Pb collisions, respectively.

tic energy loss processes, and was configured without including medium recoils in the jet reconstruction, but with accounting for the isospin effect.

The left and middle panels of Fig. 9 show the R_{AA} of photon-tagged jets and inclusive jets, respectively, in 0–10% central Pb+Pb collisions compared with the theoretical predictions. The ratio $R_{AA}^{\gamma\text{-jet}} / R_{AA}^{\text{inclusive jet}}$ is shown in the right panel, which in the theoretical predictions leads to the cancellation of some uncertainties common to both R_{AA} calculations. The inclusive jet R_{AA} , a commonly used benchmark to fix free parameters in theoretical models, is well described by all of the calculations. All the calculations except JEWEL qualitatively predict that the photon-tagged jet R_{AA} should be closer to unity than the inclusive jet R_{AA} , but the specific magnitude as a function of p_T^{jet} varies. The photon-tagged jet R_{AA} data points are generally larger than the central values of many of the calculations, but they are compatible with the LBT model and with the calculations by Takacs *et al.* and SCET_G within the range of their respective model parameters. Notably, several of the models predict the increase of the photon-tagged jet R_{AA} with decreasing p_T^{jet} observed in data at $p_T^{\text{jet}} \lesssim 80 \text{ GeV}$. The models further predict that the $R_{AA}^{\gamma\text{-jet}} / R_{AA}^{\text{inclusive jet}}$ ratio systematically decreases with increasing p_T^{jet} , as the quark-initiated fraction in the two samples become more similar, which is also qualitatively present in the data. However, the agreement with the models is worse, with only the LBT model describing the measured double ratio. Since these models otherwise described the inclusive jet R_{AA} well, this additional comparison highlights the need to test them against multiple observables simultaneously to evaluate the description of the colour-charge dependence of energy loss.

9. Conclusion

This Letter presents a measurement of photon-tagged jet production in 1.7 nb^{-1} of Pb+Pb and 260 pb^{-1} of pp collisions at $\sqrt{s_{NN}} = 5.02 \text{ TeV}$ with the ATLAS detector. The cross-section of jets produced opposite in azimuth ($\Delta\phi > 7\pi/8$) to a $p_T^\gamma > 50 \text{ GeV}$ isolated photon is reported as a function of p_T^{jet} . This selection results in a sample of jets with a steeply falling p_T distribution and a large fraction of quark-initiated jets. The nuclear modification factor, R_{AA} , for photon-tagged jets is found to be suppressed below unity in a way that varies with centrality but only weakly with p_T^{jet} in the measured range. The fractional energy loss, S_{loss} , is de-

termined to be approximately 0.10 with no strong p_T dependence within uncertainties in the 0–10% centrality interval. The photon-tagged jet R_{AA} (S_{loss}) is significantly higher (lower) than that for inclusive jets at the same p_T^{jet} and centrality, which instead have a large gluon-initiated jet fraction. The results are compared with a variety of theoretical calculations, which qualitatively describe aspects of the ordering between photon-tagged and inclusive jets, but tend to over-predict the amount of energy loss for the former. The data provide the strongest confirmation to date of larger jet quenching for gluon jets compared with quark jets.

Declaration of competing interest

The authors declare that they have no known competing financial interests or personal relationships that could have appeared to influence the work reported in this paper.

Data availability

The data for this manuscript are not available. The values in the plots and tables associated to this article are stored in HEPDATA (<https://hepdata.cedar.ac.uk>).

Acknowledgements

We thank CERN for the very successful operation of the LHC, as well as the support staff from our institutions without whom ATLAS could not be operated efficiently.

We acknowledge the support of ANPCyT, Argentina; YerPhI, Armenia; ARC, Australia; BMWFW and FWF, Austria; ANAS, Azerbaijan; CNPq and FAPESP, Brazil; NSERC, NRC and CFI, Canada; CERN; ANID, Chile; CAS, MOST and NSFC, China; Minciencias, Colombia; MEYS CR, Czech Republic; DNRF and DNSRC, Denmark; IN2P3-CNRS and CEA-DRF/IRFU, France; SRNSFG, Georgia; BMBF, HGF and MPG, Germany; GSRI, Greece; RGC and Hong Kong SAR, China; ISF and Benoziyo Center, Israel; INFN, Italy; MEXT and JSPS, Japan; CNRST, Morocco; NWO, Netherlands; RCN, Norway; MEIN, Poland; FCT, Portugal; MNE/IFA, Romania; MESTD, Serbia; MSSR, Slovakia; ARRS and MIZŠ, Slovenia; DS/ NRF, South Africa; MICINN, Spain; SRC and Wallenberg Foundation, Sweden; SERI, SNSF and Canton of Bern and Geneva, Switzerland; MOST, Taiwan; TENMAK, Türkiye; STFC, United Kingdom; DOE and NSF, United States of America. In addition, individual groups and members have received support from BCKDF, CANARIE, Compute Canada and CRC,

Canada; PRIMUS 21/SCI/017 and UNCE SCI/013, Czech Republic; COST, ERC, ERDF, Horizon 2020 and Marie Skłodowska-Curie Actions, European Union; Investissements d’Avenir Labex, Investissements d’Avenir Idex and ANR, France; DFG and AvH Foundation, Germany; Herakleitos, Thales and Aristeia programmes co-financed by EU-ESF and the Greek NSRF, Greece; BSF-NSF and MINERVA, Israel; Norwegian Financial Mechanism 2014–2021, Norway; NCN and NAWA, Poland; La Caixa Banking Foundation, CERCA Programme Generalitat de Catalunya and PROMETEO and GenT Programmes Generalitat Valenciana, Spain; Göran Gustafssons Stiftelse, Sweden; The Royal Society and Leverhulme Trust, United Kingdom.

The crucial computing support from all WLCG partners is acknowledged gratefully, in particular from CERN, the ATLAS Tier-1 facilities at TRIUMF (Canada), NDGF (Denmark, Norway, Sweden), CC-IN2P3 (France), KIT/GridKA (Germany), INFN-CNAF (Italy), NL-T1 (Netherlands), PIC (Spain), ASGC (Taiwan), RAL (UK) and BNL (USA), the Tier-2 facilities worldwide and large non-WLCG resource providers. Major contributors of computing resources are listed in Ref. [79].

References

- [1] P. Romatschke, U. Romatschke, Relativistic Fluid Dynamics in and Out of Equilibrium, Cambridge Monographs on Mathematical Physics, vol. isbn, Cambridge University Press, 2019, 978-1-108-48368-1, 978-1-108-75002-8 arXiv: 1712.05815 [nucl-th].
- [2] U. Heinz, R. Snellings, Collective flow and viscosity in relativistic heavy-ion collisions, Annu. Rev. Nucl. Part. Sci. 63 (2013) 123, arXiv:1301.2826 [nucl-th].
- [3] H. Elfner, B. Müller, The exploration of hot and dense nuclear matter: introduction to relativistic heavy-ion physics, arXiv:2210.12056 [nucl-th], 2022.
- [4] L. Cunqueiro, A.M. Sickles, Studying the QGP with jets at the LHC and RHIC, Prog. Part. Nucl. Phys. 124 (2022) 103940, arXiv:2110.14490 [nucl-ex].
- [5] M.L. Miller, K. Reiglers, S.J. Sanders, P. Steinberg, Glauber modeling in high energy nuclear collisions, Annu. Rev. Nucl. Part. Sci. 57 (2007) 205, arXiv: nucl-ex/0701025.
- [6] CMS Collaboration, Measurement of transverse momentum relative to dijet systems in PbPb and pp collisions at $\sqrt{s_{NN}} = 2.76 \text{ TeV}$, J. High Energy Phys. 01 (2016) 006, arXiv:1509.09029 [hep-ex].
- [7] ATLAS Collaboration, Measurement of angular and momentum distributions of charged particles within and around jets in Pb+Pb and pp collisions at $\sqrt{s_{NN}} = 5.02 \text{ TeV}$ with the ATLAS detector, Phys. Rev. C 100 (2019) 064901, arXiv:1908.05264 [hep-ex], Erratum: Phys. Rev. C 101 (2019) 059903.
- [8] ATLAS Collaboration, Measurement of the nuclear modification factor for inclusive jets in Pb+Pb collisions at $\sqrt{s_{NN}} = 5.02 \text{ TeV}$ with the ATLAS detector, Phys. Lett. B 790 (2019) 108, arXiv:1805.05635 [hep-ex].
- [9] CMS Collaboration, First measurement of large area jet transverse momentum spectra in heavy-ion collisions, J. High Energy Phys. 05 (2021) 284, arXiv:2102.13080 [hep-ex].
- [10] ALICE Collaboration, Measurements of inclusive jet spectra in pp and central Pb-Pb collisions at $\sqrt{s_{NN}} = 5.02 \text{ TeV}$, Phys. Rev. C 101 (2020) 034911, arXiv: 1909.09718 [nucl-ex].
- [11] K. Kovářík, et al., nCTEQ15 - Global analysis of nuclear parton distributions with uncertainties in the CTEQ framework, Phys. Rev. D 93 (2016) 085037, arXiv:1509.00792 [hep-ph].
- [12] K.J. Eskola, P. Paakkinen, H. Paukkunen, C.A. Salgado, EPPS21: a global QCD analysis of nuclear PDFs, Eur. Phys. J. C 82 (2022) 413, arXiv:2112.12462 [hep-ph].
- [13] R. Abdul Khalek, et al., nNNPDF3.0: evidence for a modified partonic structure in heavy nuclei, Eur. Phys. J. C 82 (2022) 507, arXiv:2201.12363 [hep-ph].
- [14] M. Spousta, B. Cole, Interpreting single jet measurements in Pb + Pb collisions at the LHC, Eur. Phys. J. C 76 (2016) 50, arXiv:1504.05169 [hep-ph].
- [15] Y. Mehtar-Tani, D. Pablos, K. Tywoniuk, Cone-size dependence of jet suppression in heavy-ion collisions, Phys. Rev. Lett. 127 (2021) 252301, arXiv: 2101.01742 [hep-ph].
- [16] A. Takacs, K. Tywoniuk, Quenching effects in the cumulative jet spectrum, J. High Energy Phys. 10 (2021) 038, arXiv:2103.14676 [hep-ph].
- [17] W. Ke, Y. Xu, S.A. Bass, Modified Boltzmann approach for modeling the splitting vertices induced by the hot QCD medium in the deep Landau-Pomeranchuk-Migdal region, Phys. Rev. C 100 (2019) 064911, arXiv:1810.08177 [nucl-th].
- [18] W. Ke, Y. Xu, S.A. Bass, Linearized Boltzmann-Langevin model for heavy quark transport in hot and dense QCD matter, Phys. Rev. C 98 (2018) 064901, arXiv: 1806.08848 [nucl-th].
- [19] W. Ke, X.-N. Wang, QGP modification to single inclusive jets in a calibrated transport model, J. High Energy Phys. 05 (2021) 041, arXiv:2010.13680 [hep-ph].
- [20] Z.-B. Kang, I. Vitev, H. Xing, Vector-boson-tagged jet production in heavy ion collisions at energies available at the CERN large hadron collider, Phys. Rev. C 96 (2017) 014912, arXiv:1702.07276 [hep-ph].
- [21] H.T. Li, I. Vitev, Inclusive heavy flavor jet production with semi-inclusive jet functions: from proton to heavy-ion collisions, J. High Energy Phys. 07 (2019) 148, arXiv:1811.07905 [hep-ph].
- [22] H.T. Li, I. Vitev, Jet charge modification in dense QCD matter, Phys. Rev. D 101 (2020) 076020, arXiv:1908.06979 [hep-ph].
- [23] Y. He, et al., Interplaying mechanisms behind single inclusive jet suppression in heavy-ion collisions, Phys. Rev. C 99 (2019) 054911, arXiv:1809.02525 [nucl-th].
- [24] J. Brewer, J. Thaler, A.P. Turner, Data-driven quark and gluon jet modification in heavy-ion collisions, Phys. Rev. C 103 (2021) L021901, arXiv:2008.08596 [hep-ph].
- [25] J. Brewer, Q. Brodsky, K. Rajagopal, Disentangling jet modification in jet simulations and in Z -jet data, J. High Energy Phys. 02 (2022) 175, arXiv:2110.13159 [hep-ph].
- [26] ATLAS Collaboration, Measurement of the nuclear modification factor of b -jets in 5.02 TeV Pb+Pb collisions with the ATLAS detector, Eur. Phys. J. C 83 (2022) 438, arXiv:2204.13530 [nucl-ex].
- [27] CMS Collaboration, Evidence of b -jet quenching in PbPb collisions at $\sqrt{s_{NN}} = 2.76 \text{ TeV}$, Phys. Rev. Lett. 113 (2014) 132301, arXiv:1312.4198 [hep-ex].
- [28] ATLAS Collaboration, Centrality, rapidity and transverse momentum dependence of isolated prompt photon production in lead-lead collisions at $\sqrt{s_{NN}} = 2.76 \text{ TeV}$ measured with the ATLAS detector, Phys. Rev. C 93 (2016) 034914, arXiv:1506.08552 [hep-ex].
- [29] CMS Collaboration, The production of isolated photons in PbPb and pp collisions at $\sqrt{s_{NN}} = 5.02 \text{ TeV}$, J. High Energy Phys. 07 (2020) 116, arXiv:2003.12797 [hep-ex].
- [30] ATLAS Collaboration, Measurement of W^\pm boson production in Pb+Pb collisions at $\sqrt{s_{NN}} = 5.02 \text{ TeV}$ with the ATLAS detector, Eur. Phys. J. C 79 (2019) 935, arXiv:1907.10414 [hep-ex].
- [31] CMS Collaboration, Using Z boson events to study parton–medium interactions in PbPb collisions, Phys. Rev. Lett. 128 (2021) 122301, arXiv:2103.04377 [hep-ex].
- [32] X.-N. Wang, Z. Huang, I. Sarcevic, Jet quenching in the opposite direction of a tagged photon in high-energy heavy ion collisions, Phys. Rev. Lett. 77 (1996) 231, arXiv:hep-ph/9605213.
- [33] ATLAS Collaboration, Measurement of photon-jet transverse momentum correlations in 5.02 TeV Pb+Pb and pp collisions with ATLAS, Phys. Lett. B 789 (2019) 167, arXiv:1809.07280 [hep-ex].
- [34] ATLAS Collaboration, Medium-induced modification of Z -tagged charged particle yields in Pb+Pb collisions at 5.02 TeV with the ATLAS detector, Phys. Rev. Lett. 126 (2021) 072301, arXiv:2008.09811 [hep-ex].
- [35] ATLAS Collaboration, Comparison of fragmentation functions for jets dominated by light quarks and gluons from pp and Pb+Pb collisions in ATLAS, Phys. Rev. Lett. 123 (2019) 042001, arXiv:1902.10007 [hep-ex].
- [36] PHENIX Collaboration, Formation of dense partonic matter in relativistic nucleus-nucleus collisions at RHIC: experimental evaluation by the PHENIX collaboration, Nucl. Phys. A 757 (2005) 184, arXiv:nucl-ex/0410003.
- [37] PHENIX Collaboration, Detailed study of high- p_T neutral pion suppression and azimuthal anisotropy in Au+Au Collisions at $\sqrt{s_{NN}} = 200 \text{ GeV}$, Phys. Rev. C 76 (2007) 034904, arXiv:nucl-ex/0611007.
- [38] PHENIX Collaboration, Scaling properties of fractional momentum loss of high- p_T hadrons in nucleus-nucleus collisions at $\sqrt{s_{NN}}$ from 62.4 GeV to 2.76 TeV , Phys. Rev. C 93 (2016) 024911, arXiv:1509.06735 [nucl-ex].
- [39] J. Brewer, J.G. Milhano, J. Thaler, Sorting out quenched jets, Phys. Rev. Lett. 122 (2019) 222301, arXiv:1812.05111 [hep-ph].
- [40] ATLAS Collaboration, The ATLAS experiment at the CERN large hadron collider, J. Instrum. 3 (2008) S08003.
- [41] ATLAS Collaboration, Performance of the ATLAS trigger system in 2015, Eur. Phys. J. C 77 (2017) 317, arXiv:1611.09661 [hep-ex].
- [42] ATLAS Collaboration, The ATLAS collaboration software and firmware, ATL-SOFT-PUB-2021-001, <https://cds.cern.ch/record/2767187>, 2021.
- [43] ATLAS Collaboration, Performance of electron and photon triggers in ATLAS during LHC run 2, Eur. Phys. J. C 80 (2020) 47, arXiv:1909.00761 [hep-ex].
- [44] ATLAS Collaboration, Prompt and non-prompt J/ψ and $\psi(2S)$ suppression at high transverse momentum in 5.02 TeV Pb+Pb collisions with the ATLAS experiment, Eur. Phys. J. C 78 (2018) 762, arXiv:1805.04077 [hep-ex].
- [45] ATLAS Collaboration, Electron and photon performance measurements with the ATLAS detector using the 2015–2017 LHC proton-proton collision data, J. Instrum. 14 (2019) P12006, arXiv:1908.00005 [hep-ex].
- [46] ATLAS Collaboration, Measurement of the jet radius and transverse momentum dependence of inclusive jet suppression in lead-lead collisions at $\sqrt{s_{NN}} = 2.76 \text{ TeV}$ with the ATLAS detector, Phys. Lett. B 719 (2013) 220, arXiv:1208.1967 [hep-ex].
- [47] ATLAS Collaboration, Measurement of the photon identification efficiencies with the ATLAS detector using LHC run 2 data collected in 2015 and 2016, Eur. Phys. J. C 79 (2019) 205, arXiv:1810.05087 [hep-ex].
- [48] M. Cacciari, G.P. Salam, G. Soyez, The anti- k_t jet clustering algorithm, J. High Energy Phys. 04 (2008) 063, arXiv:0802.1189 [hep-ph].

- [49] M. Cacciari, G.P. Salam, G. Soyez, Fastjet user manual, Eur. Phys. J. C 72 (2012) 1896, arXiv:1111.6097 [hep-ph].
- [50] ATLAS Collaboration, Jet energy measurement and its systematic uncertainty in proton–proton collisions at $\sqrt{s} = 7\text{ TeV}$ with the ATLAS detector, Eur. Phys. J. C 75 (2015) 17, arXiv:1406.0076 [hep-ex].
- [51] ATLAS Collaboration, Jet energy scale measurements and their systematic uncertainties in proton–proton collisions at $\sqrt{s} = 13\text{ TeV}$ with the ATLAS detector, Phys. Rev. D 96 (2017) 072002, arXiv:1703.09665 [hep-ex].
- [52] ATLAS Collaboration, Jet energy scale and its uncertainty for jets reconstructed using the ATLAS heavy ion jet algorithm, ATLAS-CONF-2015-016, <https://cds.cern.ch/record/2008677>, 2015.
- [53] T. Sjostrand, S. Mrenna, P.Z. Skands, A brief introduction to PYTHIA 8.1, Comput. Phys. Commun. 178 (2008) 852, arXiv:0710.3820 [hep-ph].
- [54] ATLAS Collaboration, ATLAS Pythia 8 tunes to 7 TeV data, ATL-PHYS-PUB-2014-021, <https://cds.cern.ch/record/1966419>, 2014.
- [55] R.D. Ball, et al., Parton distributions with LHC data, Nucl. Phys. B 867 (2013) 244, arXiv:1207.1303 [hep-ph].
- [56] E. Bothmann, et al., Event generation with Sherpa 2.2, SciPost Phys. 7 (2019) 034, arXiv:1905.09127 [hep-ph].
- [57] F. Siegert, A practical guide to event generation for prompt photon production with Sherpa, J. Phys. G 44 (2017) 044007, arXiv:1611.07226 [hep-ph].
- [58] R.D. Ball, et al., Parton distributions for the LHC Run II, J. High Energy Phys. 04 (2015) 040, arXiv:1410.8849 [hep-ph].
- [59] J. Bellm, et al., Herwig 7.0/Herwig++ 3.0 release note, Eur. Phys. J. C 76 (2016) 196, arXiv:1512.01178 [hep-ph].
- [60] L. Harland-Lang, A. Martin, P. Motylinski, R. Thorne, Parton distributions in the LHC era: MMHT 2014 PDFs, Eur. Phys. J. C 75 (2015) 204, arXiv:1412.3989 [hep-ph].
- [61] S. Agostinelli, et al., GEANT4—a simulation toolkit, Nucl. Instrum. Methods A 506 (2003) 250.
- [62] ATLAS Collaboration, Light-quark and gluon jet discrimination in pp collisions at $\sqrt{s} = 7\text{ TeV}$ with the ATLAS detector, Eur. Phys. J. C 74 (2014) 3023, arXiv:1405.6583 [hep-ex].
- [63] K.J. Eskola, P. Paakkinen, H. Paukkunen, C.A. Salgado, EPPS16: nuclear parton distributions with LHC data, Eur. Phys. J. C 77 (2017) 163, arXiv:1612.05741 [hep-ph].
- [64] ATLAS Collaboration, Dynamics of isolated-photon plus jet production in pp collisions at $\sqrt{s} = 7\text{ TeV}$ with the ATLAS detector, Nucl. Phys. B 875 (2013) 483, arXiv:1307.6795 [hep-ex].
- [65] ATLAS Collaboration, Measurement of the inclusive isolated prompt photon cross section in pp collisions at $\sqrt{s} = 8\text{ TeV}$ with the ATLAS detector, J. High Energy Phys. 08 (2016) 005, arXiv:1605.03495 [hep-ex].
- [66] ATLAS Collaboration, Measurement of the cross section for inclusive isolated-photon production in pp collisions at $\sqrt{s} = 13\text{ TeV}$ using the ATLAS detector, Phys. Lett. B 770 (2017) 473, arXiv:1701.06882 [hep-ex].
- [67] ATLAS Collaboration, Measurement of the inclusive isolated prompt photons cross section in pp collisions at $\sqrt{s} = 7\text{ TeV}$ with the ATLAS detector using 4.6 fb^{-1} , Phys. Rev. D 89 (2014) 052004, arXiv:1311.1440 [hep-ex].
- [68] ATLAS Collaboration, High- E_T isolated-photon plus jets production in pp collisions at $\sqrt{s} = 8\text{ TeV}$ with the ATLAS detector, Nucl. Phys. B 918 (2017) 257, arXiv:1611.06586 [hep-ex].
- [69] G. D’Agostini, A multidimensional unfolding method based on Bayes’ theorem, Nucl. Instrum. Methods 362 (1995) 487.
- [70] T. Adye, Unfolding Algorithms and Tests Using RooUnfold, Proceedings, PHYS-TAT 2011 Workshop on Statistical Issues Related to Discovery Claims in Search Experiments and Unfolding, CERN, Geneva, Switzerland, 17–20 January 2011 (2011), p. 313, arXiv:1105.1160 [physics.data-an].
- [71] ATLAS Collaboration, Electron and photon energy calibration with the ATLAS detector using 2015–2016 LHC proton–proton collision data, J. Instrum. 14 (2019) P03017, arXiv:1812.03848 [hep-ex].
- [72] ATLAS Collaboration, Measurements of azimuthal anisotropies of jet production in $Pb+Pb$ collisions at $\sqrt{s_{NN}} = 5.02\text{ TeV}$ with the ATLAS detector, Phys. Rev. C 105 (2021) 064903, arXiv:2111.06606 [nucl-ex].
- [73] ATLAS Collaboration, Jet energy measurement with the ATLAS detector in proton–proton collisions at $\sqrt{s} = 7\text{ TeV}$, Eur. Phys. J. C 73 (2013) 2304, arXiv:1112.6426 [hep-ex].
- [74] ATLAS Collaboration, Jet energy resolution in proton–proton collisions at $\sqrt{s} = 7\text{ TeV}$ recorded in 2010 with the ATLAS detector, Eur. Phys. J. C 73 (2013) 2306, arXiv:1210.6210 [hep-ex].
- [75] ATLAS Collaboration, Determination of jet calibration and energy resolution in proton–proton collisions at $\sqrt{s} = 8\text{ TeV}$ using the ATLAS detector, Eur. Phys. J. C 80 (2020) 1104, arXiv:1910.04482 [hep-ex].
- [76] ATLAS Collaboration, Luminosity determination in pp collisions at $\sqrt{s} = 13\text{ TeV}$ using the ATLAS detector at the LHC, arXiv:2212.09379 [hep-ex], 2022.
- [77] ATLAS Collaboration, Measurement of prompt photon production in $\sqrt{s_{NN}} = 8.16\text{ TeV}$ $p + Pb$ collisions with ATLAS, Phys. Lett. B 796 (2019) 230, arXiv:1903.02209 [hep-ex].
- [78] R. Kuninawalkam Elayavalli, K.C. Zapp, Simulating V+jet processes in heavy ion collisions with JEWEL, Eur. Phys. J. C 76 (2016) 695, arXiv:1608.03099 [hep-ph].
- [79] ATLAS Collaboration, ATLAS computing acknowledgements, ATL-SOFT-PUB-2021-003, <https://cds.cern.ch/record/2776662>, 2021.

The ATLAS Collaboration

G. Aad ^{102, ID}, B. Abbott ^{120, ID}, K. Abeling ^{55, ID}, N.J. Abicht ^{49, ID}, S.H. Abidi ^{29, ID}, A. Aboulhorma ^{35e, ID}, H. Abramowicz ^{151, ID}, H. Abreu ^{150, ID}, Y. Abulaiti ^{117, ID}, A.C. Abusleme Hoffman ^{137a, ID}, B.S. Acharya ^{69a, 69b, ID, p}, C. Adam Bourdarios ^{4, ID}, L. Adamczyk ^{85a, ID}, L. Adamek ^{155, ID}, S.V. Addepalli ^{26, ID}, M.J. Addison ^{101, ID}, J. Adelman ^{115, ID}, A. Adiguzel ^{21c, ID}, T. Adye ^{134, ID}, A.A. Affolder ^{136, ID}, Y. Afik ^{36, ID}, M.N. Agaras ^{13, ID}, J. Agarwala ^{73a, 73b, ID}, A. Aggarwal ^{100, ID}, C. Agheorghiesei ^{27c, ID}, A. Ahmad ^{36, ID}, F. Ahmadov ^{38, ID, ac}, W.S. Ahmed ^{104, ID}, S. Ahuja ^{95, ID}, X. Ai ^{62a, ID}, G. Aielli ^{76a, 76b, ID}, M. Ait Tamlihat ^{35e, ID}, B. Aitbenchikh ^{35a, ID}, I. Aizenberg ^{169, ID}, M. Akbiyik ^{100, ID}, T.P.A. Åkesson ^{98, ID}, A.V. Akimov ^{37, ID}, D. Akiyama ^{168, ID}, N.N. Akolkar ^{24, ID}, K. Al Khoury ^{41, ID}, G.L. Alberghi ^{23b, ID}, J. Albert ^{165, ID}, P. Albicocco ^{53, ID}, G.L. Albouy ^{60, ID}, S. Alderweireldt ^{52, ID}, M. Aleksa ^{36, ID}, I.N. Aleksandrov ^{38, ID}, C. Alexa ^{27b, ID}, T. Alexopoulos ^{10, ID}, A. Alfonsi ^{114, ID}, F. Alfonsi ^{23b, ID}, M. Algren ^{56, ID}, M. Alhroob ^{120, ID}, B. Ali ^{132, ID}, H.M.J. Ali ^{91, ID}, S. Ali ^{148, ID}, S.W. Alibocus ^{92, ID}, M. Aliev ^{37, ID}, G. Alimonti ^{71a, ID}, W. Alkakhi ^{55, ID}, C. Allaire ^{66, ID}, B.M.M. Allbrooke ^{146, ID}, J.F. Allen ^{52, ID}, C.A. Allendes Flores ^{137f, ID}, P.P. Allport ^{20, ID}, A. Aloisio ^{72a, 72b, ID}, F. Alonso ^{90, ID}, C. Alpigiani ^{138, ID}, M. Alvarez Estevez ^{99, ID}, A. Alvarez Fernandez ^{100, ID}, M.G. Alviggi ^{72a, 72b, ID}, M. Aly ^{101, ID}, Y. Amaral Coutinho ^{82b, ID}, A. Ambler ^{104, ID}, C. Amelung ³⁶, M. Amerl ^{101, ID}, C.G. Ames ^{109, ID}, D. Amidei ^{106, ID}, S.P. Amor Dos Santos ^{130a, ID}, K.R. Amos ^{163, ID}, V. Ananiev ^{125, ID}, C. Anastopoulos ^{139, ID}, T. Andeen ^{11, ID}, J.K. Anders ^{36, ID}, S.Y. Andreadan ^{47a, 47b, ID}, A. Andreazza ^{71a, 71b, ID}, S. Angelidakis ^{9, ID}, A. Angerami ^{41, ID, af}, A.V. Anisenkov ^{37, ID}, A. Annovi ^{74a, ID}, C. Antel ^{56, ID}, M.T. Anthony ^{139, ID}, E. Antipov ^{145, ID}, M. Antonelli ^{53, ID}, D.J.A. Antrim ^{17a, ID}, F. Anulli ^{75a, ID}, M. Aoki ^{83, ID}, T. Aoki ^{153, ID}, J.A. Aparisi Pozo ^{163, ID},

- M.A. Aparo ^{146, ID}, L. Aperio Bella ^{48, ID}, C. Appelt ^{18, ID}, N. Aranzabal ^{36, ID}, C. Arcangeletti ^{53, ID},
 A.T.H. Arce ^{51, ID}, E. Arena ^{92, ID}, J-F. Arguin ^{108, ID}, S. Argyropoulos ^{54, ID}, J.-H. Arling ^{48, ID},
 A.J. Armbruster ^{36, ID}, O. Arnaez ^{4, ID}, H. Arnold ^{114, ID}, Z.P. Arrubarrena Tame ¹⁰⁹, G. Artoni ^{75a, 75b, ID},
 H. Asada ^{111, ID}, K. Asai ^{118, ID}, S. Asai ^{153, ID}, N.A. Asbah ^{61, ID}, J. Assahsah ^{35d, ID}, K. Assamagan ^{29, ID},
 R. Astalos ^{28a, ID}, S. Atashi ^{160, ID}, R.J. Atkin ^{33a, ID}, M. Atkinson ¹⁶², N.B. Atlay ^{18, ID}, H. Atmani ^{62b},
 P.A. Atmasiddha ^{106, ID}, K. Augsten ^{132, ID}, S. Auricchio ^{72a, 72b, ID}, A.D. Auriol ^{20, ID}, V.A. Astrup ^{101, ID},
 G. Avolio ^{36, ID}, K. Axiotis ^{56, ID}, G. Azuelos ^{108, ID, aj}, D. Babal ^{28b, ID}, H. Bachacou ^{135, ID}, K. Bachas ^{152, ID, t},
 A. Bachiu ^{34, ID}, F. Backman ^{47a, 47b, ID}, A. Badea ^{61, ID}, P. Bagnaia ^{75a, 75b, ID}, M. Bahmani ^{18, ID},
 A.J. Bailey ^{163, ID}, V.R. Bailey ^{162, ID}, J.T. Baines ^{134, ID}, L. Baines ^{94, ID}, C. Bakalis ^{10, ID}, O.K. Baker ^{172, ID},
 E. Bakos ^{15, ID}, D. Bakshi Gupta ^{8, ID}, R. Balasubramanian ^{114, ID}, E.M. Baldin ^{37, ID}, P. Balek ^{85a, ID},
 E. Ballabene ^{23b, 23a, ID}, F. Balli ^{135, ID}, L.M. Baltes ^{63a, ID}, W.K. Balunas ^{32, ID}, J. Balz ^{100, ID}, E. Banas ^{86, ID},
 M. Bandieramonte ^{129, ID}, A. Bandyopadhyay ^{24, ID}, S. Bansal ^{24, ID}, L. Barak ^{151, ID}, M. Barakat ^{48, ID},
 E.L. Barberio ^{105, ID}, D. Barberis ^{57b, 57a, ID}, M. Barbero ^{102, ID}, G. Barbour ⁹⁶, K.N. Barends ^{33a, ID},
 T. Barillari ^{110, ID}, M-S. Barisits ^{36, ID}, T. Barklow ^{143, ID}, P. Baron ^{122, ID}, D.A. Baron Moreno ^{101, ID},
 A. Baroncelli ^{62a, ID}, G. Barone ^{29, ID}, A.J. Barr ^{126, ID}, J.D. Barr ^{96, ID}, L. Barranco Navarro ^{47a, 47b, ID},
 F. Barreiro ^{99, ID}, J. Barreiro Guimarães da Costa ^{14a, ID}, U. Barron ^{151, ID}, M.G. Barros Teixeira ^{130a, ID},
 S. Barsov ^{37, ID}, F. Bartels ^{63a, ID}, R. Bartoldus ^{143, ID}, A.E. Barton ^{91, ID}, P. Bartos ^{28a, ID}, A. Basan ^{100, ID},
 M. Baselga ^{49, ID}, A. Bassalat ^{66, ID, b}, M.J. Basso ^{156a, ID}, C.R. Basson ^{101, ID}, R.L. Bates ^{59, ID}, S. Batlamous ^{35e},
 J.R. Batley ^{32, ID}, B. Batool ^{141, ID}, M. Battaglia ^{136, ID}, D. Battulga ^{18, ID}, M. Bauce ^{75a, 75b, ID}, M. Bauer ^{36, ID},
 P. Bauer ^{24, ID}, L.T. Bazzano Hurrell ^{30, ID}, J.B. Beacham ^{51, ID}, T. Beau ^{127, ID}, P.H. Beauchemin ^{158, ID},
 F. Becherer ^{54, ID}, P. Bechtle ^{24, ID}, H.P. Beck ^{19, ID, s}, K. Becker ^{167, ID}, A.J. Beddall ^{21d, ID}, V.A. Bednyakov ^{38, ID},
 C.P. Bee ^{145, ID}, L.J. Beemster ¹⁵, T.A. Beermann ^{36, ID}, M. Begalli ^{82d, ID}, M. Begel ^{29, ID}, A. Behera ^{145, ID},
 J.K. Behr ^{48, ID}, J.F. Beirer ^{55, ID}, F. Beisiegel ^{24, ID}, M. Belfkir ^{159, ID}, G. Bella ^{151, ID}, L. Bellagamba ^{23b, ID},
 A. Bellerive ^{34, ID}, P. Bellos ^{20, ID}, K. Beloborodov ^{37, ID}, N.L. Belyaev ^{37, ID}, D. Benchekroun ^{35a, ID},
 F. Bendebba ^{35a, ID}, Y. Benhammou ^{151, ID}, M. Benoit ^{29, ID}, J.R. Bensinger ^{26, ID}, S. Bentvelsen ^{114, ID},
 L. Beresford ^{48, ID}, M. Beretta ^{53, ID}, E. Bergeaas Kuutmann ^{161, ID}, N. Berger ^{4, ID}, B. Bergmann ^{132, ID},
 J. Beringer ^{17a, ID}, G. Bernardi ^{5, ID}, C. Bernius ^{143, ID}, F.U. Bernlochner ^{24, ID}, F. Beron ^{36, 102, ID}, T. Berry ^{95, ID},
 P. Berta ^{133, ID}, A. Berthold ^{50, ID}, I.A. Bertram ^{91, ID}, S. Bethke ^{110, ID}, A. Betti ^{75a, 75b, ID}, A.J. Bevan ^{94, ID},
 M. Bhamjee ^{33c, ID}, S. Bhatta ^{145, ID}, D.S. Bhattacharya ^{166, ID}, P. Bhattacharai ^{26, ID}, V.S. Bhopatkar ^{121, ID},
 R. Bi ^{29, al}, R.M. Bianchi ^{129, ID}, G. Bianco ^{23b, 23a, ID}, O. Biebel ^{109, ID}, R. Bielski ^{123, ID}, M. Biglietti ^{77a, ID},
 T.R.V. Billoud ^{132, ID}, M. Bindi ^{55, ID}, A. Bingul ^{21b, ID}, C. Bini ^{75a, 75b, ID}, A. Biondini ^{92, ID},
 C.J. Birch-sykes ^{101, ID}, G.A. Bird ^{20, 134, ID}, M. Birman ^{169, ID}, M. Biros ^{133, ID}, T. Bisanz ^{49, ID},
 E. Bisceglie ^{43b, 43a, ID}, D. Biswas ^{141, ID}, A. Bitadze ^{101, ID}, K. Bjørke ^{125, ID}, I. Bloch ^{48, ID}, C. Blocker ^{26, ID},
 A. Blue ^{59, ID}, U. Blumenschein ^{94, ID}, J. Blumenthal ^{100, ID}, G.J. Bobbink ^{114, ID}, V.S. Bobrovnikov ^{37, ID},
 M. Boehler ^{54, ID}, B. Boehm ^{166, ID}, D. Bogavac ^{36, ID}, A.G. Bogdanchikov ^{37, ID}, C. Bohm ^{47a, ID},
 V. Boisvert ^{95, ID}, P. Bokan ^{48, ID}, T. Bold ^{85a, ID}, M. Bomben ^{5, ID}, M. Bona ^{94, ID}, M. Boonekamp ^{135, ID},
 C.D. Booth ^{95, ID}, A.G. Borbély ^{59, ID}, I.S. Bordulev ^{37, ID}, H.M. Borecka-Bielska ^{108, ID}, L.S. Borgna ^{96, ID},
 G. Borissov ^{91, ID}, D. Bortoletto ^{126, ID}, D. Boscherini ^{23b, ID}, M. Bosman ^{13, ID}, J.D. Bossio Sola ^{36, ID},
 K. Bouaouda ^{35a, ID}, N. Bouchhar ^{163, ID}, J. Boudreau ^{129, ID}, E.V. Bouhova-Thacker ^{91, ID}, D. Boumediene ^{40, ID},
 R. Bouquet ^{5, ID}, A. Boveia ^{119, ID}, J. Boyd ^{36, ID}, D. Boye ^{29, ID}, I.R. Boyko ^{38, ID}, J. Bracinik ^{20, ID},
 N. Brahimi ^{62d, ID}, G. Brandt ^{171, ID}, O. Brandt ^{32, ID}, F. Braren ^{48, ID}, B. Brau ^{103, ID}, J.E. Brau ^{123, ID},
 R. Brener ^{169, ID}, L. Brenner ^{114, ID}, R. Brenner ^{161, ID}, S. Bressler ^{169, ID}, D. Britton ^{59, ID}, D. Britzger ^{110, ID},

- I. Brock 24, ^{IB}, G. Brooijmans 41, ^{IB}, W.K. Brooks 137f, ^{IB}, E. Brost 29, ^{IB}, L.M. Brown 165, ^{IB}, L.E. Bruce 61, ^{IB}, T.L. Bruckler 126, ^{IB}, P.A. Bruckman de Renstrom 86, ^{IB}, B. Brüers 48, ^{IB}, D. Bruncko 28b, ^{IB}, A. Bruni 23b, ^{IB}, G. Bruni 23b, ^{IB}, M. Bruschi 23b, ^{IB}, N. Bruscino 75a, 75b, ^{IB}, T. Buanes 16, ^{IB}, Q. Buat 138, ^{IB}, D. Buchin 110, ^{IB}, A.G. Buckley 59, ^{IB}, M.K. Bugge 125, ^{IB}, O. Bulekov 37, ^{IB}, B.A. Bullard 143, ^{IB}, S. Burdin 92, ^{IB}, C.D. Burgard 49, ^{IB}, A.M. Burger 40, ^{IB}, B. Burghgrave 8, ^{IB}, O. Burlayenko 54, ^{IB}, J.T.P. Burr 32, ^{IB}, C.D. Burton 11, ^{IB}, J.C. Burzynski 142, ^{IB}, E.L. Busch 41, ^{IB}, V. Büscher 100, ^{IB}, P.J. Bussey 59, ^{IB}, J.M. Butler 25, ^{IB}, C.M. Buttar 59, ^{IB}, J.M. Butterworth 96, ^{IB}, W. Buttlinger 134, ^{IB}, C.J. Buxo Vazquez 107, A.R. Buzykaev 37, ^{IB}, G. Cabras 23b, ^{IB}, S. Cabrera Urbán 163, ^{IB}, D. Caforio 58, ^{IB}, H. Cai 129, ^{IB}, Y. Cai 14a, 14e, ^{IB}, V.M.M. Cairo 36, ^{IB}, O. Cakir 3a, ^{IB}, N. Calace 36, ^{IB}, P. Calafiura 17a, ^{IB}, G. Calderini 127, ^{IB}, P. Calfayan 68, ^{IB}, G. Callea 59, ^{IB}, L.P. Caloba 82b, D. Calvet 40, ^{IB}, S. Calvet 40, ^{IB}, T.P. Calvet 102, ^{IB}, M. Calvetti 74a, 74b, ^{IB}, R. Camacho Toro 127, ^{IB}, S. Camarda 36, ^{IB}, D. Camarero Munoz 26, ^{IB}, P. Camarri 76a, 76b, ^{IB}, M.T. Camerlingo 72a, 72b, ^{IB}, D. Cameron 125, ^{IB}, C. Camincher 165, ^{IB}, M. Campanelli 96, ^{IB}, A. Camplani 42, ^{IB}, V. Canale 72a, 72b, ^{IB}, A. Canesse 104, ^{IB}, M. Cano Bret 80, ^{IB}, J. Cantero 163, ^{IB}, Y. Cao 162, ^{IB}, F. Capocasa 26, ^{IB}, M. Capua 43b, 43a, ^{IB}, A. Carbone 71a, 71b, ^{IB}, R. Cardarelli 76a, ^{IB}, J.C.J. Cardenas 8, ^{IB}, F. Cardillo 163, ^{IB}, T. Carli 36, ^{IB}, G. Carlino 72a, ^{IB}, J.I. Carlotto 13, ^{IB}, B.T. Carlson 129, ^{IB}, u, E.M. Carlson 165, 156a, ^{IB}, L. Carminati 71a, 71b, ^{IB}, A. Carnelli 135, ^{IB}, M. Carnesale 75a, 75b, ^{IB}, S. Caron 113, ^{IB}, E. Carquin 137f, ^{IB}, S. Carrá 71a, 71b, ^{IB}, G. Carratta 23b, 23a, ^{IB}, F. Carrio Argos 33g, ^{IB}, J.W.S. Carter 155, ^{IB}, T.M. Carter 52, ^{IB}, M.P. Casado 13, ^{IB}, j, M. Caspar 48, ^{IB}, E.G. Castiglia 172, ^{IB}, F.L. Castillo 4, ^{IB}, L. Castillo Garcia 13, ^{IB}, V. Castillo Gimenez 163, ^{IB}, N.F. Castro 130a, 130e, ^{IB}, A. Catinaccio 36, ^{IB}, J.R. Catmore 125, ^{IB}, V. Cavaliere 29, ^{IB}, N. Cavalli 23b, 23a, ^{IB}, V. Cavasinni 74a, 74b, ^{IB}, Y.C. Cekmecelioglu 48, ^{IB}, E. Celebi 21a, ^{IB}, F. Celli 126, ^{IB}, M.S. Centonze 70a, 70b, ^{IB}, K. Cerny 122, ^{IB}, A.S. Cerqueira 82a, ^{IB}, A. Cerri 146, ^{IB}, L. Cerrito 76a, 76b, ^{IB}, F. Cerutti 17a, ^{IB}, B. Cervato 141, ^{IB}, A. Cervelli 23b, ^{IB}, G. Cesarini 53, ^{IB}, S.A. Cetin 21d, ^{IB}, Z. Chadi 35a, ^{IB}, D. Chakraborty 115, ^{IB}, M. Chala 130f, ^{IB}, J. Chan 170, ^{IB}, W.Y. Chan 153, ^{IB}, J.D. Chapman 32, ^{IB}, E. Chapon 135, ^{IB}, B. Chargeishvili 149b, ^{IB}, D.G. Charlton 20, ^{IB}, T.P. Charman 94, ^{IB}, M. Chatterjee 19, ^{IB}, C. Chauhan 133, ^{IB}, S. Chekanov 6, ^{IB}, S.V. Chekulaev 156a, ^{IB}, G.A. Chelkov 38, ^{IB}, a, A. Chen 106, ^{IB}, B. Chen 151, ^{IB}, B. Chen 165, ^{IB}, H. Chen 14c, ^{IB}, H. Chen 29, ^{IB}, J. Chen 62c, ^{IB}, J. Chen 142, ^{IB}, M. Chen 126, ^{IB}, S. Chen 153, ^{IB}, S.J. Chen 14c, ^{IB}, X. Chen 62c, ^{IB}, X. Chen 14b, ^{IB}, ai, Y. Chen 62a, ^{IB}, C.L. Cheng 170, ^{IB}, H.C. Cheng 64a, ^{IB}, S. Cheong 143, ^{IB}, A. Cheplakov 38, ^{IB}, E. Cheremushkina 48, ^{IB}, E. Cherepanova 114, ^{IB}, R. Cherkaoui El Moursli 35e, ^{IB}, E. Cheu 7, ^{IB}, K. Cheung 65, ^{IB}, L. Chevalier 135, ^{IB}, V. Chiarella 53, ^{IB}, G. Chiarelli 74a, ^{IB}, N. Chiedde 102, ^{IB}, G. Chiodini 70a, ^{IB}, A.S. Chisholm 20, ^{IB}, A. Chitan 27b, ^{IB}, M. Chitishvili 163, ^{IB}, M.V. Chizhov 38, ^{IB}, K. Choi 11, ^{IB}, A.R. Chomont 75a, 75b, ^{IB}, Y. Chou 103, ^{IB}, E.Y.S. Chow 114, ^{IB}, T. Chowdhury 33g, ^{IB}, K.L. Chu 169, M.C. Chu 64a, ^{IB}, X. Chu 14a, 14e, ^{IB}, J. Chudoba 131, ^{IB}, J.J. Chwastowski 86, ^{IB}, D. Cieri 110, ^{IB}, K.M. Ciesla 85a, ^{IB}, V. Cindro 93, ^{IB}, A. Ciocio 17a, ^{IB}, F. Cirotto 72a, 72b, ^{IB}, Z.H. Citron 169, ^{IB}, n, M. Citterio 71a, ^{IB}, D.A. Ciubotaru 27b, B.M. Ciungu 155, ^{IB}, A. Clark 56, ^{IB}, P.J. Clark 52, ^{IB}, J.M. Clavijo Columbie 48, ^{IB}, S.E. Clawson 48, ^{IB}, C. Clement 47a, 47b, ^{IB}, J. Clercx 48, ^{IB}, L. Clissa 23b, 23a, ^{IB}, Y. Coadou 102, ^{IB}, M. Cobal 69a, 69c, ^{IB}, A. Coccaro 57b, ^{IB}, R.F. Coelho Barrue 130a, ^{IB}, R. Coelho Lopes De Sa 103, ^{IB}, S. Coelli 71a, ^{IB}, H. Cohen 151, ^{IB}, A.E.C. Coimbra 71a, 71b, ^{IB}, B. Cole 41, ^{IB}, J. Collot 60, ^{IB}, P. Conde Muiño 130a, 130g, ^{IB}, M.P. Connell 33c, ^{IB}, S.H. Connell 33c, ^{IB}, I.A. Connolly 59, ^{IB}, E.I. Conroy 126, ^{IB}, F. Conventi 72a, ^{IB}, ak, H.G. Cooke 20, ^{IB}, A.M. Cooper-Sarkar 126, ^{IB}, A. Cordeiro Oudot Choi 127, ^{IB}, F. Cormier 164, ^{IB}, L.D. Corpe 40, ^{IB}, M. Corradi 75a, 75b, ^{IB}, F. Corriveau 104, ^{IB}, aa, A. Cortes-Gonzalez 18, ^{IB}, M.J. Costa 163, ^{IB}, F. Costanza 4, ^{IB}, D. Costanzo 139, ^{IB}, B.M. Cote 119, ^{IB}, G. Cowan 95, ^{IB}, K. Cranmer 170, ^{IB}, D. Cremonini 23b, 23a, ^{IB}, S. Crépé-Renaudin 60, ^{IB}, F. Crescioli 127, ^{IB}, M. Cristinziani 141, ^{IB}, M. Cristoforetti 78a, 78b, ^{IB}, V. Croft 114, ^{IB},

- J.E. Crosby 121, ID, G. Crosetti 43b, 43a, ID, A. Cueto 99, ID, T. Cuhadar Donszelmann 160, ID, H. Cui 14a, 14e, ID,
 Z. Cui 7, ID, W.R. Cunningham 59, ID, F. Curcio 43b, 43a, ID, P. Czodrowski 36, ID, M.M. Czurylo 63b, ID,
 M.J. Da Cunha Sargedas De Sousa 62a, ID, J.V. Da Fonseca Pinto 82b, ID, C. Da Via 101, ID, W. Dabrowski 85a, ID,
 T. Dado 49, ID, S. Dahbi 33g, ID, T. Dai 106, ID, C. Dallapiccola 103, ID, M. Dam 42, ID, G. D'amen 29, ID,
 V. D'Amico 109, ID, J. Damp 100, ID, J.R. Dandoy 128, ID, M.F. Daneri 30, ID, M. Danninger 142, ID, V. Dao 36, ID,
 G. Darbo 57b, ID, S. Darmora 6, ID, S.J. Das 29, ID, al, S. D'Auria 71a, 71b, ID, C. David 156b, ID, T. Davidek 133, ID,
 B. Davis-Purcell 34, ID, I. Dawson 94, ID, H.A. Day-hall 132, ID, K. De 8, ID, R. De Asmundis 72a, ID,
 N. De Biase 48, ID, S. De Castro 23b, 23a, ID, N. De Groot 113, ID, P. de Jong 114, ID, H. De la Torre 107, ID,
 A. De Maria 14c, ID, A. De Salvo 75a, ID, U. De Sanctis 76a, 76b, ID, A. De Santo 146, ID,
 J.B. De Vivie De Regie 60, ID, D.V. Dedovich 38, J. Degens 114, ID, A.M. Deiana 44, ID, F. Del Corso 23b, 23a, ID,
 J. Del Peso 99, ID, F. Del Rio 63a, ID, F. Deliot 135, ID, C.M. Delitzsch 49, ID, M. Della Pietra 72a, 72b, ID,
 D. Della Volpe 56, ID, A. Dell'Acqua 36, ID, L. Dell'Asta 71a, 71b, ID, M. Delmastro 4, ID, P.A. Delsart 60, ID,
 S. Demers 172, ID, M. Demichev 38, ID, S.P. Denisov 37, ID, L. D'Eramo 40, ID, D. Derendarz 86, ID, F. Derue 127, ID,
 P. Dervan 92, ID, K. Desch 24, ID, C. Deutsch 24, ID, F.A. Di Bello 57b, 57a, ID, A. Di Ciaccio 76a, 76b, ID,
 L. Di Ciaccio 4, ID, A. Di Domenico 75a, 75b, ID, C. Di Donato 72a, 72b, ID, A. Di Girolamo 36, ID,
 G. Di Gregorio 5, ID, A. Di Luca 78a, 78b, ID, B. Di Micco 77a, 77b, ID, R. Di Nardo 77a, 77b, ID, C. Diaconu 102, ID,
 F.A. Dias 114, ID, T. Dias Do Vale 142, ID, M.A. Diaz 137a, 137b, ID, F.G. Diaz Capriles 24, ID, M. Didenko 163, ID,
 E.B. Diehl 106, ID, L. Diehl 54, ID, S. Díez Cornell 48, ID, C. Diez Pardos 141, ID, C. Dimitriadi 24, 161, ID,
 A. Dimitrievska 17a, ID, J. Dingfelder 24, ID, I-M. Dinu 27b, ID, S.J. Dittmeier 63b, ID, F. Dittus 36, ID,
 F. Djama 102, ID, T. Djobava 149b, ID, J.I. Djuvsland 16, ID, C. Doglioni 101, 98, ID, J. Dolejsi 133, ID, Z. Dolezal 133, ID,
 M. Donadelli 82c, ID, B. Dong 107, ID, J. Donini 40, ID, A. D'Onofrio 77a, 77b, ID, M. D'Onofrio 92, ID, J. Dopke 134, ID,
 A. Doria 72a, ID, N. Dos Santos Fernandes 130a, ID, M.T. Dova 90, ID, A.T. Doyle 59, ID, M.A. Draguet 126, ID,
 E. Dreyer 169, ID, I. Drivas-koulouris 10, ID, A.S. Drobac 158, ID, M. Drozdova 56, ID, D. Du 62a, ID,
 T.A. du Pree 114, ID, F. Dubinin 37, ID, M. Dubovsky 28a, ID, E. Duchovni 169, ID, G. Duckeck 109, ID,
 O.A. Ducu 27b, ID, D. Duda 52, ID, A. Dudarev 36, ID, E.R. Duden 26, ID, M. D'uffizi 101, ID, L. Duflot 66, ID,
 M. Dührssen 36, ID, C. Dülsen 171, ID, A.E. Dumitriu 27b, ID, M. Dunford 63a, ID, S. Dungs 49, ID,
 K. Dunne 47a, 47b, ID, A. Duperrin 102, ID, H. Duran Yildiz 3a, ID, M. Düren 58, ID, A. Durglishvili 149b, ID,
 B.L. Dwyer 115, ID, G.I. Dyckes 17a, ID, M. Dyndal 85a, ID, S. Dysch 101, ID, B.S. Dziedzic 86, ID,
 Z.O. Earnshaw 146, ID, G.H. Eberwein 126, ID, B. Eckerova 28a, ID, S. Eggebrecht 55, ID, M.G. Eggleston 51,
 E. Egidio Purcino De Souza 127, ID, L.F. Ehrke 56, ID, G. Eigen 16, ID, K. Einsweiler 17a, ID, T. Ekelof 161, ID,
 P.A. Ekman 98, ID, Y. El Ghazali 35b, ID, H. El Jarrari 35e, 148, ID, A. El Moussaouy 35a, ID, V. Ellajosyula 161, ID,
 M. Ellert 161, ID, F. Ellinghaus 171, ID, A.A. Elliot 94, ID, N. Ellis 36, ID, J. Elmsheuser 29, ID, M. Elsing 36, ID,
 D. Emeliyanov 134, ID, Y. Enari 153, ID, I. Ene 17a, ID, S. Epari 13, ID, J. Erdmann 49, ID, P.A. Erland 86, ID,
 M. Errenst 171, ID, M. Escalier 66, ID, C. Escobar 163, ID, E. Etzion 151, ID, G. Evans 130a, ID, H. Evans 68, ID,
 L.S. Evans 95, ID, M.O. Evans 146, ID, A. Ezhilov 37, ID, S. Ezzarqtouni 35a, ID, F. Fabbri 59, ID, L. Fabbri 23b, 23a, ID,
 G. Facini 96, ID, V. Fadeyev 136, ID, R.M. Fakhrutdinov 37, ID, S. Falciano 75a, ID, L.F. Falda Ulhoa Coelho 36, ID,
 P.J. Falke 24, ID, J. Faltova 133, ID, C. Fan 162, ID, Y. Fan 14a, ID, Y. Fang 14a, 14e, ID, M. Fanti 71a, 71b, ID,
 M. Faraj 69a, 69b, ID, Z. Farazpay 97, A. Farbin 8, ID, A. Farilla 77a, ID, T. Farooque 107, ID, S.M. Farrington 52, ID,
 F. Fassi 35e, ID, D. Fassouliotis 9, ID, M. Faucci Giannelli 76a, 76b, ID, W.J. Fawcett 32, ID, L. Fayard 66, ID,
 P. Federic 133, ID, P. Federicova 131, ID, O.L. Fedin 37, ID, a, G. Fedotov 37, ID, M. Feickert 170, ID, L. Feligioni 102, ID,
 A. Fell 139, ID, D.E. Fellers 123, ID, C. Feng 62b, ID, M. Feng 14b, ID, Z. Feng 114, ID, M.J. Fenton 160, ID,
 A.B. Fenyuk 37, L. Ferencz 48, ID, R.A.M. Ferguson 91, ID, S.I. Fernandez Luengo 137f, ID, M.J.V. Fernoux 102, ID,

- J. Ferrando 48, [ID](#), A. Ferrari 161, [ID](#), P. Ferrari 114, 113, [ID](#), R. Ferrari 73a, [ID](#), D. Ferrere 56, [ID](#), C. Ferretti 106, [ID](#),
 F. Fiedler 100, [ID](#), A. Filipčič 93, [ID](#), E.K. Filmer 1, [ID](#), F. Filthaut 113, [ID](#), M.C.N. Fiolhais 130a, 130c, [ID](#), [d](#),
 L. Fiorini 163, [ID](#), W.C. Fisher 107, [ID](#), T. Fitschen 101, [ID](#), P.M. Fitzhugh 135, I. Fleck 141, [ID](#), P. Fleischmann 106, [ID](#),
 T. Flick 171, [ID](#), L. Flores 128, [ID](#), M. Flores 33d, [ID](#), [ag](#), L.R. Flores Castillo 64a, [ID](#), L. Flores Sanz De Acedo 36, [ID](#),
 F.M. Follega 78a, 78b, [ID](#), N. Fomin 16, [ID](#), J.H. Foo 155, [ID](#), B.C. Forland 68, A. Formica 135, [ID](#), A.C. Forti 101, [ID](#),
 E. Fortin 36, [ID](#), A.W. Fortman 61, [ID](#), M.G. Foti 17a, [ID](#), L. Fountas 9, [ID](#), [k](#), D. Fournier 66, [ID](#), H. Fox 91, [ID](#),
 P. Francavilla 74a, 74b, [ID](#), S. Francescato 61, [ID](#), S. Franchellucci 56, [ID](#), M. Franchini 23b, 23a, [ID](#),
 S. Franchino 63a, [ID](#), D. Francis 36, L. Franco 113, [ID](#), L. Franconi 48, [ID](#), M. Franklin 61, [ID](#), G. Frattari 26, [ID](#),
 A.C. Freegard 94, [ID](#), W.S. Freund 82b, [ID](#), Y.Y. Frid 151, [ID](#), N. Fritzschke 50, [ID](#), A. Froch 54, [ID](#), D. Froidevaux 36, [ID](#),
 J.A. Frost 126, [ID](#), Y. Fu 62a, [ID](#), M. Fujimoto 118, [ID](#), E. Fullana Torregrosa 163, [ID](#), [*](#), K.Y. Fung 64a, [ID](#),
 E. Furtado De Simas Filho 82b, [ID](#), M. Furukawa 153, [ID](#), J. Fuster 163, [ID](#), A. Gabrielli 23b, 23a, [ID](#),
 A. Gabrielli 155, [ID](#), P. Gadow 48, [ID](#), G. Gagliardi 57b, 57a, [ID](#), L.G. Gagnon 17a, [ID](#), E.J. Gallas 126, [ID](#),
 B.J. Gallop 134, [ID](#), K.K. Gan 119, [ID](#), S. Ganguly 153, [ID](#), J. Gao 62a, [ID](#), Y. Gao 52, [ID](#), F.M. Garay Walls 137a, 137b, [ID](#),
 B. Garcia 29, [al](#), C. García 163, [ID](#), A. Garcia Alonso 114, [ID](#), A.G. Garcia Caffaro 172, [ID](#), J.E. García Navarro 163, [ID](#),
 M. Garcia-Sciveres 17a, [ID](#), G.L. Gardner 128, [ID](#), R.W. Gardner 39, [ID](#), N. Garelli 158, [ID](#), D. Garg 80, [ID](#),
 R.B. Garg 143, [ID](#), [r](#), J.M. Gargan 52, C.A. Garner 155, S.J. Gasiorowski 138, [ID](#), P. Gaspar 82b, [ID](#), G. Gaudio 73a, [ID](#),
 V. Gautam 13, P. Gauzzi 75a, 75b, [ID](#), I.L. Gavrilenko 37, [ID](#), A. Gavrilyuk 37, [ID](#), C. Gay 164, [ID](#), G. Gaycken 48, [ID](#),
 E.N. Gazis 10, [ID](#), A.A. Geanta 27b, [ID](#), C.M. Gee 136, [ID](#), C. Gemme 57b, [ID](#), M.H. Genest 60, [ID](#), S. Gentile 75a, 75b, [ID](#),
 S. George 95, [ID](#), W.F. George 20, [ID](#), T. Geralis 46, [ID](#), P. Gessinger-Befurt 36, [ID](#), M.E. Geyik 171, [ID](#),
 M. Ghneimat 141, [ID](#), K. Ghorbanian 94, [ID](#), A. Ghosal 141, [ID](#), A. Ghosh 160, [ID](#), A. Ghosh 7, [ID](#), B. Giacobbe 23b, [ID](#),
 S. Giagu 75a, 75b, [ID](#), P. Giannetti 74a, [ID](#), A. Giannini 62a, [ID](#), S.M. Gibson 95, [ID](#), M. Gignac 136, [ID](#), D.T. Gil 85b, [ID](#),
 A.K. Gilbert 85a, [ID](#), B.J. Gilbert 41, [ID](#), D. Gillberg 34, [ID](#), G. Gilles 114, [ID](#), N.E.K. Gillwald 48, [ID](#), L. Ginabat 127, [ID](#),
 D.M. Gingrich 2, [ID](#), [aj](#), M.P. Giordani 69a, 69c, [ID](#), P.F. Giraud 135, [ID](#), G. Giugliarelli 69a, 69c, [ID](#), D. Giugni 71a, [ID](#),
 F. Giuli 36, [ID](#), I. Gkialas 9, [ID](#), [k](#), L.K. Gladilin 37, [ID](#), C. Glasman 99, [ID](#), G.R. Gledhill 123, [ID](#), M. Glisic 123,
 I. Gnesi 43b, [ID](#), [g](#), Y. Go 29, [ID](#), [al](#), M. Goblirsch-Kolb 36, [ID](#), B. Gocke 49, [ID](#), D. Godin 108, B. Gokturk 21a, [ID](#),
 S. Goldfarb 105, [ID](#), T. Golling 56, [ID](#), M.G.D. Gololo 33g, D. Golubkov 37, [ID](#), J.P. Gombas 107, [ID](#),
 A. Gomes 130a, 130b, [ID](#), G. Gomes Da Silva 141, [ID](#), A.J. Gomez Delegido 163, [ID](#), R. Gonçalo 130a, 130c, [ID](#),
 G. Gonella 123, [ID](#), L. Gonella 20, [ID](#), A. Gongadze 38, [ID](#), F. Gonnella 20, [ID](#), J.L. Gonski 41, [ID](#),
 R.Y. González Andana 52, [ID](#), S. González de la Hoz 163, [ID](#), S. Gonzalez Fernandez 13, [ID](#),
 R. Gonzalez Lopez 92, [ID](#), C. Gonzalez Renteria 17a, [ID](#), R. Gonzalez Suarez 161, [ID](#), S. Gonzalez-Sevilla 56, [ID](#),
 G.R. Gonzalvo Rodriguez 163, [ID](#), L. Goossens 36, [ID](#), P.A. Gorbounov 37, [ID](#), B. Gorini 36, [ID](#), E. Gorini 70a, 70b, [ID](#),
 A. Gorišek 93, [ID](#), T.C. Gosart 128, [ID](#), A.T. Goshaw 51, [ID](#), M.I. Gostkin 38, [ID](#), S. Goswami 121, [ID](#),
 C.A. Gottardo 36, [ID](#), M. Gouighri 35b, [ID](#), V. Goumarre 48, [ID](#), A.G. Goussiou 138, [ID](#), N. Govender 33c, [ID](#),
 I. Grabowska-Bold 85a, [ID](#), K. Graham 34, [ID](#), E. Gramstad 125, [ID](#), S. Grancagnolo 70a, 70b, [ID](#), M. Grandi 146, [ID](#),
 V. Gratchev 37, [*](#), P.M. Gravila 27f, [ID](#), F.G. Gravili 70a, 70b, [ID](#), H.M. Gray 17a, [ID](#), M. Greco 70a, 70b, [ID](#), C. Grefe 24, [ID](#),
 I.M. Gregor 48, [ID](#), P. Grenier 143, [ID](#), C. Grieco 13, [ID](#), A.A. Grillo 136, [ID](#), K. Grimm 31, [ID](#), S. Grinstein 13, [ID](#), [w](#),
 J.-F. Grivaz 66, [ID](#), E. Gross 169, [ID](#), J. Grosse-Knetter 55, [ID](#), C. Grud 106, J.C. Grundy 126, [ID](#), L. Guan 106, [ID](#),
 W. Guan 170, [ID](#), C. Gubbels 164, [ID](#), J.G.R. Guerrero Rojas 163, [ID](#), G. Guerrieri 69a, 69b, [ID](#), F. Guescini 110, [ID](#),
 R. Gugel 100, [ID](#), J.A.M. Guhit 106, [ID](#), A. Guida 18, [ID](#), T. Guillemin 4, [ID](#), E. Guilloton 167, 134, [ID](#), S. Guindon 36, [ID](#),
 F. Guo 14a, 14e, [ID](#), J. Guo 62c, [ID](#), L. Guo 48, [ID](#), Y. Guo 106, [ID](#), R. Gupta 48, [ID](#), S. Gurbuz 24, [ID](#), S.S. Gurdasani 54, [ID](#),
 G. Gustavino 36, [ID](#), M. Guth 56, [ID](#), P. Gutierrez 120, [ID](#), L.F. Gutierrez Zagazeta 128, [ID](#), C. Gutschow 96, [ID](#),
 C. Gwenlan 126, [ID](#), C.B. Gwilliam 92, [ID](#), E.S. Haaland 125, [ID](#), A. Haas 117, [ID](#), M. Habedank 48, [ID](#),

- C. Haber ^{17a, ID}, H.K. Hadavand ^{8, ID}, A. Hadef ^{100, ID}, S. Hadzic ^{110, ID}, J.J. Hahn ^{141, ID}, E.H. Haines ^{96, ID}, M. Haleem ^{166, ID}, J. Haley ^{121, ID}, J.J. Hall ^{139, ID}, G.D. Hallewell ^{102, ID}, L. Halser ^{19, ID}, K. Hamano ^{165, ID}, H. Hamdaoui ^{35e, ID}, M. Hamer ^{24, ID}, G.N. Hamity ^{52, ID}, E.J. Hampshire ^{95, ID}, J. Han ^{62b, ID}, K. Han ^{62a, ID}, L. Han ^{14c, ID}, L. Han ^{62a, ID}, S. Han ^{17a, ID}, Y.F. Han ^{155, ID}, K. Hanagaki ^{83, ID}, M. Hance ^{136, ID}, D.A. Hangal ^{41, ID, af}, H. Hanif ^{142, ID}, M.D. Hank ^{128, ID}, R. Hankache ^{101, ID}, J.B. Hansen ^{42, ID}, J.D. Hansen ^{42, ID}, P.H. Hansen ^{42, ID}, K. Hara ^{157, ID}, D. Harada ^{56, ID}, T. Harenberg ^{171, ID}, S. Harkusha ^{37, ID}, Y.T. Harris ^{126, ID}, J. Harrison ^{13, ID}, N.M. Harrison ^{119, ID}, P.F. Harrison ¹⁶⁷, N.M. Hartman ^{143, ID}, N.M. Hartmann ^{109, ID}, Y. Hasegawa ^{140, ID}, A. Hasib ^{52, ID}, S. Haug ^{19, ID}, R. Hauser ^{107, ID}, C.M. Hawkes ^{20, ID}, R.J. Hawkings ^{36, ID}, Y. Hayashi ^{153, ID}, S. Hayashida ^{111, ID}, D. Hayden ^{107, ID}, C. Hayes ^{106, ID}, R.L. Hayes ^{114, ID}, C.P. Hays ^{126, ID}, J.M. Hays ^{94, ID}, H.S. Hayward ^{92, ID}, F. He ^{62a, ID}, M. He ^{14a, 14e, ID}, Y. He ^{154, ID}, Y. He ^{127, ID}, N.B. Heatley ^{94, ID}, V. Hedberg ^{98, ID}, A.L. Heggelund ^{125, ID}, N.D. Hehir ^{94, ID}, C. Heidegger ^{54, ID}, K.K. Heidegger ^{54, ID}, W.D. Heidorn ^{81, ID}, J. Heilman ^{34, ID}, S. Heim ^{48, ID}, T. Heim ^{17a, ID}, J.G. Heinlein ^{128, ID}, J.J. Heinrich ^{123, ID}, L. Heinrich ^{110, ID, ah}, J. Hejbal ^{131, ID}, L. Helary ^{48, ID}, A. Held ^{170, ID}, S. Hellesund ^{16, ID}, C.M. Helling ^{164, ID}, S. Hellman ^{47a, 47b, ID}, C. Helsens ^{36, ID}, R.C.W. Henderson ⁹¹, L. Henkelmann ^{32, ID}, A.M. Henriques Correia ³⁶, H. Herde ^{98, ID}, Y. Hernández Jiménez ^{145, ID}, L.M. Herrmann ^{24, ID}, T. Herrmann ^{50, ID}, G. Herten ^{54, ID}, R. Hertenberger ^{109, ID}, L. Hervas ^{36, ID}, M.E. Hesping ^{100, ID}, N.P. Hessey ^{156a, ID}, H. Hibi ^{84, ID}, S.J. Hillier ^{20, ID}, J.R. Hinds ^{107, ID}, F. Hinterkeuser ^{24, ID}, M. Hirose ^{124, ID}, S. Hirose ^{157, ID}, D. Hirschbuehl ^{171, ID}, T.G. Hitchings ^{101, ID}, B. Hiti ^{93, ID}, J. Hobbs ^{145, ID}, R. Hobincu ^{27e, ID}, N. Hod ^{169, ID}, M.C. Hodgkinson ^{139, ID}, B.H. Hodkinson ^{32, ID}, A. Hoecker ^{36, ID}, J. Hofer ^{48, ID}, T. Holm ^{24, ID}, M. Holzbock ^{110, ID}, L.B.A.H. Hommels ^{32, ID}, B.P. Honan ^{101, ID}, J. Hong ^{62c, ID}, T.M. Hong ^{129, ID}, B.H. Hooberman ^{162, ID}, W.H. Hopkins ^{6, ID}, Y. Horii ^{111, ID}, S. Hou ^{148, ID}, A.S. Howard ^{93, ID}, J. Howarth ^{59, ID}, J. Hoya ^{6, ID}, M. Hrabovsky ^{122, ID}, A. Hrynevich ^{48, ID}, T. Hrynn'ova ^{4, ID}, P.J. Hsu ^{65, ID}, S.-C. Hsu ^{138, ID}, Q. Hu ^{41, ID}, Y.F. Hu ^{14a, 14e, ID}, S. Huang ^{64b, ID}, X. Huang ^{14c, ID}, Y. Huang ^{62a, ID}, Y. Huang ^{14a, ID}, Z. Huang ^{101, ID}, Z. Hubacek ^{132, ID}, M. Huebner ^{24, ID}, F. Huegging ^{24, ID}, T.B. Huffman ^{126, ID}, C.A. Hugli ^{48, ID}, M. Huhtinen ^{36, ID}, S.K. Huiberts ^{16, ID}, R. Hulskens ^{104, ID}, N. Huseynov ^{12, ID, a}, J. Huston ^{107, ID}, J. Huth ^{61, ID}, R. Hyneman ^{143, ID}, G. Iacobucci ^{56, ID}, G. Iakovidis ^{29, ID}, I. Ibragimov ^{141, ID}, L. Iconomidou-Fayard ^{66, ID}, P. Iengo ^{72a, 72b, ID}, R. Iguchi ^{153, ID}, T. Iizawa ^{83, ID}, Y. Ikegami ^{83, ID}, N. Ilic ^{155, ID}, H. Imam ^{35a, ID}, M. Ince Lezki ^{56, ID}, T. Ingebretsen Carlson ^{47a, 47b, ID}, G. Introzzi ^{73a, 73b, ID}, M. Iodice ^{77a, ID}, V. Ippolito ^{75a, 75b, ID}, R.K. Irwin ^{92, ID}, M. Ishino ^{153, ID}, W. Islam ^{170, ID}, C. Issever ^{18, 48, ID}, S. Istin ^{21a, ID, an}, H. Ito ^{168, ID}, J.M. Iturbe Ponce ^{64a, ID}, R. Iuppa ^{78a, 78b, ID}, A. Ivina ^{169, ID}, J.M. Izen ^{45, ID}, V. Izzo ^{72a, ID}, P. Jacka ^{131, 132, ID}, P. Jackson ^{1, ID}, R.M. Jacobs ^{48, ID}, B.P. Jaeger ^{142, ID}, C.S. Jagfeld ^{109, ID}, P. Jain ^{54, ID}, G. Jäkel ^{171, ID}, K. Jakobs ^{54, ID}, T. Jakoubek ^{169, ID}, J. Jamieson ^{59, ID}, K.W. Janas ^{85a, ID}, A.E. Jaspan ^{92, ID}, M. Javurkova ^{103, ID}, F. Jeanneau ^{135, ID}, L. Jeanty ^{123, ID}, J. Jejelava ^{149a, ID, ad}, P. Jenni ^{54, ID, h}, C.E. Jessiman ^{34, ID}, S. Jézéquel ^{4, ID}, C. Jia ^{62b}, J. Jia ^{145, ID}, X. Jia ^{61, ID}, X. Jia ^{14a, 14e, ID}, Z. Jia ^{14c, ID}, Y. Jiang ^{62a, ID}, S. Jiggins ^{48, ID}, J. Jimenez Pena ^{13, ID}, S. Jin ^{14c, ID}, A. Jinaru ^{27b, ID}, O. Jinnouchi ^{154, ID}, P. Johansson ^{139, ID}, K.A. Johns ^{7, ID}, J.W. Johnson ^{136, ID}, D.M. Jones ^{32, ID}, E. Jones ^{48, ID}, P. Jones ^{32, ID}, R.W.L. Jones ^{91, ID}, T.J. Jones ^{92, ID}, R. Joshi ^{119, ID}, J. Jovicevic ^{15, ID}, X. Ju ^{17a, ID}, J.J. Junggeburth ^{36, ID}, T. Junkermann ^{63a, ID}, A. Juste Rozas ^{13, ID, w}, M.K. Juzek ^{86, ID}, S. Kabana ^{137e, ID}, A. Kaczmarska ^{86, ID}, M. Kado ^{110, ID}, H. Kagan ^{119, ID}, M. Kagan ^{143, ID}, A. Kahn ⁴¹, A. Kahn ^{128, ID}, C. Kahra ^{100, ID}, T. Kaji ^{168, ID}, E. Kajomovitz ^{150, ID}, N. Kakati ^{169, ID}, I. Kalaitzidou ^{54, ID}, C.W. Kalderon ^{29, ID}, A. Kamenshchikov ^{155, ID}, S. Kanayama ^{154, ID}, N.J. Kang ^{136, ID}, D. Kar ^{33g, ID}, K. Karava ^{126, ID}, M.J. Kareem ^{156b, ID}, E. Karentzos ^{54, ID}, I. Karkanias ^{152, ID}, O. Karkout ^{114, ID}, S.N. Karpov ^{38, ID}, Z.M. Karpova ^{38, ID}, V. Kartvelishvili ^{91, ID},

- A.N. Karyukhin ^{37, ID}, E. Kasimi ^{152, ID}, J. Katzy ^{48, ID}, S. Kaur ^{34, ID}, K. Kawade ^{140, ID}, T. Kawamoto ^{135, ID},
 E.F. Kay ^{36, ID}, F.I. Kaya ^{158, ID}, S. Kazakos ^{107, ID}, V.F. Kazanin ^{37, ID}, Y. Ke ^{145, ID}, J.M. Keaveney ^{33a, ID},
 R. Keeler ^{165, ID}, G.V. Kehris ^{61, ID}, J.S. Keller ^{34, ID}, A.S. Kelly ⁹⁶, J.J. Kempster ^{146, ID}, K.E. Kennedy ^{41, ID},
 P.D. Kennedy ^{100, ID}, O. Kepka ^{131, ID}, B.P. Kerridge ^{167, ID}, S. Kersten ^{171, ID}, B.P. Kerševan ^{93, ID}, S. Keshri ^{66, ID},
 L. Keszeghova ^{28a, ID}, S. Ketabchi Haghight ^{155, ID}, M. Khandoga ^{127, ID}, A. Khanov ^{121, ID},
 A.G. Kharlamov ^{37, ID}, T. Kharlamova ^{37, ID}, E.E. Khoda ^{138, ID}, T.J. Khoo ^{18, ID}, G. Khoriauli ^{166, ID},
 J. Khubua ^{149b, ID}, Y.A.R. Khwaira ^{66, ID}, M. Kiehn ^{36, ID}, A. Kilgallon ^{123, ID}, D.W. Kim ^{47a, 47b, ID}, Y.K. Kim ^{39, ID},
 N. Kimura ^{96, ID}, A. Kirchhoff ^{55, ID}, C. Kirfel ^{24, ID}, F. Kirfel ^{24, ID}, J. Kirk ^{134, ID}, A.E. Kiryunin ^{110, ID},
 C. Kitsaki ^{10, ID}, O. Kivernyk ^{24, ID}, M. Klassen ^{63a, ID}, C. Klein ^{34, ID}, L. Klein ^{166, ID}, M.H. Klein ^{106, ID},
 M. Klein ^{92, ID}, S.B. Klein ^{56, ID}, U. Klein ^{92, ID}, P. Klimek ^{36, ID}, A. Klimentov ^{29, ID}, T. Klioutchnikova ^{36, ID},
 P. Kluit ^{114, ID}, S. Kluth ^{110, ID}, E. Kneringer ^{79, ID}, T.M. Knight ^{155, ID}, A. Knue ^{54, ID}, R. Kobayashi ^{87, ID},
 S.F. Koch ^{126, ID}, M. Kocian ^{143, ID}, P. Kodyš ^{133, ID}, D.M. Koeck ^{123, ID}, P.T. Koenig ^{24, ID}, T. Koffas ^{34, ID},
 M. Kolb ^{135, ID}, I. Koletsou ^{4, ID}, T. Komarek ^{122, ID}, K. Köneke ^{54, ID}, A.X.Y. Kong ^{1, ID}, T. Kono ^{118, ID},
 N. Konstantinidis ^{96, ID}, B. Konya ^{98, ID}, R. Kopeliansky ^{68, ID}, S. Koperny ^{85a, ID}, K. Korcyl ^{86, ID},
 K. Kordas ^{152, ID, f}, G. Koren ^{151, ID}, A. Korn ^{96, ID}, S. Korn ^{55, ID}, I. Korolkov ^{13, ID}, N. Korotkova ^{37, ID},
 B. Kortman ^{114, ID}, O. Kortner ^{110, ID}, S. Kortner ^{110, ID}, W.H. Kostecka ^{115, ID}, V.V. Kostyukhin ^{141, ID},
 A. Kotsokechagia ^{135, ID}, A. Kotwal ^{51, ID}, A. Koulouris ^{36, ID}, A. Kourkoumeli-Charalampidi ^{73a, 73b, ID},
 C. Kourkoumelis ^{9, ID}, E. Kourlitis ^{6, ID}, O. Kovanda ^{146, ID}, R. Kowalewski ^{165, ID}, W. Kozanecki ^{135, ID},
 A.S. Kozhin ^{37, ID}, V.A. Kramarenko ^{37, ID}, G. Kramberger ^{93, ID}, P. Kramer ^{100, ID}, M.W. Krasny ^{127, ID},
 A. Krasznahorkay ^{36, ID}, J.W. Kraus ^{171, ID}, J.A. Kremer ^{100, ID}, T. Kresse ^{50, ID}, J. Kretzschmar ^{92, ID},
 K. Kreul ^{18, ID}, P. Krieger ^{155, ID}, S. Krishnamurthy ^{103, ID}, M. Krivos ^{133, ID}, K. Krizka ^{20, ID}, K. Kroeninger ^{49, ID},
 H. Kroha ^{110, ID}, J. Kroll ^{131, ID}, J. Kroll ^{128, ID}, K.S. Krowpman ^{107, ID}, U. Kruchonak ^{38, ID}, H. Krüger ^{24, ID},
 N. Krumnack ⁸¹, M.C. Kruse ^{51, ID}, J.A. Krzysiak ^{86, ID}, O. Kuchinskaia ^{37, ID}, S. Kuday ^{3a, ID}, S. Kuehn ^{36, ID},
 R. Kuesters ^{54, ID}, T. Kuhl ^{48, ID}, V. Kukhtin ^{38, ID}, Y. Kulchitsky ^{37, ID, a}, S. Kuleshov ^{137d, 137b, ID},
 M. Kumar ^{33g, ID}, N. Kumari ^{102, ID}, A. Kupco ^{131, ID}, T. Kupfer ⁴⁹, A. Kupich ^{37, ID}, O. Kuprash ^{54, ID},
 H. Kurashige ^{84, ID}, L.L. Kurchaninov ^{156a, ID}, O. Kurdysh ^{66, ID}, Y.A. Kurochkin ^{37, ID}, A. Kurova ^{37, ID},
 M. Kuze ^{154, ID}, A.K. Kvam ^{103, ID}, J. Kvita ^{122, ID}, T. Kwan ^{104, ID}, N.G. Kyriacou ^{106, ID}, L.A.O. Laatu ^{102, ID},
 C. Lacasta ^{163, ID}, F. Lacava ^{75a, 75b, ID}, H. Lacker ^{18, ID}, D. Lacour ^{127, ID}, N.N. Lad ^{96, ID}, E. Ladygin ^{38, ID},
 B. Laforge ^{127, ID}, T. Lagouri ^{137e, ID}, S. Lai ^{55, ID}, I.K. Lakomiec ^{85a, ID}, N. Lalloue ^{60, ID}, J.E. Lambert ^{165, ID, m},
 S. Lammers ^{68, ID}, W. Lampl ^{7, ID}, C. Lampoudis ^{152, ID, f}, A.N. Lancaster ^{115, ID}, E. Lançon ^{29, ID},
 U. Landgraf ^{54, ID}, M.P.J. Landon ^{94, ID}, V.S. Lang ^{54, ID}, R.J. Langenberg ^{103, ID}, O.K.B. Langrekken ^{125, ID},
 A.J. Lankford ^{160, ID}, F. Lanni ^{36, ID}, K. Lantzsch ^{24, ID}, A. Lanza ^{73a, ID}, A. Lapertosa ^{57b, 57a, ID},
 J.F. Laporte ^{135, ID}, T. Lari ^{71a, ID}, F. Lasagni Manghi ^{23b, ID}, M. Lassnig ^{36, ID}, V. Latonova ^{131, ID},
 A. Laudrain ^{100, ID}, A. Laurier ^{150, ID}, S.D. Lawlor ^{95, ID}, Z. Lawrence ^{101, ID}, M. Lazzaroni ^{71a, 71b, ID}, B. Le ¹⁰¹,
 E.M. Le Boulicaut ^{51, ID}, B. Leban ^{93, ID}, A. Lebedev ^{81, ID}, M. LeBlanc ^{36, ID}, F. Ledroit-Guillon ^{60, ID},
 A.C.A. Lee ⁹⁶, S.C. Lee ^{148, ID}, S. Lee ^{47a, 47b, ID}, T.F. Lee ^{92, ID}, L.L. Leeuw ^{33c, ID}, H.P. Lefebvre ^{95, ID},
 M. Lefebvre ^{165, ID}, C. Leggett ^{17a, ID}, G. Lehmann Miotto ^{36, ID}, M. Leigh ^{56, ID}, W.A. Leight ^{103, ID},
 W. Leinonen ^{113, ID}, A. Leisos ^{152, ID, v}, M.A.L. Leite ^{82c, ID}, C.E. Leitgeb ^{48, ID}, R. Leitner ^{133, ID},
 K.J.C. Leney ^{44, ID}, T. Lenz ^{24, ID}, S. Leone ^{74a, ID}, C. Leonidopoulos ^{52, ID}, A. Leopold ^{144, ID}, C. Leroy ^{108, ID},
 R. Les ^{107, ID}, C.G. Lester ^{32, ID}, M. Levchenko ^{37, ID}, J. Levêque ^{4, ID}, D. Levin ^{106, ID}, L.J. Levinson ^{169, ID},
 M.P. Lewicki ^{86, ID}, D.J. Lewis ^{4, ID}, A. Li ^{5, ID}, B. Li ^{62b, ID}, C. Li ^{62a}, C-Q. Li ^{62c, ID}, H. Li ^{62a, ID}, H. Li ^{62b, ID},
 H. Li ^{14c, ID}, H. Li ^{62b, ID}, K. Li ^{138, ID}, L. Li ^{62c, ID}, M. Li ^{14a, 14e, ID}, Q.Y. Li ^{62a, ID}, S. Li ^{14a, 14e, ID}, S. Li ^{62d, 62c, ID, e},

- T. Li ^{5, ID, c}, X. Li ^{104, ID}, Z. Li ^{126, ID}, Z. Li ^{104, ID}, Z. Li ^{92, ID}, Z. Li ^{14a, 14e, ID}, Z. Liang ^{14a, ID}, M. Liberatore ^{48, ID},
 B. Liberti ^{76a, ID}, K. Lie ^{64c, ID}, J. Lieber Marin ^{82b, ID}, H. Lien ^{68, ID}, K. Lin ^{107, ID}, R.E. Lindley ^{7, ID},
 J.H. Lindon ^{2, ID}, A. Linss ^{48, ID}, E. Lipeles ^{128, ID}, A. Lipniacka ^{16, ID}, A. Lister ^{164, ID}, J.D. Little ^{4, ID}, B. Liu ^{14a, ID},
 B.X. Liu ^{142, ID}, D. Liu ^{62d, 62c, ID}, J.B. Liu ^{62a, ID}, J.K.K. Liu ^{32, ID}, K. Liu ^{62d, 62c, ID}, M. Liu ^{62a, ID}, M.Y. Liu ^{62a, ID},
 P. Liu ^{14a, ID}, Q. Liu ^{62d, 138, 62c, ID}, X. Liu ^{62a, ID}, Y. Liu ^{14d, 14e, ID}, Y.L. Liu ^{106, ID}, Y.W. Liu ^{62a, ID},
 J. Llorente Merino ^{142, ID}, S.L. Lloyd ^{94, ID}, E.M. Lobodzinska ^{48, ID}, P. Loch ^{7, ID}, S. Loffredo ^{76a, 76b, ID},
 T. Lohse ^{18, ID}, K. Lohwasser ^{139, ID}, E. Loiacono ^{48, ID}, M. Lokajicek ^{131, ID, *}, J.D. Lomas ^{20, ID}, J.D. Long ^{162, ID},
 I. Longarini ^{160, ID}, L. Longo ^{70a, 70b, ID}, R. Longo ^{162, ID}, I. Lopez Paz ^{67, ID}, A. Lopez Solis ^{48, ID}, J. Lorenz ^{109, ID},
 N. Lorenzo Martinez ^{4, ID}, A.M. Lory ^{109, ID}, O. Loseva ^{37, ID}, X. Lou ^{47a, 47b, ID}, X. Lou ^{14a, 14e, ID}, A. Lounis ^{66, ID},
 J. Love ^{6, ID}, P.A. Love ^{91, ID}, G. Lu ^{14a, 14e, ID}, M. Lu ^{80, ID}, S. Lu ^{128, ID}, Y.J. Lu ^{65, ID}, H.J. Lubatti ^{138, ID},
 C. Luci ^{75a, 75b, ID}, F.L. Lucio Alves ^{14c, ID}, A. Lucotte ^{60, ID}, F. Luehring ^{68, ID}, I. Luise ^{145, ID}, O. Lukianchuk ^{66, ID},
 O. Lundberg ^{144, ID}, B. Lund-Jensen ^{144, ID}, N.A. Luongo ^{123, ID}, M.S. Lutz ^{151, ID}, D. Lynn ^{29, ID}, H. Lyons ⁹²,
 R. Lysak ^{131, ID}, E. Lytken ^{98, ID}, V. Lyubushkin ^{38, ID}, T. Lyubushkina ^{38, ID}, M.M. Lyukova ^{145, ID}, H. Ma ^{29, ID},
 L.L. Ma ^{62b, ID}, Y. Ma ^{121, ID}, D.M. Mac Donell ^{165, ID}, G. Maccarrone ^{53, ID}, J.C. MacDonald ^{100, ID},
 R. Madar ^{40, ID}, W.F. Mader ^{50, ID}, J. Maeda ^{84, ID}, T. Maeno ^{29, ID}, M. Maerker ^{50, ID}, H. Maguire ^{139, ID},
 V. Maiboroda ^{135, ID}, A. Maio ^{130a, 130b, 130d, ID}, K. Maj ^{85a, ID}, O. Majersky ^{48, ID}, S. Majewski ^{123, ID},
 N. Makovec ^{66, ID}, V. Maksimovic ^{15, ID}, B. Malaescu ^{127, ID}, Pa. Malecki ^{86, ID}, V.P. Maleev ^{37, ID}, F. Malek ^{60, ID},
 M. Mali ^{93, ID}, D. Malito ^{95, ID, q}, U. Mallik ^{80, ID}, S. Maltezos ¹⁰, S. Malyukov ³⁸, J. Mamuzic ^{13, ID},
 G. Mancini ^{53, ID}, G. Manco ^{73a, 73b, ID}, J.P. Mandalia ^{94, ID}, I. Mandić ^{93, ID},
 L. Manhaes de Andrade Filho ^{82a, ID}, I.M. Maniatis ^{169, ID}, J. Manjarres Ramos ^{102, ID, ae}, D.C. Mankad ^{169, ID},
 A. Mann ^{109, ID}, B. Mansoulie ^{135, ID}, S. Manzoni ^{36, ID}, A. Marantis ^{152, ID, v}, G. Marchiori ^{5, ID},
 M. Marcisovsky ^{131, ID}, C. Marcon ^{71a, 71b, ID}, M. Marinescu ^{20, ID}, M. Marjanovic ^{120, ID}, E.J. Marshall ^{91, ID},
 Z. Marshall ^{17a, ID}, S. Marti-Garcia ^{163, ID}, T.A. Martin ^{167, ID}, V.J. Martin ^{52, ID}, B. Martin dit Latour ^{16, ID},
 L. Martinelli ^{75a, 75b, ID}, M. Martinez ^{13, ID, w}, P. Martinez Agullo ^{163, ID}, V.I. Martinez Outschoorn ^{103, ID},
 P. Martinez Suarez ^{13, ID}, S. Martin-Haugh ^{134, ID}, V.S. Martoiu ^{27b, ID}, A.C. Martyniuk ^{96, ID}, A. Marzin ^{36, ID},
 D. Mascione ^{78a, 78b, ID}, L. Masetti ^{100, ID}, T. Mashimo ^{153, ID}, J. Masik ^{101, ID}, A.L. Maslennikov ^{37, ID},
 L. Massa ^{23b, ID}, P. Massarotti ^{72a, 72b, ID}, P. Mastrandrea ^{74a, 74b, ID}, A. Mastroberardino ^{43b, 43a, ID},
 T. Masubuchi ^{153, ID}, T. Mathisen ^{161, ID}, J. Matousek ^{133, ID}, N. Matsuzawa ¹⁵³, J. Maurer ^{27b, ID},
 B. Maček ^{93, ID}, D.A. Maximov ^{37, ID}, R. Mazini ^{148, ID}, I. Maznas ^{152, ID}, M. Mazza ^{107, ID}, S.M. Mazza ^{136, ID},
 E. Mazzeo ^{71a, 71b, ID}, C. Mc Ginn ^{29, ID}, J.P. Mc Gowan ^{104, ID}, S.P. Mc Kee ^{106, ID}, E.F. McDonald ^{105, ID},
 A.E. McDougall ^{114, ID}, J.A. Mcfayden ^{146, ID}, R.P. McGovern ^{128, ID}, G. Mchedlidze ^{149b, ID},
 R.P. Mckenzie ^{33g, ID}, T.C. McLachlan ^{48, ID}, D.J. McLaughlin ^{96, ID}, K.D. McLean ^{165, ID}, S.J. McMahon ^{134, ID},
 P.C. McNamara ^{105, ID}, C.M. Mcpartland ^{92, ID}, R.A. McPherson ^{165, ID, aa}, S. Mehlhase ^{109, ID}, A. Mehta ^{92, ID},
 D. Melini ^{150, ID}, B.R. Mellado Garcia ^{33g, ID}, A.H. Melo ^{55, ID}, F. Meloni ^{48, ID},
 A.M. Mendes Jacques Da Costa ^{101, ID}, H.Y. Meng ^{155, ID}, L. Meng ^{91, ID}, S. Menke ^{110, ID}, M. Mentink ^{36, ID},
 E. Meoni ^{43b, 43a, ID}, C. Merlassino ^{126, ID}, L. Merola ^{72a, 72b, ID}, C. Meroni ^{71a, ID}, G. Merz ¹⁰⁶, O. Meshkov ^{37, ID},
 J. Metcalfe ^{6, ID}, A.S. Mete ^{6, ID}, C. Meyer ^{68, ID}, J-P. Meyer ^{135, ID}, R.P. Middleton ^{134, ID}, L. Mijović ^{52, ID},
 G. Mikenberg ^{169, ID}, M. Mikestikova ^{131, ID}, M. Mikuž ^{93, ID}, H. Mildner ^{100, ID}, A. Milic ^{36, ID}, C.D. Milke ^{44, ID},
 D.W. Miller ^{39, ID}, L.S. Miller ^{34, ID}, A. Milov ^{169, ID}, D.A. Milstead ^{47a, 47b}, T. Min ^{14c}, A.A. Minaenko ^{37, ID},
 I.A. Minashvili ^{149b, ID}, L. Mince ^{59, ID}, A.I. Mincer ^{117, ID}, B. Mindur ^{85a, ID}, M. Mineev ^{38, ID}, Y. Mino ^{87, ID},
 L.M. Mir ^{13, ID}, M. Miralles Lopez ^{163, ID}, M. Mironova ^{17a, ID}, A. Mishima ¹⁵³, M.C. Missio ^{113, ID},
 T. Mitani ^{168, ID}, A. Mitra ^{167, ID}, V.A. Mitsou ^{163, ID}, O. Miu ^{155, ID}, P.S. Miyagawa ^{94, ID}, Y. Miyazaki ⁸⁹,

- A. Mizukami 83, ID, T. Mkrtchyan 63a, ID, M. Mlinarevic 96, ID, T. Mlinarevic 96, ID, M. Mlynarikova 36, ID,
 S. Mobius 19, ID, K. Mochizuki 108, ID, P. Moder 48, ID, P. Mogg 109, ID, A.F. Mohammed 14a, 14e, ID,
 S. Mohapatra 41, ID, G. Mokgatitswane 33g, ID, L. Moleri 169, ID, B. Mondal 141, ID, S. Mondal 132, ID,
 G. Monig 146, ID, K. Mönig 48, ID, E. Monnier 102, ID, L. Monsonis Romero 163, J. Montejo Berlingen 13, 83, ID,
 M. Montella 119, ID, F. Monticelli 90, ID, S. Monzani 69a, 69c, ID, N. Morange 66, ID,
 A.L. Moreira De Carvalho 130a, ID, M. Moreno Llácer 163, ID, C. Moreno Martinez 56, ID, P. Morettini 57b, ID,
 S. Morgenstern 36, ID, M. Morii 61, ID, M. Morinaga 153, ID, A.K. Morley 36, ID, F. Morodei 75a, 75b, ID,
 L. Morvaj 36, ID, P. Moschovakos 36, ID, B. Moser 36, ID, M. Mosidze 149b, T. Moskalets 54, ID,
 P. Moskvitina 113, ID, J. Moss 31, ID, o, E.J.W. Moyse 103, ID, O. Mtintsilana 33g, ID, S. Muanza 102, ID,
 J. Mueller 129, ID, D. Muenstermann 91, ID, R. Müller 19, ID, G.A. Mullier 161, ID, A.J. Mullin 32, J.J. Mullin 128,
 D.P. Mungo 155, ID, D. Munoz Perez 163, ID, F.J. Munoz Sanchez 101, ID, M. Murin 101, ID, W.J. Murray 167, 134, ID,
 A. Murrone 71a, 71b, ID, J.M. Muse 120, ID, M. Muškinja 17a, ID, C. Mwewa 29, ID, A.G. Myagkov 37, ID, a,
 A.J. Myers 8, ID, A.A. Myers 129, G. Myers 68, ID, M. Myska 132, ID, B.P. Nachman 17a, ID, O. Nackenhorst 49, ID,
 A. Nag 50, ID, K. Nagai 126, ID, K. Nagano 83, ID, J.L. Nagle 29, ID, al, E. Nagy 102, ID, A.M. Nairz 36, ID,
 Y. Nakahama 83, ID, K. Nakamura 83, ID, K. Nakkalil 5, ID, H. Nanjo 124, ID, R. Narayan 44, ID,
 E.A. Narayanan 112, ID, I. Naryshkin 37, ID, M. Naseri 34, ID, S. Nasri 159, ID, C. Nass 24, ID, G. Navarro 22a, ID,
 J. Navarro-Gonzalez 163, ID, R. Nayak 151, ID, A. Nayaz 18, ID, P.Y. Nechaeva 37, ID, F. Nechansky 48, ID,
 L. Nedic 126, ID, T.J. Neep 20, ID, A. Negri 73a, 73b, ID, M. Negrini 23b, ID, C. Nellist 114, ID, C. Nelson 104, ID,
 K. Nelson 106, ID, S. Nemecek 131, ID, M. Nessi 36, ID, i, M.S. Neubauer 162, ID, F. Neuhaus 100, ID,
 J. Neundorf 48, ID, R. Newhouse 164, ID, P.R. Newman 20, ID, C.W. Ng 129, ID, Y.W.Y. Ng 48, ID, B. Ngair 35e, ID,
 H.D.N. Nguyen 108, ID, R.B. Nickerson 126, ID, R. Nicolaïdou 135, ID, J. Nielsen 136, ID, M. Niemeyer 55, ID,
 J. Niermann 55, 36, ID, N. Nikiforou 36, ID, V. Nikolaenko 37, ID, a, I. Nikolic-Audit 127, ID, K. Nikolopoulos 20, ID,
 P. Nilsson 29, ID, I. Ninca 48, ID, H.R. Nindhito 56, ID, G. Ninio 151, ID, A. Nisati 75a, ID, N. Nishu 2, ID,
 R. Nisius 110, ID, J-E. Nitschke 50, ID, E.K. Nkademeng 33g, ID, S.J. Noacco Rosende 90, ID, T. Nobe 153, ID,
 D.L. Noel 32, ID, T. Nommensen 147, ID, M.B. Norfolk 139, ID, R.R.B. Norisam 96, ID, B.J. Norman 34, ID,
 J. Novak 93, ID, T. Novak 48, ID, L. Novotny 132, ID, R. Novotny 112, ID, L. Nozka 122, ID, K. Ntekas 160, ID,
 N.M.J. Nunes De Moura Junior 82b, ID, E. Nurse 96, J. Ocariz 127, ID, A. Ochi 84, ID, I. Ochoa 130a, ID,
 S. Oerdekk 161, ID, J.T. Offermann 39, ID, A. Ogrodnik 133, ID, A. Oh 101, ID, C.C. Ohm 144, ID, H. Oide 83, ID,
 R. Oishi 153, ID, M.L. Ojeda 48, ID, Y. Okazaki 87, ID, M.W. O'Keefe 92, Y. Okumura 153, ID,
 L.F. Oleiro Seabra 130a, ID, S.A. Olivares Pino 137d, ID, D. Oliveira Damazio 29, ID, D. Oliveira Goncalves 82a, ID,
 J.L. Oliver 160, ID, M.J.R. Olsson 160, ID, A. Olszewski 86, ID, Ö.O. Öncel 54, ID, D.C. O'Neil 142, ID, A.P. O'Neill 19, ID,
 A. Onofre 130a, 130e, ID, P.U.E. Onyisi 11, ID, M.J. Oreglia 39, ID, G.E. Orellana 90, ID, D. Orestano 77a, 77b, ID,
 N. Orlando 13, ID, R.S. Orr 155, ID, V. O'Shea 59, ID, L.M. Osojnak 128, ID, R. Ospanov 62a, ID,
 G. Otero y Garzon 30, ID, H. Otono 89, ID, P.S. Ott 63a, ID, G.J. Ottino 17a, ID, M. Ouchrif 35d, ID, J. Ouellette 29, ID,
 F. Ould-Saada 125, ID, M. Owen 59, ID, R.E. Owen 134, ID, K.Y. Oyulmaz 21a, ID, V.E. Ozcan 21a, ID, N. Ozturk 8, ID,
 S. Ozturk 21d, ID, H.A. Pacey 32, ID, A. Pacheco Pages 13, ID, C. Padilla Aranda 13, ID, G. Padovano 75a, 75b, ID,
 S. Pagan Griso 17a, ID, G. Palacino 68, ID, A. Palazzo 70a, 70b, ID, S. Palestini 36, ID, J. Pan 172, ID, T. Pan 64a, ID,
 D.K. Panchal 11, ID, C.E. Pandini 114, ID, J.G. Panduro Vazquez 95, ID, H. Pang 14b, ID, P. Pani 48, ID,
 G. Panizzo 69a, 69c, ID, L. Paolozzi 56, ID, C. Papadatos 108, ID, S. Parajuli 44, ID, A. Paramonov 6, ID,
 C. Paraskevopoulos 10, ID, D. Paredes Hernandez 64b, ID, T.H. Park 155, ID, M.A. Parker 32, ID, F. Parodi 57b, 57a, ID,
 E.W. Parrish 115, ID, V.A. Parrish 52, ID, J.A. Parsons 41, ID, U. Parzefall 54, ID, B. Pascual Dias 108, ID,
 L. Pascual Dominguez 151, ID, F. Pasquali 114, ID, E. Pasqualucci 75a, ID, S. Passaggio 57b, ID, F. Pastore 95, ID,

- P. Pasuwan ^{47a,47b, ID}, P. Patel ^{86, ID}, U.M. Patel ^{51, ID}, J.R. Pater ^{101, ID}, T. Pauly ^{36, ID}, J. Pearkes ^{143, ID}, M. Pedersen ^{125, ID}, R. Pedro ^{130a, ID}, S.V. Peleganchuk ^{37, ID}, O. Penc ^{36, ID}, E.A. Pender ^{52, ID}, H. Peng ^{62a, ID}, K.E. Penski ^{109, ID}, M. Penzin ^{37, ID}, B.S. Peralva ^{82d, ID}, A.P. Pereira Peixoto ^{60, ID}, L. Pereira Sanchez ^{47a,47b, ID}, D.V. Perepelitsa ^{29, ID, al}, E. Perez Codina ^{156a, ID}, M. Perganti ^{10, ID}, L. Perini ^{71a,71b, ID, *}, H. Pernegger ^{36, ID}, A. Perrevoort ^{113, ID}, O. Perrin ^{40, ID}, K. Peters ^{48, ID}, R.F.Y. Peters ^{101, ID}, B.A. Petersen ^{36, ID}, T.C. Petersen ^{42, ID}, E. Petit ^{102, ID}, V. Petousis ^{132, ID}, C. Petridou ^{152, ID, f}, A. Petrukhin ^{141, ID}, M. Pettee ^{17a, ID}, N.E. Pettersson ^{36, ID}, A. Petukhov ^{37, ID}, K. Petukhova ^{133, ID}, A. Peyaud ^{135, ID}, R. Pezoa ^{137f, ID}, L. Pezzotti ^{36, ID}, G. Pezzullo ^{172, ID}, T.M. Pham ^{170, ID}, T. Pham ^{105, ID}, P.W. Phillips ^{134, ID}, G. Piacquadio ^{145, ID}, E. Pianori ^{17a, ID}, F. Piazza ^{71a,71b, ID}, R. Piegaia ^{30, ID}, D. Pietreanu ^{27b, ID}, A.D. Pilkington ^{101, ID}, M. Pinamonti ^{69a,69c, ID}, J.L. Pinfold ^{2, ID}, B.C. Pinheiro Pereira ^{130a, ID}, A.E. Pinto Pinoargote ^{135, ID}, K.M. Piper ^{146, ID}, C. Pitman Donaldson ⁹⁶, D.A. Pizzi ^{34, ID}, L. Pizzimento ^{76a,76b, ID}, A. Pizzini ^{114, ID}, M.-A. Pleier ^{29, ID}, V. Plesanovs ⁵⁴, V. Pleskot ^{133, ID}, E. Plotnikova ³⁸, G. Poddar ^{4, ID}, R. Poettgen ^{98, ID}, L. Poggioli ^{127, ID}, I. Pokharel ^{55, ID}, S. Polacek ^{133, ID}, G. Polesello ^{73a, ID}, A. Poley ^{142,156a, ID}, R. Polifka ^{132, ID}, A. Polini ^{23b, ID}, C.S. Pollard ^{167, ID}, Z.B. Pollock ^{119, ID}, V. Polychronakos ^{29, ID}, E. Pompa Pacchi ^{75a,75b, ID}, D. Ponomarenko ^{113, ID}, L. Pontecorvo ^{36, ID}, S. Popa ^{27a, ID}, G.A. Popeneiciu ^{27d, ID}, A. Poreba ^{36, ID}, D.M. Portillo Quintero ^{156a, ID}, S. Pospisil ^{132, ID}, M.A. Postill ^{139, ID}, P. Postolache ^{27c, ID}, K. Potamianos ^{167, ID}, P.A. Potepa ^{85a, ID}, I.N. Potrap ^{38, ID}, C.J. Potter ^{32, ID}, H. Potti ^{1, ID}, T. Poulsen ^{48, ID}, J. Poveda ^{163, ID}, M.E. Pozo Astigarraga ^{36, ID}, A. Prades Ibanez ^{163, ID}, J. Pretel ^{54, ID}, D. Price ^{101, ID}, M. Primavera ^{70a, ID}, M.A. Principe Martin ^{99, ID}, R. Privara ^{122, ID}, T. Procter ^{59, ID}, M.L. Proffitt ^{138, ID}, N. Proklova ^{128, ID}, K. Prokofiev ^{64c, ID}, G. Proto ^{110, ID}, S. Protopopescu ^{29, ID}, J. Proudfoot ^{6, ID}, M. Przybycien ^{85a, ID}, W.W. Przygoda ^{85b, ID}, J.E. Puddefoot ^{139, ID}, D. Pudzha ^{37, ID}, D. Pyatiizbyantseva ^{37, ID}, J. Qian ^{106, ID}, D. Qichen ^{101, ID}, Y. Qin ^{101, ID}, T. Qiu ^{52, ID}, A. Quadt ^{55, ID}, M. Queitsch-Maitland ^{101, ID}, G. Quetant ^{56, ID}, G. Rabanal Bolanos ^{61, ID}, D. Rafanoharana ^{54, ID}, F. Ragusa ^{71a,71b, ID}, J.L. Rainbolt ^{39, ID}, J.A. Raine ^{56, ID}, S. Rajagopalan ^{29, ID}, E. Ramakoti ^{37, ID}, K. Ran ^{48,14e, ID}, N.P. Rapheeha ^{33g, ID}, H. Rasheed ^{27b, ID}, V. Raskina ^{127, ID}, D.F. Rassloff ^{63a, ID}, S. Rave ^{100, ID}, B. Ravina ^{55, ID}, I. Ravinovich ^{169, ID}, M. Raymond ^{36, ID}, A.L. Read ^{125, ID}, N.P. Readioff ^{139, ID}, D.M. Rebuzzi ^{73a,73b, ID}, G. Redlinger ^{29, ID}, A.S. Reed ^{110, ID}, K. Reeves ^{26, ID}, J.A. Reidelsturz ^{171, ID}, D. Reikher ^{151, ID}, A. Rej ^{141, ID}, C. Rembser ^{36, ID}, A. Renardi ^{48, ID}, M. Renda ^{27b, ID}, M.B. Rendel ¹¹⁰, F. Renner ^{48, ID}, A.G. Rennie ^{59, ID}, S. Resconi ^{71a, ID}, M. Ressegotti ^{57b,57a, ID}, S. Rettie ^{36, ID}, J.G. Reyes Rivera ^{107, ID}, B. Reynolds ¹¹⁹, E. Reynolds ^{17a, ID}, O.L. Rezanova ^{37, ID}, P. Reznicek ^{133, ID}, N. Ribaric ^{91, ID}, E. Ricci ^{78a,78b, ID}, R. Richter ^{110, ID}, S. Richter ^{47a,47b, ID}, E. Richter-Was ^{85b, ID}, M. Ridel ^{127, ID}, S. Ridouani ^{35d, ID}, P. Rieck ^{117, ID}, P. Riedler ^{36, ID}, M. Rijssenbeek ^{145, ID}, A. Rimoldi ^{73a,73b, ID}, M. Rimoldi ^{48, ID}, L. Rinaldi ^{23b,23a, ID}, T.T. Rinn ^{29, ID}, M.P. Rinnagel ^{109, ID}, G. Ripellino ^{161, ID}, I. Riu ^{13, ID}, P. Rivadeneira ^{48, ID}, J.C. Rivera Vergara ^{165, ID}, F. Rizatdinova ^{121, ID}, E. Rizvi ^{94, ID}, B.A. Roberts ^{167, ID}, B.R. Roberts ^{17a, ID}, S.H. Robertson ^{104, ID, aa}, M. Robin ^{48, ID}, D. Robinson ^{32, ID}, C.M. Robles Gajardo ^{137f}, M. Robles Manzano ^{100, ID}, A. Robson ^{59, ID}, A. Rocchi ^{76a,76b, ID}, C. Roda ^{74a,74b, ID}, S. Rodriguez Bosca ^{63a, ID}, Y. Rodriguez Garcia ^{22a, ID}, A. Rodriguez Rodriguez ^{54, ID}, A.M. Rodriguez Vera ^{156b, ID}, S. Roe ³⁶, J.T. Roemer ^{160, ID}, A.R. Roepe-Gier ^{136, ID}, J. Roggel ^{171, ID}, O. Røhne ^{125, ID}, R.A. Rojas ^{103, ID}, C.P.A. Roland ^{68, ID}, J. Roloff ^{29, ID}, A. Romaniouk ^{37, ID}, E. Romano ^{73a,73b, ID}, M. Romano ^{23b, ID}, A.C. Romero Hernandez ^{162, ID}, N. Rompotis ^{92, ID}, L. Roos ^{127, ID}, S. Rosati ^{75a, ID}, B.J. Rosser ^{39, ID}, E. Rossi ^{126, ID}, E. Rossi ^{72a,72b, ID}, L.P. Rossi ^{57b, ID}, L. Rossini ^{48, ID}, R. Rosten ^{119, ID}, M. Rotaru ^{27b, ID}, B. Rottler ^{54, ID}, C. Rougier ^{102, ID, ae}, D. Rousseau ^{66, ID}, D. Rousso ^{32, ID}, A. Roy ^{162, ID}, S. Roy-Garand ^{155, ID}, A. Rozanov ^{102, ID}, Y. Rozen ^{150, ID},

- X. Ruan ^{33g, ID}, A. Rubio Jimenez ^{163, ID}, A.J. Ruby ^{92, ID}, V.H. Ruelas Rivera ^{18, ID}, T.A. Ruggieri ^{1, ID},
 A. Ruggiero ^{126, ID}, A. Ruiz-Martinez ^{163, ID}, A. Rummller ^{36, ID}, Z. Rurikova ^{54, ID}, N.A. Rusakovich ^{38, ID},
 H.L. Russell ^{165, ID}, G. Russo ^{75a, 75b, ID}, J.P. Rutherford ^{7, ID}, S. Rutherford Colmenares ^{32, ID}, K. Rybacki ⁹¹,
 M. Rybar ^{133, ID}, E.B. Rye ^{125, ID}, A. Ryzhov ^{44, ID}, J.A. Sabater Iglesias ^{56, ID}, P. Sabatini ^{163, ID},
 L. Sabetta ^{75a, 75b, ID}, H.F-W. Sadrozinski ^{136, ID}, F. Safai Tehrani ^{75a, ID}, B. Safarzadeh Samani ^{146, ID},
 M. Safdari ^{143, ID}, S. Saha ^{165, ID}, M. Sahinsoy ^{110, ID}, M. Saimpert ^{135, ID}, M. Saito ^{153, ID}, T. Saito ^{153, ID},
 D. Salamani ^{36, ID}, A. Salnikov ^{143, ID}, J. Salt ^{163, ID}, A. Salvador Salas ^{13, ID}, D. Salvatore ^{43b, 43a, ID},
 F. Salvatore ^{146, ID}, A. Salzburger ^{36, ID}, D. Sammel ^{54, ID}, D. Sampsonidis ^{152, ID, f}, D. Sampsonidou ^{123, ID},
 J. Sánchez ^{163, ID}, A. Sanchez Pineda ^{4, ID}, V. Sanchez Sebastian ^{163, ID}, H. Sandaker ^{125, ID}, C.O. Sander ^{48, ID},
 J.A. Sandesara ^{103, ID}, M. Sandhoff ^{171, ID}, C. Sandoval ^{22b, ID}, D.P.C. Sankey ^{134, ID}, T. Sano ^{87, ID},
 A. Sansoni ^{53, ID}, L. Santi ^{75a, 75b, ID}, C. Santoni ^{40, ID}, H. Santos ^{130a, 130b, ID}, S.N. Santpur ^{17a, ID},
 A. Santra ^{169, ID}, K.A. Saoucha ^{139, ID}, J.G. Saraiva ^{130a, 130d, ID}, J. Sardain ^{7, ID}, O. Sasaki ^{83, ID}, K. Sato ^{157, ID},
 C. Sauer ^{63b}, F. Sauerburger ^{54, ID}, E. Sauvan ^{4, ID}, P. Savard ^{155, ID, aj}, R. Sawada ^{153, ID}, C. Sawyer ^{134, ID},
 L. Sawyer ^{97, ID}, I. Sayago Galvan ¹⁶³, C. Sbarra ^{23b, ID}, A. Sbrizzi ^{23b, 23a, ID}, T. Scanlon ^{96, ID},
 J. Schaarschmidt ^{138, ID}, P. Schacht ^{110, ID}, D. Schaefer ^{39, ID}, U. Schäfer ^{100, ID}, A.C. Schaffer ^{66, 44, ID},
 D. Schaile ^{109, ID}, R.D. Schamberger ^{145, ID}, C. Scharf ^{18, ID}, M.M. Schefer ^{19, ID}, V.A. Schegelsky ^{37, ID},
 D. Scheirich ^{133, ID}, F. Schenck ^{18, ID}, M. Schernau ^{160, ID}, C. Scheulen ^{55, ID}, C. Schiavi ^{57b, 57a, ID},
 E.J. Schioppa ^{70a, 70b, ID}, M. Schioppa ^{43b, 43a, ID}, B. Schlag ^{143, ID, r}, K.E. Schleicher ^{54, ID}, S. Schlenker ^{36, ID},
 J. Schmeing ^{171, ID}, M.A. Schmidt ^{171, ID}, K. Schmieden ^{100, ID}, C. Schmitt ^{100, ID}, S. Schmitt ^{48, ID},
 L. Schoeffel ^{135, ID}, A. Schoening ^{63b, ID}, P.G. Scholer ^{54, ID}, E. Schopf ^{126, ID}, M. Schott ^{100, ID},
 J. Schovancova ^{36, ID}, S. Schramm ^{56, ID}, F. Schroeder ^{171, ID}, T. Schroer ^{56, ID}, H-C. Schultz-Coulon ^{63a, ID},
 M. Schumacher ^{54, ID}, B.A. Schumm ^{136, ID}, Ph. Schune ^{135, ID}, A.J. Schuy ^{138, ID}, H.R. Schwartz ^{136, ID},
 A. Schwartzman ^{143, ID}, T.A. Schwarz ^{106, ID}, Ph. Schwemling ^{135, ID}, R. Schwienhorst ^{107, ID},
 A. Sciandra ^{136, ID}, G. Sciolla ^{26, ID}, F. Scuri ^{74a, ID}, C.D. Sebastiani ^{92, ID}, K. Sedlaczek ^{115, ID}, P. Seema ^{18, ID},
 S.C. Seidel ^{112, ID}, A. Seiden ^{136, ID}, B.D. Seidlitz ^{41, ID}, C. Seitz ^{48, ID}, J.M. Seixas ^{82b, ID}, G. Sekhniaidze ^{72a, ID},
 S.J. Sekula ^{44, ID}, L. Selem ^{60, ID}, N. Semprini-Cesari ^{23b, 23a, ID}, D. Sengupta ^{56, ID}, V. Senthilkumar ^{163, ID},
 L. Serin ^{66, ID}, L. Serkin ^{69a, 69b, ID}, M. Sessa ^{76a, 76b, ID}, H. Severini ^{120, ID}, F. Sforza ^{57b, 57a, ID}, A. Sfyrla ^{56, ID},
 E. Shabalina ^{55, ID}, R. Shaheen ^{144, ID}, J.D. Shahinian ^{128, ID}, D. Shaked Renous ^{169, ID}, L.Y. Shan ^{14a, ID},
 M. Shapiro ^{17a, ID}, A. Sharma ^{36, ID}, A.S. Sharma ^{164, ID}, P. Sharma ^{80, ID}, S. Sharma ^{48, ID}, P.B. Shatalov ^{37, ID},
 K. Shaw ^{146, ID}, S.M. Shaw ^{101, ID}, A. Shcherbakova ^{37, ID}, Q. Shen ^{62c, 5, ID}, P. Sherwood ^{96, ID}, L. Shi ^{96, ID},
 X. Shi ^{14a, ID}, C.O. Shimmin ^{172, ID}, Y. Shimogama ^{168, ID}, J.D. Shinner ^{95, ID}, I.P.J. Shipsey ^{126, ID},
 S. Shirabe ^{56, ID, i}, M. Shiyakova ^{38, ID, y}, J. Shlomi ^{169, ID}, M.J. Shochet ^{39, ID}, J. Shojaei ^{105, ID}, D.R. Shope ^{125, ID},
 S. Shrestha ^{119, ID, am}, E.M. Shrif ^{33g, ID}, M.J. Shroff ^{165, ID}, P. Sicho ^{131, ID}, A.M. Sickles ^{162, ID},
 E. Sideras Haddad ^{33g, ID}, A. Sidoti ^{23b, ID}, F. Siegert ^{50, ID}, Dj. Sijacki ^{15, ID}, R. Sikora ^{85a, ID}, F. Sili ^{90, ID},
 J.M. Silva ^{20, ID}, M.V. Silva Oliveira ^{29, ID}, S.B. Silverstein ^{47a, ID}, S. Simion ⁶⁶, R. Simoniello ^{36, ID},
 E.L. Simpson ^{59, ID}, H. Simpson ^{146, ID}, L.R. Simpson ^{106, ID}, N.D. Simpson ⁹⁸, S. Simsek ^{21d, ID}, S. Sindhu ^{55, ID},
 P. Sinervo ^{155, ID}, S. Singh ^{155, ID}, S. Sinha ^{48, ID}, S. Sinha ^{101, ID}, M. Sioli ^{23b, 23a, ID}, I. Siral ^{36, ID},
 E. Sitnikova ^{48, ID}, S.Yu. Sivoklokov ^{37, ID, *}, J. Sjölin ^{47a, 47b, ID}, A. Skaf ^{55, ID}, E. Skorda ^{98, ID}, P. Skubic ^{120, ID},
 M. Slawinska ^{86, ID}, V. Smakhtin ¹⁶⁹, B.H. Smart ^{134, ID}, J. Smiesko ^{36, ID}, S.Yu. Smirnov ^{37, ID}, Y. Smirnov ^{37, ID},
 L.N. Smirnova ^{37, ID, a}, O. Smirnova ^{98, ID}, A.C. Smith ^{41, ID}, E.A. Smith ^{39, ID}, H.A. Smith ^{126, ID}, J.L. Smith ^{92, ID},
 R. Smith ¹⁴³, M. Smizanska ^{91, ID}, K. Smolek ^{132, ID}, A.A. Snesarev ^{37, ID}, S.R. Snider ^{155, ID}, H.L. Snoek ^{114, ID},
 S. Snyder ^{29, ID}, R. Sobie ^{165, ID, aa}, A. Soffer ^{151, ID}, C.A. Solans Sanchez ^{36, ID}, E.Yu. Soldatov ^{37, ID},

- U. Soldevila ^{163, ID}, A.A. Solodkov ^{37, ID}, S. Solomon ^{26, ID}, A. Soloshenko ^{38, ID}, K. Solovieva ^{54, ID},
 O.V. Solovyanov ^{40, ID}, V. Solovyev ^{37, ID}, P. Sommer ^{36, ID}, A. Sonay ^{13, ID}, W.Y. Song ^{156b, ID},
 J.M. Sonneveld ^{114, ID}, A. Sopczak ^{132, ID}, A.L. Sopio ^{96, ID}, F. Sopkova ^{28b, ID}, V. Sothilingam ^{63a},
 S. Sottocornola ^{68, ID}, R. Soualah ^{116b, ID}, Z. Soumaimi ^{35e, ID}, D. South ^{48, ID}, S. Spagnolo ^{70a, 70b, ID},
 M. Spalla ^{110, ID}, D. Sperlich ^{54, ID}, G. Spigo ^{36, ID}, M. Spina ^{146, ID}, S. Spinali ^{91, ID}, D.P. Spiteri ^{59, ID},
 M. Spousta ^{133, ID}, E.J. Staats ^{34, ID}, A. Stabile ^{71a, 71b, ID}, R. Stamen ^{63a, ID}, M. Stamenkovic ^{114, ID},
 A. Stampekkis ^{20, ID}, M. Standke ^{24, ID}, E. Stanecka ^{86, ID}, M.V. Stange ^{50, ID}, B. Stanislaus ^{17a, ID},
 M.M. Stanitzki ^{48, ID}, B. Stapf ^{48, ID}, E.A. Starchenko ^{37, ID}, G.H. Stark ^{136, ID}, J. Stark ^{102, ID, ae}, D.M. Starko ^{156b},
 P. Staroba ^{131, ID}, P. Starovoitov ^{63a, ID}, S. Stärz ^{104, ID}, R. Staszewski ^{86, ID}, G. Stavropoulos ^{46, ID},
 J. Steentoft ^{161, ID}, P. Steinberg ^{29, ID}, B. Stelzer ^{142, 156a, ID}, H.J. Stelzer ^{129, ID}, O. Stelzer-Chilton ^{156a, ID},
 H. Stenzel ^{58, ID}, T.J. Stevenson ^{146, ID}, G.A. Stewart ^{36, ID}, J.R. Stewart ^{121, ID}, M.C. Stockton ^{36, ID},
 G. Stoicea ^{27b, ID}, M. Stolarski ^{130a, ID}, S. Stonjek ^{110, ID}, A. Straessner ^{50, ID}, J. Strandberg ^{144, ID},
 S. Strandberg ^{47a, 47b, ID}, M. Strauss ^{120, ID}, T. Strebler ^{102, ID}, P. Strizenec ^{28b, ID}, R. Ströhmer ^{166, ID},
 D.M. Strom ^{123, ID}, L.R. Strom ^{48, ID}, R. Stroynowski ^{44, ID}, A. Strubig ^{47a, 47b, ID}, S.A. Stucci ^{29, ID}, B. Stugu ^{16, ID},
 J. Stupak ^{120, ID}, N.A. Styles ^{48, ID}, D. Su ^{143, ID}, S. Su ^{62a, ID}, W. Su ^{62d, ID}, X. Su ^{62a, 66, ID}, K. Sugizaki ^{153, ID},
 V.V. Sulin ^{37, ID}, M.J. Sullivan ^{92, ID}, D.M.S. Sultan ^{78a, 78b, ID}, L. Sultanaliyeva ^{37, ID}, S. Sultansoy ^{3b, ID},
 T. Sumida ^{87, ID}, S. Sun ^{106, ID}, S. Sun ^{170, ID}, O. Sunneborn Gudnadottir ^{161, ID}, M.R. Sutton ^{146, ID},
 H. Suzuki ^{157, ID}, M. Svatos ^{131, ID}, M. Swiatlowski ^{156a, ID}, T. Swirski ^{166, ID}, I. Sykora ^{28a, ID}, M. Sykora ^{133, ID},
 T. Sykora ^{133, ID}, D. Ta ^{100, ID}, K. Tackmann ^{48, ID, x}, A. Taffard ^{160, ID}, R. Tafirout ^{156a, ID}, J.S. Tafoya Vargas ^{66, ID},
 R. Takashima ^{88, ID}, E.P. Takeva ^{52, ID}, Y. Takubo ^{83, ID}, M. Talby ^{102, ID}, A.A. Talyshев ^{37, ID}, K.C. Tam ^{64b, ID},
 N.M. Tamir ¹⁵¹, A. Tanaka ^{153, ID}, J. Tanaka ^{153, ID}, R. Tanaka ^{66, ID}, M. Tanasini ^{57b, 57a, ID}, Z. Tao ^{164, ID},
 S. Tapia Araya ^{137f, ID}, S. Tapprogge ^{100, ID}, A. Tarek Abouelfadl Mohamed ^{107, ID}, S. Tarem ^{150, ID},
 K. Tariq ^{62b, ID}, G. Tarna ^{102, 27b, ID}, G.F. Tartarelli ^{71a, ID}, P. Tas ^{133, ID}, M. Tasevsky ^{131, ID}, E. Tassi ^{43b, 43a, ID},
 A.C. Tate ^{162, ID}, G. Tateno ^{153, ID}, Y. Tayalati ^{35e, ID, z}, G.N. Taylor ^{105, ID}, W. Taylor ^{156b, ID}, H. Teagle ⁹²,
 A.S. Tee ^{170, ID}, R. Teixeira De Lima ^{143, ID}, P. Teixeira-Dias ^{95, ID}, J.J. Teoh ^{155, ID}, K. Terashi ^{153, ID},
 J. Terron ^{99, ID}, S. Terzo ^{13, ID}, M. Testa ^{53, ID}, R.J. Teuscher ^{155, ID, aa}, A. Thaler ^{79, ID}, O. Theiner ^{56, ID},
 N. Themistokleous ^{52, ID}, T. Theveneaux-Pelzer ^{102, ID}, O. Thielmann ^{171, ID}, D.W. Thomas ⁹⁵,
 J.P. Thomas ^{20, ID}, E.A. Thompson ^{17a, ID}, P.D. Thompson ^{20, ID}, E. Thomson ^{128, ID}, Y. Tian ^{55, ID},
 V. Tikhomirov ^{37, ID, a}, Yu.A. Tikhonov ^{37, ID}, S. Timoshenko ³⁷, D. Timoshyn ^{133, ID}, E.X.L. Ting ^{1, ID},
 P. Tipton ^{172, ID}, S.H. Tlou ^{33g, ID}, A. Tnourji ^{40, ID}, K. Todome ^{23b, 23a, ID}, S. Todorova-Nova ^{133, ID}, S. Todt ⁵⁰,
 M. Togawa ^{83, ID}, J. Tojo ^{89, ID}, S. Tokár ^{28a, ID}, K. Tokushuku ^{83, ID}, O. Toldaiev ^{68, ID}, R. Tombs ^{32, ID},
 M. Tomoto ^{83, 111, ID}, L. Tompkins ^{143, ID, r}, K.W. Topolnicki ^{85b, ID}, E. Torrence ^{123, ID}, H. Torres ^{102, ID, ae},
 E. Torró Pastor ^{163, ID}, M. Toscani ^{30, ID}, C. Tosciri ^{39, ID}, M. Tost ^{11, ID}, D.R. Tovey ^{139, ID}, A. Traeet ¹⁶,
 I.S. Trandafir ^{27b, ID}, T. Trefzger ^{166, ID}, A. Tricoli ^{29, ID}, I.M. Trigger ^{156a, ID}, S. Trincaz-Duvoud ^{127, ID},
 D.A. Trischuk ^{26, ID}, B. Trocmé ^{60, ID}, C. Troncon ^{71a, ID}, L. Truong ^{33c, ID}, M. Trzebinski ^{86, ID}, A. Trzupek ^{86, ID},
 F. Tsai ^{145, ID}, M. Tsai ^{106, ID}, A. Tsiamis ^{152, ID, f}, P.V. Tsiareshka ³⁷, S. Tsigaridas ^{156a, ID}, A. Tsirigotis ^{152, ID, v},
 V. Tsiskaridze ^{155, ID}, E.G. Tskhadadze ^{149a}, M. Tsopoulou ^{152, ID, f}, Y. Tsujikawa ^{87, ID}, I.I. Tsukerman ^{37, ID},
 V. Tsulaia ^{17a, ID}, S. Tsuno ^{83, ID}, O. Tsur ¹⁵⁰, K. Tsuri ¹¹⁸, D. Tsybychev ^{145, ID}, Y. Tu ^{64b, ID},
 A. Tudorache ^{27b, ID}, V. Tudorache ^{27b, ID}, A.N. Tuna ^{36, ID}, S. Turchikhin ^{38, ID}, I. Turk Cakir ^{3a, ID},
 R. Turra ^{71a, ID}, T. Turtuvshin ^{38, ID, ab}, P.M. Tuts ^{41, ID}, S. Tzamarias ^{152, ID, f}, P. Tzanis ^{10, ID}, E. Tzovara ^{100, ID},
 K. Uchida ¹⁵³, F. Ukegawa ^{157, ID}, P.A. Ulloa Poblete ^{137c, 137b, ID}, E.N. Umaka ^{29, ID}, G. Unal ^{36, ID},
 M. Unal ^{11, ID}, A. Undrus ^{29, ID}, G. Unel ^{160, ID}, J. Urban ^{28b, ID}, P. Urquijo ^{105, ID}, G. Usai ^{8, ID}, R. Ushioda ^{154, ID}

- M. Usman 108, ID, Z. Uysal 21b, ID, L. Vacavant 102, ID, V. Vacek 132, ID, B. Vachon 104, ID, K.O.H. Vadla 125, ID,
 T. Vafeiadis 36, ID, A. Vaitkus 96, ID, C. Valderanis 109, ID, E. Valdes Santurio 47a, 47b, ID, M. Valente 156a, ID,
 S. Valentini 23b, 23a, ID, A. Valero 163, ID, E. Valiente Moreno 163, ID, A. Vallier 102, ID, ae,
 J.A. Valls Ferrer 163, ID, D.R. Van Arneman 114, ID, T.R. Van Daalen 138, ID, A. Van Der Graaf 49, ID,
 P. Van Gemmeren 6, ID, M. Van Rijnbach 125, 36, ID, S. Van Stroud 96, ID, I. Van Vulpen 114, ID,
 M. Vanadia 76a, 76b, ID, W. Vandelli 36, ID, M. Vandenbroucke 135, ID, E.R. Vandewall 121, ID, D. Vannicola 151, ID,
 L. Vannoli 57b, 57a, ID, R. Vari 75a, ID, E.W. Varnes 7, ID, C. Varni 17a, ID, T. Varol 148, ID, D. Varouchas 66, ID,
 L. Varriale 163, ID, K.E. Varvell 147, ID, M.E. Vasile 27b, ID, L. Vaslin 40, G.A. Vasquez 165, ID, F. Vazeille 40, ID,
 T. Vazquez Schroeder 36, ID, J. Veatch 31, ID, V. Vecchio 101, ID, M.J. Veen 103, ID, I. Veliscek 126, ID,
 L.M. Veloce 155, ID, F. Veloso 130a, 130c, ID, S. Veneziano 75a, ID, A. Ventura 70a, 70b, ID, A. Verbytskyi 110, ID,
 M. Verducci 74a, 74b, ID, C. Vergis 24, ID, M. Verissimo De Araujo 82b, ID, W. Verkerke 114, ID,
 J.C. Vermeulen 114, ID, C. Vernieri 143, ID, P.J. Verschuur 95, ID, M. Vessella 103, ID, M.C. Vetterli 142, ID, aj,
 A. Vgenopoulos 152, ID, f, N. Viaux Maira 137f, ID, T. Vickey 139, ID, O.E. Vickey Boeriu 139, ID,
 G.H.A. Viehhauser 126, ID, L. Vigani 63b, ID, M. Villa 23b, 23a, ID, M. Villaplana Perez 163, ID, E.M. Villhauer 52,
 E. Vilucchi 53, ID, M.G. Vincter 34, ID, G.S. Virdee 20, ID, A. Vishwakarma 52, ID, A. Visibile 114, C. Vittori 36, ID,
 I. Vivarelli 146, ID, V. Vladimirov 167, E. Voevodina 110, ID, F. Vogel 109, ID, P. Vokac 132, ID, J. Von Ahnen 48, ID,
 E. Von Toerne 24, ID, B. Vormwald 36, ID, V. Vorobel 133, ID, K. Vorobev 37, ID, M. Vos 163, ID, K. Voss 141, ID,
 J.H. Vossebeld 92, ID, M. Vozak 114, ID, L. Vozdecky 94, ID, N. Vranjes 15, ID, M. Vranjes Milosavljevic 15, ID,
 M. Vreeswijk 114, ID, N.K. Vu 62d, 62c, ID, R. Vuillermet 36, ID, O. Vujinovic 100, ID, I. Vukotic 39, ID,
 S. Wada 157, ID, C. Wagner 103, J.M. Wagner 17a, ID, W. Wagner 171, ID, S. Wahdan 171, ID, H. Wahlberg 90, ID,
 R. Wakasa 157, ID, M. Wakida 111, ID, J. Walder 134, ID, R. Walker 109, ID, W. Walkowiak 141, ID, A. Wall 128, ID,
 T. Wamorkar 6, ID, A.Z. Wang 170, ID, C. Wang 100, ID, C. Wang 62c, ID, H. Wang 17a, ID, J. Wang 64a, ID,
 R.-J. Wang 100, ID, R. Wang 61, ID, R. Wang 6, ID, S.M. Wang 148, ID, S. Wang 62b, ID, T. Wang 62a, ID,
 W.T. Wang 80, ID, W. Wang 14a, ID, X. Wang 14c, ID, X. Wang 162, ID, X. Wang 62c, ID, Y. Wang 62d, ID,
 Y. Wang 14c, ID, Z. Wang 106, ID, Z. Wang 62d, 51, 62c, ID, Z. Wang 106, ID, A. Warburton 104, ID, R.J. Ward 20, ID,
 N. Warrack 59, ID, A.T. Watson 20, ID, H. Watson 59, ID, M.F. Watson 20, ID, E. Watton 59, 134, ID, G. Watts 138, ID,
 B.M. Waugh 96, ID, C. Weber 29, ID, H.A. Weber 18, ID, M.S. Weber 19, ID, S.M. Weber 63a, ID, C. Wei 62a,
 Y. Wei 126, ID, A.R. Weidberg 126, ID, E.J. Weik 117, ID, J. Weingarten 49, ID, M. Weirich 100, ID, C. Weiser 54, ID,
 C.J. Wells 48, ID, T. Wenaus 29, ID, B. Wendland 49, ID, T. Wengler 36, ID, N.S. Wenke 110, N. Wermes 24, ID,
 M. Wessels 63a, ID, K. Whalen 123, ID, A.M. Wharton 91, ID, A.S. White 61, ID, A. White 8, ID, M.J. White 1, ID,
 D. Whiteson 160, ID, L. Wickremasinghe 124, ID, W. Wiedenmann 170, ID, C. Wiel 50, ID, M. Wielers 134, ID,
 C. Wiglesworth 42, ID, D.J. Wilbern 120, H.G. Wilkens 36, ID, D.M. Williams 41, ID, H.H. Williams 128,
 S. Williams 32, ID, S. Willocq 103, ID, B.J. Wilson 101, ID, P.J. Windischhofer 39, ID, F.I. Winkel 30, ID,
 F. Winklmeier 123, ID, B.T. Winter 54, ID, J.K. Winter 101, ID, M. Wittgen 143, M. Wobisch 97, ID, Z. Wolffs 114, ID,
 R. Wölker 126, ID, J. Wollrath 160, M.W. Wolter 86, ID, H. Wolters 130a, 130c, ID, A.F. Wongel 48, ID,
 S.D. Worm 48, ID, B.K. Wosiek 86, ID, K.W. Woźniak 86, ID, S. Wozniewski 55, ID, K. Wright 59, ID, C. Wu 20, ID,
 J. Wu 14a, 14e, ID, M. Wu 64a, ID, M. Wu 113, ID, S.L. Wu 170, ID, X. Wu 56, ID, Y. Wu 62a, ID, Z. Wu 135, ID,
 J. Wuerzinger 110, ID, T.R. Wyatt 101, ID, B.M. Wynne 52, ID, S. Xella 42, ID, L. Xia 14c, ID, M. Xia 14b, ID,
 J. Xiang 64c, ID, X. Xiao 106, ID, M. Xie 62a, ID, X. Xie 62a, ID, S. Xin 14a, 14e, ID, J. Xiong 17a, ID, D. Xu 14a, ID,
 H. Xu 62a, ID, L. Xu 62a, ID, R. Xu 128, ID, T. Xu 106, ID, Y. Xu 14b, ID, Z. Xu 52, ID, Z. Xu 14a, ID, B. Yabsley 147, ID,
 S. Yacoob 33a, ID, N. Yamaguchi 89, ID, Y. Yamaguchi 154, ID, E. Yamashita 153, ID, H. Yamauchi 157, ID,
 T. Yamazaki 17a, ID, Y. Yamazaki 84, ID, J. Yan 62c, S. Yan 126, ID, Z. Yan 25, ID, H.J. Yang 62c, 62d, ID,

- H.T. Yang 62a, ¹, S. Yang 62a, ¹, T. Yang 64c, ¹, X. Yang 62a, ¹, X. Yang 14a, ¹, Y. Yang 44, ¹, Y. Yang 62a,
 Z. Yang 62a, ¹, W-M. Yao 17a, ¹, Y.C. Yap 48, ¹, H. Ye 14c, ¹, H. Ye 55, ¹, J. Ye 44, ¹, S. Ye 29, ¹, X. Ye 62a, ¹,
 Y. Yeh 96, ¹, I. Yeletskikh 38, ¹, B.K. Yeo 17a, ¹, M.R. Yexley 96, ¹, P. Yin 41, ¹, K. Yorita 168, ¹, S. Younas 27b, ¹,
 C.J.S. Young 54, ¹, C. Young 143, ¹, Y. Yu 62a, ¹, M. Yuan 106, ¹, R. Yuan 62b, ¹, L. Yue 96, ¹, M. Zaazoua 62a, ¹,
 B. Zabinski 86, ¹, E. Zaid 52, T. Zakareishvili 149b, ¹, N. Zakharchuk 34, ¹, S. Zambito 56, ¹,
 J.A. Zamora Saa 137d, 137b, ¹, J. Zang 153, ¹, D. Zanzi 54, ¹, O. Zaplatilek 132, ¹, C. Zeitnitz 171, ¹,
 H. Zeng 14a, ¹, J.C. Zeng 162, ¹, D.T. Zenger Jr 26, ¹, O. Zenin 37, ¹, T. Ženiš 28a, ¹, S. Zenz 94, ¹,
 S. Zerradi 35a, ¹, D. Zerwas 66, ¹, M. Zhai 14a, 14e, ¹, B. Zhang 14c, ¹, D.F. Zhang 139, ¹, J. Zhang 62b, ¹,
 J. Zhang 6, ¹, K. Zhang 14a, 14e, ¹, L. Zhang 14c, ¹, P. Zhang 14a, 14e, R. Zhang 170, ¹, S. Zhang 106, ¹,
 T. Zhang 153, ¹, X. Zhang 62c, ¹, X. Zhang 62b, ¹, Y. Zhang 62c, 5, ¹, Y. Zhang 96, ¹, Z. Zhang 17a, ¹,
 Z. Zhang 66, ¹, H. Zhao 138, ¹, P. Zhao 51, ¹, T. Zhao 62b, ¹, Y. Zhao 136, ¹, Z. Zhao 62a, ¹,
 A. Zhemchugov 38, ¹, K. Zheng 162, ¹, X. Zheng 62a, ¹, Z. Zheng 143, ¹, D. Zhong 162, ¹, B. Zhou 106, ¹,
 H. Zhou 7, ¹, N. Zhou 62c, ¹, Y. Zhou 7, C.G. Zhu 62b, ¹, J. Zhu 106, ¹, Y. Zhu 62c, ¹, Y. Zhu 62a, ¹,
 X. Zhuang 14a, ¹, K. Zhukov 37, ¹, V. Zhulanov 37, ¹, N.I. Zimine 38, ¹, J. Zinsser 63b, ¹, M. Ziolkowski 141, ¹,
 L. Živković 15, ¹, A. Zoccoli 23b, 23a, ¹, K. Zoch 56, ¹, T.G. Zorbas 139, ¹, O. Zormpa 46, ¹, W. Zou 41, ¹,
 L. Zwalinski 36, ¹

¹ Department of Physics, University of Adelaide, Adelaide; Australia² Department of Physics, University of Alberta, Edmonton AB; Canada³ ^(a) Department of Physics, Ankara University, Ankara; ^(b) Division of Physics, TOBB University of Economics and Technology, Ankara; Türkiye⁴ LAPP, Université Savoie Mont Blanc, CNRS/IN2P3, Annecy; France⁵ APC, Université Paris Cité, CNRS/IN2P3, Paris; France⁶ High Energy Physics Division, Argonne National Laboratory, Argonne IL; United States of America⁷ Department of Physics, University of Arizona, Tucson AZ; United States of America⁸ Department of Physics, University of Texas at Arlington, Arlington TX; United States of America⁹ Physics Department, National and Kapodistrian University of Athens, Athens; Greece¹⁰ Physics Department, National Technical University of Athens, Zografou; Greece¹¹ Department of Physics, University of Texas at Austin, Austin TX; United States of America¹² Institute of Physics, Azerbaijan Academy of Sciences, Baku; Azerbaijan¹³ Institut de Física d'Altes Energies (IFAE), Barcelona Institute of Science and Technology, Barcelona; Spain¹⁴ ^(a) Institute of High Energy Physics, Chinese Academy of Sciences, Beijing; ^(b) Physics Department, Tsinghua University, Beijing; ^(c) Department of Physics, Nanjing University, Nanjing;^(d) School of Science, Shenzhen – Campus of Sun Yat-sen University China; ^(e) University of Chinese Academy of Science (UCAS), Beijing; China¹⁵ Institute of Physics, University of Belgrade, Belgrade; Serbia¹⁶ Department for Physics and Technology, University of Bergen, Bergen; Norway¹⁷ ^(a) Physics Division, Lawrence Berkeley National Laboratory, Berkeley CA; ^(b) University of California, Berkeley CA; United States of America¹⁸ Institut für Physik, Humboldt Universität zu Berlin, Berlin; Germany¹⁹ Albert Einstein Center for Fundamental Physics and Laboratory for High Energy Physics, University of Bern, Bern; Switzerland²⁰ School of Physics and Astronomy, University of Birmingham, Birmingham; United Kingdom²¹ ^(a) Department of Physics, Bogaziçi University, Istanbul; ^(b) Department of Physics Engineering, Gaziantep University, Gaziantep; ^(c) Department of Physics, İstanbul University, İstanbul;^(d) İstinye University, Sarıyer, İstanbul; Türkiye²² ^(a) Facultad de Ciencias y Centro de Investigaciones, Universidad Antonio Nariño, Bogotá; ^(b) Departamento de Física, Universidad Nacional de Colombia, Bogotá; ^(c) Pontificia Universidad Javeriana, Bogota; Colombia²³ ^(a) Dipartimento di Fisica e Astronomia A. Righi, Università di Bologna, Bologna; ^(b) INFN Sezione di Bologna; Italy²⁴ Physikalisches Institut, Universität Bonn, Bonn; Germany²⁵ Department of Physics, Boston University, Boston MA; United States of America²⁶ Department of Physics, Brandeis University, Waltham MA; United States of America²⁷ ^(a) Transilvania University of Brasov, Brasov; ^(b) Horia Hulubei National Institute of Physics and Nuclear Engineering, Bucharest; ^(c) Department of Physics, Alexandru Ioan Cuza University of Iasi, Iasi; ^(d) National Institute for Research and Development of Isotopic and Molecular Technologies, Physics Department, Cluj-Napoca; ^(e) University Politehnica Bucharest, Bucharest; ^(f) West University in Timisoara, Timisoara; ^(g) Faculty of Physics, University of Bucharest, Bucharest; Romania²⁸ ^(a) Faculty of Mathematics, Physics and Informatics, Comenius University, Bratislava; ^(b) Department of Subnuclear Physics, Institute of Experimental Physics of the Slovak Academy of Sciences, Kosice; Slovak Republic²⁹ Physics Department, Brookhaven National Laboratory, Upton NY; United States of America³⁰ Universidad de Buenos Aires, Facultad de Ciencias Exactas y Naturales, Departamento de Física, y CONICET, Instituto de Física de Buenos Aires (IFIBA), Buenos Aires; Argentina³¹ California State University, CA; United States of America³² Cavendish Laboratory, University of Cambridge, Cambridge; United Kingdom³³ ^(a) Department of Physics, University of Cape Town, Cape Town; ^(b) iThemba Labs, Western Cape; ^(c) Department of Mechanical Engineering Science, University of Johannesburg, Johannesburg; ^(d) National Institute of Physics, University of the Philippines Diliman (Philippines); ^(e) University of South Africa, Department of Physics, Pretoria; ^(f) University of Zululand, KwaDlangezwa; ^(g) School of Physics, University of the Witwatersrand, Johannesburg; South Africa³⁴ Department of Physics, Carleton University, Ottawa ON; Canada³⁵ ^(a) Faculté des Sciences Ain Chock, Réseau Universitaire de Physique des Hautes Energies - Université Hassan II, Casablanca; ^(b) Faculté des Sciences, Université Ibn-Tofail, Kénitra;^(c) Faculté des Sciences Semlalia, Université Cadi Ayyad, LPHEA-Marrakech; ^(d) LPMR, Faculté des Sciences, Université Mohamed Premier, Oujda; ^(e) Faculté des sciences, Université Mohammed V, Rabat; ^(f) Institute of Applied Physics, Mohammed VI Polytechnic University, Ben Guerir; Morocco³⁶ CERN, Geneva; Switzerland³⁷ Affiliated with an institute covered by a cooperation agreement with CERN³⁸ Affiliated with an international laboratory covered by a cooperation agreement with CERN³⁹ Enrico Fermi Institute, University of Chicago, Chicago IL; United States of America

- 40 ^{a)}LPC, Université Clermont Auvergne, CNRS/IN2P3, Clermont-Ferrand; France
 41 Nevis Laboratory, Columbia University, Irvington NY; United States of America
 42 Niels Bohr Institute, University of Copenhagen, Copenhagen; Denmark
 43 ^(a)Dipartimento di Fisica, Università della Calabria, Rende; ^(b)INFN Gruppo Collegato di Cosenza, Laboratori Nazionali di Frascati; Italy
 44 Physics Department, Southern Methodist University, Dallas TX; United States of America
 45 Physics Department, University of Texas at Dallas, Richardson TX; United States of America
 46 National Centre for Scientific Research "Demokritos", Agia Paraskevi; Greece
 47 ^(a)Department of Physics, Stockholm University; ^(b)Oskar Klein Centre, Stockholm; Sweden
 48 Deutsches Elektronen-Synchrotron DESY, Hamburg and Zeuthen; Germany
 49 Fakultät Physik, Technische Universität Dortmund, Dortmund; Germany
 50 Institut für Kern- und Teilchenphysik, Technische Universität Dresden, Dresden; Germany
 51 Department of Physics, Duke University, Durham NC; United States of America
 52 SUPA - School of Physics and Astronomy, University of Edinburgh, Edinburgh; United Kingdom
 53 INFN e Laboratori Nazionali di Frascati, Frascati; Italy
 54 Physikalisches Institut, Albert-Ludwigs-Universität Freiburg, Freiburg; Germany
 55 II. Physikalisches Institut, Georg-August-Universität Göttingen, Göttingen; Germany
 56 Département de Physique Nucléaire et Corpusculaire, Université de Genève, Genève; Switzerland
 57 ^(a)Dipartimento di Fisica, Università di Genova, Genova; ^(b)INFN Sezione di Genova; Italy
 58 II. Physikalisches Institut, Justus-Liebig-Universität Giessen, Giessen; Germany
 59 SUPA - School of Physics and Astronomy, University of Glasgow, Glasgow; United Kingdom
 60 LPSC, Université Grenoble Alpes, CNRS/IN2P3, Grenoble INP, Grenoble; France
 61 Laboratory for Particle Physics and Cosmology, Harvard University, Cambridge MA; United States of America
 62 ^(a)Department of Modern Physics and State Key Laboratory of Particle Detection and Electronics, University of Science and Technology of China, Hefei; ^(b)Institute of Frontier and Interdisciplinary Science and Key Laboratory of Particle Physics and Particle Irradiation (MOE), Shandong University, Qingdao; ^(c)School of Physics and Astronomy, Shanghai Jiao Tong University, Key Laboratory for Particle Astrophysics and Cosmology (MOE), SKLPPC, Shanghai; ^(d)Tsung-Dao Lee Institute, Shanghai; China
 63 ^(a)Kirchhoff-Institut für Physik, Ruprecht-Karls-Universität Heidelberg, Heidelberg; ^(b)Physikalisches Institut, Ruprecht-Karls-Universität Heidelberg, Heidelberg; Germany
 64 ^(a)Department of Physics, Chinese University of Hong Kong, Shatin, N.T., Hong Kong; ^(b)Department of Physics, University of Hong Kong, Hong Kong; ^(c)Department of Physics and Institute for Advanced Study, Hong Kong University of Science and Technology, Clear Water Bay, Kowloon, Hong Kong; China
 65 Department of Physics, National Tsing Hua University, Hsinchu; Taiwan
 66 IJCLab, Université Paris-Saclay, CNRS/IN2P3, 91405, Orsay; France
 67 Centro Nacional de Microelectrónica (IMB-CNM-CSIC), Barcelona; Spain
 68 Department of Physics, Indiana University, Bloomington IN; United States of America
 69 ^(a)INFN Gruppo Collegato di Udine, Sezione di Trieste, Udine; ^(b)ICTP, Trieste; ^(c)Dipartimento Politecnico di Ingegneria e Architettura, Università di Udine, Udine; Italy
 70 ^(a)INFN Sezione di Lecce; ^(b)Dipartimento di Matematica e Fisica, Università del Salento, Lecce; Italy
 71 ^(a)INFN Sezione di Milano; ^(b)Dipartimento di Fisica, Università di Milano, Milano; Italy
 72 ^(a)INFN Sezione di Napoli; ^(b)Dipartimento di Fisica, Università di Napoli, Napoli; Italy
 73 ^(a)INFN Sezione di Pavia; ^(b)Dipartimento di Fisica, Università di Pavia, Pavia; Italy
 74 ^(a)INFN Sezione di Pisa; ^(b)Dipartimento di Fisica E. Fermi, Università di Pisa, Pisa; Italy
 75 ^(a)INFN Sezione di Roma; ^(b)Dipartimento di Fisica, Sapienza Università di Roma, Roma; Italy
 76 ^(a)INFN Sezione di Roma Tor Vergata; ^(b)Dipartimento di Fisica, Università di Roma Tor Vergata, Roma; Italy
 77 ^(a)INFN Sezione di Roma Tre; ^(b)Dipartimento di Matematica e Fisica, Università Roma Tre, Roma; Italy
 78 ^(a)INFN-TIFPA; ^(b)Università degli Studi di Trento, Trento; Italy
 79 Universität Innsbruck, Department of Astroparticle Physics, Innsbruck; Austria
 80 University of Iowa, Iowa City IA; United States of America
 81 Department of Physics and Astronomy, Iowa State University, Ames IA; United States of America
 82 ^(a)Departamento de Engenharia Elétrica, Universidade Federal de Juiz de Fora (UFJF), Juiz de Fora; ^(b)Universidade Federal do Rio De Janeiro COPPE/EE/IF, Rio de Janeiro; ^(c)Instituto de Física, Universidade de São Paulo, São Paulo; ^(d)Rio de Janeiro State University, Rio de Janeiro; Brazil
 83 KEK, High Energy Accelerator Research Organization, Tsukuba; Japan
 84 Graduate School of Science, Kobe University, Kobe; Japan
 85 ^(a)AGH University of Krakow, Faculty of Physics and Applied Computer Science, Krakow, Poland; ^(b)Marian Smoluchowski Institute of Physics, Jagiellonian University, Krakow; Poland
 86 Institute of Nuclear Physics Polish Academy of Sciences, Krakow; Poland
 87 Faculty of Science, Kyoto University, Kyoto; Japan
 88 Kyoto University of Education, Kyoto; Japan
 89 Research Center for Advanced Particle Physics and Department of Physics, Kyushu University, Fukuoka; Japan
 90 Instituto de Física La Plata, Universidad Nacional de La Plata and CONICET, La Plata; Argentina
 91 Physics Department, Lancaster University, Lancaster; United Kingdom
 92 Oliver Lodge Laboratory, University of Liverpool, Liverpool; United Kingdom
 93 Department of Experimental Particle Physics, Jožef Stefan Institute and Department of Physics, University of Ljubljana, Ljubljana; Slovenia
 94 School of Physics and Astronomy, Queen Mary University of London, London; United Kingdom
 95 Department of Physics, Royal Holloway University of London, Egham; United Kingdom
 96 Department of Physics and Astronomy, University College London, London; United Kingdom
 97 Louisiana Tech University, Ruston LA; United States of America
 98 Fysiska institutionen, Lunds universitet, Lund; Sweden
 99 Departamento de Física Teórica C-15 and CIAFF, Universidad Autónoma de Madrid, Madrid; Spain
 100 Institut für Physik, Universität Mainz, Mainz; Germany
 101 School of Physics and Astronomy, University of Manchester, Manchester; United Kingdom
 102 CPPM, Aix-Marseille Université, CNRS/IN2P3, Marseille; France
 103 Department of Physics, University of Massachusetts, Amherst MA; United States of America
 104 Department of Physics, McGill University, Montreal QC; Canada
 105 School of Physics, University of Melbourne, Victoria; Australia
 106 Department of Physics, University of Michigan, Ann Arbor MI; United States of America
 107 Department of Physics and Astronomy, Michigan State University, East Lansing MI; United States of America
 108 Group of Particle Physics, University of Montreal, Montreal QC; Canada
 109 Fakultät für Physik, Ludwig-Maximilians-Universität München, München; Germany
 110 Max-Planck-Institut für Physik (Werner-Heisenberg-Institut), München; Germany
 111 Graduate School of Science and Kobayashi-Maskawa Institute, Nagoya University, Nagoya; Japan
 112 Department of Physics and Astronomy, University of New Mexico, Albuquerque NM; United States of America
 113 Institute for Mathematics, Astrophysics and Particle Physics, Radboud University/Nikhef, Nijmegen; Netherlands
 114 Nikhef National Institute for Subatomic Physics and University of Amsterdam, Amsterdam; Netherlands
 115 Department of Physics, Northern Illinois University, DeKalb IL; United States of America

- 116 ^(a) New York University Abu Dhabi, Abu Dhabi; ^(b) University of Sharjah, Sharjah; United Arab Emirates
 117 Department of Physics, New York University, New York NY; United States of America
 118 Ochanomizu University, Otsuka, Bunkyo-ku, Tokyo; Japan
 119 Ohio State University, Columbus OH; United States of America
 120 Homer L. Dodge Department of Physics and Astronomy, University of Oklahoma, Norman OK; United States of America
 121 Department of Physics, Oklahoma State University, Stillwater OK; United States of America
 122 Palacký University, Joint Laboratory of Optics, Olomouc; Czech Republic
 123 Institute for Fundamental Science, University of Oregon, Eugene, OR; United States of America
 124 Graduate School of Science, Osaka University, Osaka; Japan
 125 Department of Physics, University of Oslo, Oslo; Norway
 126 Department of Physics, Oxford University, Oxford; United Kingdom
 127 LPNHE, Sorbonne Université, Université Paris Cité, CNRS/IN2P3, Paris; France
 128 Department of Physics, University of Pennsylvania, Philadelphia PA; United States of America
 129 Department of Physics and Astronomy, University of Pittsburgh, Pittsburgh PA; United States of America
 130 ^(a) Laboratório de Instrumentação e Física Experimental de Partículas - LIP, Lisboa; ^(b) Departamento de Física, Faculdade de Ciências, Universidade de Lisboa, Lisboa; ^(c) Departamento de Física, Universidade de Coimbra, Coimbra; ^(d) Centro de Física Nuclear da Universidade de Lisboa, Lisboa; ^(e) Departamento de Física, Universidade do Minho, Braga; ^(f) Departamento de Física Teórica y del Cosmos, Universidad de Granada, Granada (Spain); ^(g) Departamento de Física, Instituto Superior Técnico, Universidade de Lisboa, Lisboa; Portugal
 131 Institute of Physics of the Czech Academy of Sciences, Prague; Czech Republic
 132 Czech Technical University in Prague, Prague; Czech Republic
 133 Charles University, Faculty of Mathematics and Physics, Prague; Czech Republic
 134 Particle Physics Department, Rutherford Appleton Laboratory, Didcot; United Kingdom
 135 IRFU, CEA, Université Paris-Saclay, Gif-sur-Yvette; France
 136 Santa Cruz Institute for Particle Physics, University of California Santa Cruz, Santa Cruz CA; United States of America
 137 ^(a) Departamento de Física, Pontificia Universidad Católica de Chile, Santiago; ^(b) Millennium Institute for Subatomic physics at high energy frontier (SAPHIR), Santiago; ^(c) Instituto de Investigación Multidisciplinario en Ciencia y Tecnología, y Departamento de Física, Universidad de La Serena; ^(d) Universidad Andres Bello, Department of Physics, Santiago; ^(e) Instituto de Alta Investigación, Universidad de Tarapacá, Arica; ^(f) Departamento de Física, Universidad Técnica Federico Santa María, Valparaíso; Chile
 138 Department of Physics, University of Washington, Seattle WA; United States of America
 139 Department of Physics and Astronomy, University of Sheffield, Sheffield; United Kingdom
 140 Department of Physics, Shinshu University, Nagano; Japan
 141 Department Physik, Universität Siegen, Siegen; Germany
 142 Department of Physics, Simon Fraser University, Burnaby BC; Canada
 143 SLAC National Accelerator Laboratory, Stanford CA; United States of America
 144 Department of Physics, Royal Institute of Technology, Stockholm; Sweden
 145 Departments of Physics and Astronomy, Stony Brook University, Stony Brook NY; United States of America
 146 Department of Physics and Astronomy, University of Sussex, Brighton; United Kingdom
 147 School of Physics, University of Sydney, Sydney; Australia
 148 Institute of Physics, Academia Sinica, Taipei; Taiwan
 149 ^(a) E. Andronikashvili Institute of Physics, Iv. Javakhishvili Tbilisi State University, Tbilisi; ^(b) High Energy Physics Institute, Tbilisi State University, Tbilisi; ^(c) University of Georgia, Tbilisi; Georgia
 150 Department of Physics, Technion, Israel Institute of Technology, Haifa; Israel
 151 Raymond and Beverly Sackler School of Physics and Astronomy, Tel Aviv University, Tel Aviv; Israel
 152 Department of Physics, Aristotle University of Thessaloniki, Thessaloniki; Greece
 153 International Center for Elementary Particle Physics and Department of Physics, University of Tokyo, Tokyo; Japan
 154 Department of Physics, Tokyo Institute of Technology, Tokyo; Japan
 155 Department of Physics, University of Toronto, Toronto ON; Canada
 156 ^(a) TRIUMF, Vancouver BC; ^(b) Department of Physics and Astronomy, York University, Toronto ON; Canada
 157 Division of Physics and Tomonaga Center for the History of the Universe, Faculty of Pure and Applied Sciences, University of Tsukuba, Tsukuba; Japan
 158 Department of Physics and Astronomy, Tufts University, Medford MA; United States of America
 159 United Arab Emirates University, Al Ain; United Arab Emirates
 160 Department of Physics and Astronomy, University of California Irvine, Irvine CA; United States of America
 161 Department of Physics and Astronomy, University of Uppsala, Uppsala; Sweden
 162 Department of Physics, University of Illinois, Urbana IL; United States of America
 163 Instituto de Física Corpuscular (IFIC), Centro Mixto Universidad de Valencia - CSIC, Valencia; Spain
 164 Department of Physics, University of British Columbia, Vancouver BC; Canada
 165 Department of Physics and Astronomy, University of Victoria, Victoria BC; Canada
 166 Fakultät für Physik und Astronomie, Julius-Maximilians-Universität Würzburg, Würzburg; Germany
 167 Department of Physics, University of Warwick, Coventry; United Kingdom
 168 Waseda University, Tokyo; Japan
 169 Department of Particle Physics and Astrophysics, Weizmann Institute of Science, Rehovot; Israel
 170 Department of Physics, University of Wisconsin, Madison WI; United States of America
 171 Fakultät für Mathematik und Naturwissenschaften, Fachgruppe Physik, Bergische Universität Wuppertal, Wuppertal; Germany
 172 Department of Physics, Yale University, New Haven CT; United States of America

^a Also Affiliated with an institute covered by a cooperation agreement with CERN.^b Also at An-Najah National University, Nablus; Palestine.^c Also at APC, Université Paris Cité, CNRS/IN2P3, Paris; France.^d Also at Borough of Manhattan Community College, City University of New York, New York NY; United States of America.^e Also at Center for High Energy Physics, Peking University; China.^f Also at Center for Interdisciplinary Research and Innovation (CIRI-AUTH), Thessaloniki; Greece.^g Also at Centro Studi e Ricerche Enrico Fermi; Italy.^h Also at CERN, Geneva; Switzerland.ⁱ Also at Département de Physique Nucléaire et Corpusculaire, Université de Genève, Genève; Switzerland.^j Also at Departament de Fisica de la Universitat Autònoma de Barcelona, Barcelona; Spain.^k Also at Department of Financial and Management Engineering, University of the Aegean, Chios; Greece.^l Also at Department of Physics and Astronomy, Michigan State University, East Lansing MI; United States of America.^m Also at Department of Physics and Astronomy, University of Victoria, Victoria BC; Canada.ⁿ Also at Department of Physics, Ben Gurion University of the Negev, Beer Sheva; Israel.^o Also at Department of Physics, California State University, Sacramento; United States of America.

- ^p Also at Department of Physics, King's College London, London; United Kingdom.
- ^q Also at Department of Physics, Royal Holloway University of London, Egham; United Kingdom.
- ^r Also at Department of Physics, Stanford University, Stanford CA; United States of America.
- ^s Also at Department of Physics, University of Fribourg, Fribourg; Switzerland.
- ^t Also at Department of Physics, University of Thessaly; Greece.
- ^u Also at Department of Physics, Westmont College, Santa Barbara; United States of America.
- ^v Also at Hellenic Open University, Patras; Greece.
- ^w Also at Institutio Catalana de Recerca i Estudis Avancats, ICREA, Barcelona; Spain.
- ^x Also at Institut für Experimentalphysik, Universität Hamburg, Hamburg; Germany.
- ^y Also at Institute for Nuclear Research and Nuclear Energy (INRNE) of the Bulgarian Academy of Sciences, Sofia; Bulgaria.
- ^z Also at Institute of Applied Physics, Mohammed VI Polytechnic University, Ben Guerir; Morocco.
- ^{aa} Also at Institute of Particle Physics (IPP); Canada.
- ^{ab} Also at Institute of Physics and Technology, Ulaanbaatar; Mongolia.
- ^{ac} Also at Institute of Physics, Azerbaijan Academy of Sciences, Baku; Azerbaijan.
- ^{ad} Also at Institute of Theoretical Physics, Ilia State University, Tbilisi; Georgia.
- ^{ae} Also at L2IT, Université de Toulouse, CNRS/IN2P3, UPS, Toulouse; France.
- ^{af} Also at Lawrence Livermore National Laboratory, Livermore; United States of America.
- ^{ag} Also at National Institute of Physics, University of the Philippines Diliman (Philippines); Philippines.
- ^{ah} Also at Technical University of Munich, Munich; Germany.
- ^{ai} Also at The Collaborative Innovation Center of Quantum Matter (CICQM), Beijing; China.
- ^{aj} Also at TRIUMF, Vancouver BC; Canada.
- ^{ak} Also at Università di Napoli Parthenope, Napoli; Italy.
- ^{al} Also at University of Colorado Boulder, Department of Physics, Colorado; United States of America.
- ^{am} Also at Washington College, Chestertown, MD; United States of America.
- ^{an} Also at Yeditepe University, Physics Department, İstanbul; Türkiye.
- * Deceased.